Negative microfilm
received from university

64–8156

EL–GAALY, Mohamed Ali, 1936–
ANALYSIS OF MULTI–CELL BOX GATES
FOR DRY DOCKS.

The University of Michigan, Sc.D., 1963
Engineering, civil

University Microfilms, Inc., Ann Arbor, Michigan

ANALYSIS OF MULTI-CELL BOX GATES FOR DRY DOCKS

Mohamed Ali El-Gaaly

A dissertation submitted in partial fulfillment
of the requirements for the degree of
Doctor of Science in the
University of Michigan
1963

Doctoral Committee:

Professor Glen V. Berg, Chairman
Associate Professor Bernard A. Galler
Professor Bruce G. Johnston
Professor Lawrence C. Maugh
Associate Professor Raymond A. Yagle

ACKNOWLEDGMENTS

The author wishes to express his sincere appreciation to Professor G. V. Berg for his advice and guidance during the course of this study, and to Professor L. C. Maugh for his guidance and advice, particularly in the experimental work in this study. Special thanks are also due to Professor B. G. Johnston for his friendly encouragement and instructions about the application of plate theory to the analysis.

The author also wishes to express his gratitude to each of the other committee members for their interest and cooperation, and extends his thanks to the many other people with whom he has been associated while doing his work, and by whome his work has been greatly accelerated.

TABLE OF CONTENTS

		Page
ACKNOWLEDGMENTS		ii
LIST OF FIGURES		v
LIST OF PLATES		viii
NOMENCLATURE		ix
CHAPTER		
I.	INTRODUCTION	1
II.	ANALYTICAL SOLUTION	8
2.1	Idealization of the Structure	8
2.2	Simplifying Assumptions	8
2.3	The Stiffness Matrix of the Individual Elements	10
2.4	The Formulation of the Stiffness Matrix	16
2.5	Boundary (Support) Conditions	31
2.6	The Flexibility Matrix	32
2.7	The First Approach	33
2.8	The Second Approach	35
2.9	Stress Calculations	39
III.	ANALYSIS OF A SPECIFIC CASE	41
IV.	EXPERIMENTAL ANALYSIS	53
4.1	Material Used	53
4.2	Properties of the Material	53
4.3	The Model	58
4.4	The Supporting Frame	58
4.5	The Test Load	61
4.6	The Measuring Instruments	61
4.7	Preliminary Tests	63
4.8	The Test	64
4.9	Test Results and Comparison with Analytical Answers	66
V.	THIN ISOTROPIC PLATE SOLUTION VS. FINITE ELEMENT SOLUTION	70
5.1	Thin Isotropic Plate Solution	70
5.2	Stresses	75
5.3	Evaluation of the Plate Solution	79

TABLE OF CONTENTS CONT'D

		Page
5.4	Comparison Between the Finite Element Solution and the Plate Solution	81
5.5	Concluding Remarks	96
VI.	SUMMARY AND CONCLUSIONS	98
APPENDIX		
I.	PLANE STRESS PLATE-ELEMENT STIFFNESS MATRIX	101
II.	WEB-ELEMENT STIFFNESS MATRIX	110
REFERENCES		114
SELECTED BIBLIOGRAPHY		116

LIST OF FIGURES

Figure		Page
1	Plane Elements Assembly.....	9
2a	Assumed Stress Pattern in Cover Plate Element.....	11
2b	Joint Moments and Rotations in Cover Plate Element...	11
3	Stiffness Coefficients of the Cover Plates.....	14
4	Moments, Reactions, Rotations, and Deflections in a Web Element.....	15
5	Stiffness Coefficients of the Web.....	17
6	Unit Displacement at Joint 0, and the Forces at the Neighboring Joints.....	20
7	Dock-Gate Example Dimensions.....	42
8	Deflections (Considering and Neglecting Shear Deformations).....	44
9	Normal Stresses in the Cover Plate in the x-Direction (Considering and Neglecting Shear Deformations).	45
10	Normal Stresses in the Cover Plate in the y-Direction (Considering and Neglecting Shear Deformations).	47
11	Shear Stresses in the Cover Plate (Considering and Neglecting Shear Deformations).....	48
12	Shear Stresses in the Horizontal Webs (Considering and Neglecting Shear Deformations).....	49
13	Shear Stresses in the Vertical Webs (Considering and Neglecting Shear Deformations).....	50
14	Reactions (Considering and Neglecting Shear Deformations).....	51
15	Arrangements for the Tensile Test.....	55
16	Load-Strain Curve.....	56
17	Dimensions of the Model.....	59

LIST OF FIGURES CONT'D

Figure		Page
18	Locations of Strain Gages.....	65
19	Strains in the Horizontal Direction.....	67
20	Strains in the Vertical Direction.....	68
21	Plate Simply Supported on Three Sides and Subjected to a Hydrostatic Pressure.....	71
22	Directions of Positive Load, Moments, and Shears.....	76
23	Vertical Shears Due to Twisting Moments.....	78
24	Locations Where Moments and Shears are Calculated....	80
25	Deflections (Finite Element vs. Idealized Plate).....	82
26	Normal Stresses in the Cover Plate in the x-Direction (Finite Element vs. Idealized Plate).....	83
27	Normal Stresses in the Cover Plate in the y-Direction (Finite Element vs. Idealized Plate).....	84
28	Shear Stresses in the Cover Plate (Finite Element vs. Idealized Plate).....	85
29	Shear Stresses in the Horizontal Webs (Finite Element vs. Idealized Plate).....	87
30	Shear Stresses in the Vertical Webs (Finite Element vs. Idealized Plate).....	88
31	Reactions (Finite Element vs. Idealized Plate).....	89
32	Comparison Between the Deflections in Three Gates With Different Cover Plate Thicknesses.....	90
33	Comparison Between the Deflections in Three Gates With Different Web Spacings.....	93
34	Comparison Between the Deflections in Three Gates With Different Cover Plate Spacings.....	95

ACKNOWLEDGMENTS

The author wishes to express his sincere appreciation to Professor G. V. Berg for his advice and guidance during the course of this study, and to Professor L. C. Maugh for his guidance and advice, particularly in the experimental work in this study. Special thanks are also due to Professor B. G. Johnston for his friendly encouragement and instructions about the application of plate theory to the analysis.

The author also wishes to express his gratitude to each of the other committee members for their interest and cooperation, and extends his thanks to the many other people with whom he has been associated while doing his work, and by whome his work has been greatly accelerated.

TABLE OF CONTENTS

		Page
ACKNOWLEDGMENTS		ii
LIST OF FIGURES		v
LIST OF PLATES		viii
NOMENCLATURE		ix
CHAPTER		
I.	INTRODUCTION	1
II.	ANALYTICAL SOLUTION	8
2.1	Idealization of the Structure	8
2.2	Simplifying Assumptions	8
2.3	The Stiffness Matrix of the Individual Elements	10
2.4	The Formulation of the Stiffness Matrix	16
2.5	Boundary (Support) Conditions	31
2.6	The Flexibility Matrix	32
2.7	The First Approach	33
2.8	The Second Approach	35
2.9	Stress Calculations	39
III.	ANALYSIS OF A SPECIFIC CASE	41
IV.	EXPERIMENTAL ANALYSIS	53
4.1	Material Used	53
4.2	Properties of the Material	53
4.3	The Model	58
4.4	The Supporting Frame	58
4.5	The Test Load	61
4.6	The Measuring Instruments	61
4.7	Preliminary Tests	63
4.8	The Test	64
4.9	Test Results and Comparison with Analytical Answers	66
V.	THIN ISOTROPIC PLATE SOLUTION VS. FINITE ELEMENT SOLUTION	70
5.1	Thin Isotropic Plate Solution	70
5.2	Stresses	75
5.3	Evaluation of the Plate Solution	79

TABLE OF CONTENTS CONT'D

		Page
5.4	Comparison Between the Finite Element Solution and the Plate Solution	81
5.5	Concluding Remarks	96
VI.	SUMMARY AND CONCLUSIONS	98
APPENDIX		
I.	PLANE STRESS PLATE-ELEMENT STIFFNESS MATRIX	101
II.	WEB-ELEMENT STIFFNESS MATRIX	110
REFERENCES		114
SELECTED BIBLIOGRAPHY		116

LIST OF FIGURES

Figure		Page
1	Plane Elements Assembly.....	9
2a	Assumed Stress Pattern in Cover Plate Element.....	11
2b	Joint Moments and Rotations in Cover Plate Element...	11
3	Stiffness Coefficients of the Cover Plates.....	14
4	Moments, Reactions, Rotations, and Deflections in a Web Element.....	15
5	Stiffness Coefficients of the Web.....	17
6	Unit Displacement at Joint O, and the Forces at the Neighboring Joints.....	20
7	Dock-Gate Example Dimensions.....	42
8	Deflections (Considering and Neglecting Shear Deformations).....	44
9	Normal Stresses in the Cover Plate in the x-Direction (Considering and Neglecting Shear Deformations).	45
10	Normal Stresses in the Cover Plate in the y-Direction (Considering and Neglecting Shear Deformations).	47
11	Shear Stresses in the Cover Plate (Considering and Neglecting Shear Deformations).....	48
12	Shear Stresses in the Horizontal Webs (Considering and Neglecting Shear Deformations).....	49
13	Shear Stresses in the Vertical Webs (Considering and Neglecting Shear Deformations).....	50
14	Reactions (Considering and Neglecting Shear Deformations).....	51
15	Arrangements for the Tensile Test.....	55
16	Load-Strain Curve.....	56
17	Dimensions of the Model.....	59

LIST OF FIGURES CONT'D

Figure		Page
18	Locations of Strain Gages.....	65
19	Strains in the Horizontal Direction.....	67
20	Strains in the Vertical Direction.....	68
21	Plate Simply Supported on Three Sides and Subjected to a Hydrostatic Pressure.....	71
22	Directions of Positive Load, Moments, and Shears.....	76
23	Vertical Shears Due to Twisting Moments.....	78
24	Locations Where Moments and Shears are Calculated....	80
25	Deflections (Finite Element vs. Idealized Plate).....	82
26	Normal Stresses in the Cover Plate in the x-Direction (Finite Element vs. Idealized Plate).....	83
27	Normal Stresses in the Cover Plate in the y-Direction (Finite Element vs. Idealized Plate).....	84
28	Shear Stresses in the Cover Plate (Finite Element vs. Idealized Plate).....	85
29	Shear Stresses in the Horizontal Webs (Finite Element vs. Idealized Plate).....	87
30	Shear Stresses in the Vertical Webs (Finite Element vs. Idealized Plate).....	88
31	Reactions (Finite Element vs. Idealized Plate).....	89
32	Comparison Between the Deflections in Three Gates With Different Cover Plate Thicknesses.....	90
33	Comparison Between the Deflections in Three Gates With Different Web Spacings.....	93
34	Comparison Between the Deflections in Three Gates With Different Cover Plate Spacings.....	95

LIST OF FIGURES CONT'D

Figure		Page
A1	Assumed Stress and Corresponding Deformation Patterns.....	102
A2	Plate Distortions for Support Displacements.....	107
A3	Web Displacements Required in Developing the Web Stiffness Matrix.....	111

LIST OF PLATES

Plate		Page
1	The Test Set-Up.....	60
2	The Loaded Model.....	60
3	Support Details.....	62

NOMENCLATURE

Symbol	Description
a	Depth of the gate, or the dimension of the cover plate element in the y-direction.
b	The span of the gate, or the dimension of the cover plate element in the x-direction.
D	Flexural rigidity, $Et_c h^2/2(1-\nu^2)$
$\overline{D}$	Deformation vector
E	Young's modulus of elasticity
[F]	Flexibility matrix; the matrix whose influence coefficients f_{ij} represent the displacement at i due to a unit force at j.
G	Shear modulus, or modulus of rigidity
h	Distance between the cover plates
I	Moment of inertia of the web element, $t_w h^3/12$
[K]	Stiffness matrix; the matrix whose influence coefficients k_{ij} represent the force at i due to a unit displacement at j.
$\overline{L}$	Load vector
L	Length of web element
m	Number of webs parallel to the x-axis, or ratio between the sides of the cover plate element, b/a
Mx	Moment about the x-axis
My	Moment about the y-axis
Mxy	Twisting moment
n	Number of webs parallel to the y-axis, or shear deformation factor in the web element; $3EI/Ght_w L^2$
N	Number of joints

Symbol	Description
q	Specific weight of water, 62.4 lb/ft^3
R	Force in the z-direction
Rx, Ry	Uniformly distributed reactions along the supported edges $x = \pm b/2$, and $y = a$.
rx, ry	Displacements in the cover plates in the x- and the y-directions, respectively.
t_c	Thickness of cover plates
t_w	Thickness of webs
Vx, Vy	Shearing forces in the webs parallel to the x- and the y-axes, respectively.
w	Deflection in the z-direction
α	Ratio between the gate depth and span, a/b
$\epsilon x, \epsilon y$	Strains in the cover plates in the x and the y directions, respectively.
$\theta x, \theta y$	Rotations about the x- and the y-axes, respectively.
τ_{xy}	Shearing stresses in the cover plates
τ_{xz}, τ_{yz}	Shearing stresses in the webs parallel to the x- and y-axes, respectively.
ν	Poisson's ratio
σ_{xx}, σ_{yy}	Normal stresses in the cover plates in the x and the y directions, respectively.
$[\ ]^T$	Transpose of a matrix
$[\ ]^{-1}$	Inverse of a matrix

I. INTRODUCTION

In recent years the falling-leaf or box-flap gate has been increasingly used for dry docks where circumstances permit. In practically all new or reconstructed dry docks completed during the past ten years, this type has been adopted.[1] The gate consists of a single leaf hinged horizontally at the level of the bottom sill. It is extremely simple and speedy in operation; it can be raised or lowered by one man, if necessary, in a few minutes by means of an electrically driven winch placed on one side of the dock.

An important advantage of the flap gate is that, in the open or lowered position, it can usually be accommodated in the outer basin or waterway adjoining the dry dock. In comparison with the mitre type of gates, which require recesses in the dock walls for the accommodation of the gates in the open position, the box gate offers a considerable saving in cost of dock wall construction. The cost of forming the apron in front of the gate is usually much less than that of the additional length of the side wall. Alternatively, if a given space is available, a greater useful length of the dock can be obtained with this gate than with the mitre type. This length-saving feature of the flap gate can increase by 20 to 40 feet the effective length of an existing dock, or with a new dock, can reduce the general cost of construction by an amount approximating to the cost of the gate.[1]

Gates of this type have now been built for dock entrances of 130 feet in width and larger sizes, up to 160 feet. The dock gate at Wallsend, England,[2] is of this type; it is 111 feet 4 inches in width, 35 feet deep, and 7 feet 9 inches thick. It weighs 240 tons. The gate for the Queen Elizabeth graving dock at Falmouth, England,[3,4] is 133 feet 4 inches wide, 40 feet 3 inches deep, and 9 feet 6 inches thick. Five hundred tons of steel were used for the all-welded structure of the gate.

The gate is of cellular steel construction, which in its early forms was riveted. However, present-day practice favors fabrication entirely by welding.

The system of framing adopted may be varied according to the size and the width-height ratio of the gate. The usual arrangement consists of a series of horizontal webs spanning between the side jambs of the entrance, vertical webs spanning from the keel to the top, and the skin plating on both sides.

The usual structural design for the gate is based essentially on considering it as a rectangular slab supported on three sides and carrying a hydrostatic pressure. This is based on the idea that the contribution of the cover plates to the flexural rigidity of the gate greatly exceed that of the webs, and that the webs are close enough to assure that the cover plates are fully effective. Also, shear deformations of the webs are assumed to be negligible. If these assumptions are valid, then the gate behavior is essentially the same as that of a hypothetical thin isotropic plate with flexural rigidity $D = Et_c h^2/2(1-\nu^2)$, where:

E = Young's modulus of elasticity

ν = Poisson's ratio

t_c = the thickness of cover plates, and

h = the distance between the cover plates.[5-7]

Experimental work carried out by L. G. Jaeger,[8] in which deflections only were measured, indicated that this assumption may be accepted. However, a considerable difference may result by comparing actual stresses with the calculated ones using this assumption.

The assumed plate is in reality a box composed of an outer plate and a two-directional webbing in the form of interconnecting bulkheads or trusses. (The civil engineer will find that a considerable amount of work has been done in the analysis of similar structures in the aircraft industry, such as delta wings. The aircraft engineer is much more concerned about the weight of his structure than is the civil engineer.) D. Williams[9] suggested that the plate theory can be followed in the solution of thick-walled structures. S. U. Benscoter and R. H. MacNeal[10] derived an equivalent plate theory to take the shear deformations of the webs into consideration. This theory is based on various simplifying assumptions, such as assuming normal stresses to be carried in equivalent flanges located at the juncture of the webs and the cover plates, while the webs and the cover plates carry only shear flows. They presented the solution in first-order finite difference equations, to be solved by analog computer.

For a more realistic analysis we must deal with a highly indeterminate structure. The development on high-speed digital computing machines has permitted a solution for such a highly indeterminate structure.

The degree of statical indeterminacy of the structure is strictly infinite. To obtain a solution, we must first idealize the structure by considering it to be an assembly of a large number of members interconnected at a finite number of connections. For a given idealized structure, the analysis of stresses and deflections due to a given system of loads is purely a mathematical problem. Two conditions must be satisfied in the analysis:

1) The forces developed in the members must be in equilibrium.
2) The deformations of the members must be compatible, that is to say, consistent with each other and with the boundary conditions.

In addition, the forces and deflections in each member must be related in accordance with the stress-strain relationship assumed for the material.

The analysis may be approached from two different points of view. In one case the forces acting in the members of the structure are considered as unknowns. In a statically indeterminate system an infinite number of such force systems exist which will satisfy the equations of equilibrium; the correct system is then selected by satisfying the conditions of compatible deformations

in the members. In the other approach the displacements of the joints in the structure are considered as unknown quantities. Also, an infinite number of systems of compatible deformations in the members are possible; the correct one is that for which the equations of equilibrium are satisfied. The first method is usually called the force method, while the second is called the displacement method. In both methods, use of matrices is desirable, because this allows a systematic approach to the tremendous number of calculations, and simplifies programming of the problem for the electronic digital computer.

The idealization of the structure depends upon the method of approach to be used in the analysis of the structure. Levy[11] has considered the structure as an assemblage of shear panels with uniformly distributed shear flows along the edges, and axially loaded flanges at the intersections of webs and cover plates. He made use of the stress analysis based primarily on equilibrium considerations, together with Castigliano's energy theorem for deriving displacements under load from the elastic energy stored in the structure. Wehle and Lansing[12] made use of Levy's idea and presented a solution to the whole structure which is systematic and in a matrix form easily adapted for high-speed digital computer programming. Argyris[13] presented a force-method analysis which involves idealizations similar to those considered by Levy. Several other idealizations have been proposed.[14,15] In some cases the plate-lattice analogy[16,17] was considered as a means of simulating the behavior of the cover plate element.

The force method of analysis of such a highly redundant structure involves severe computational difficulties and the method is not particularly well adapted to the use of high-speed computing machines. For this reason, the displacement method is used in the analysis presented in this work.

The structure is considered as an assemblage of cover-plate elements and web elements. We define the middle plane between the cover plates as the x-y plane, and the direction perpendicular to it as the z-direction. Because the structure is symmetric about the x-y plane and the loads are applied normal to this plane, we define only three displacement components at each web intersection (joint), these displacement components are Θx, and Θy, the rotations about the x- and y-axes and w the deflection in the z-direction. We displace one joint in only one of the three displacement components and calculate the forces that arise at the neighboring joints in terms of this component, assuming that the stiffness of the individual elements of the assemblage is known. If we repeat this with respect to the other two displacement components and do the same thing for all other joints, we will obtain the forces at the different joints in terms of the defined displacements. From the three equilibrium conditions at each joint, namely,

1. The sum of the forces in the z-direction = 0,
2. The sum of the moments about the x-axis = 0, and
3. The sum of the moments about the y-axis = 0,

we are able to evaluate the three displacement components. As mentioned

before, the stiffness of each individual element of the assemblage must be known. The stiffness of the web element is based on the beam theory which is modified to include shear deformations. The cover plate is relatively thin so that its stiffness in the lateral direction (z-direction) can be neglected without introducing any considerable errors. Plate stiffness for the cover plate element can be derived by assuming a stress or a strain pattern.[13,18,19] The calculations involved in the analysis demand the use of high-speed electronic digital computers.

In Chapter II the analysis is described in detail. Two different schemes are proposed to reduce the amount of computations involved. The analysis is presented in a matrix notation; the reader unfamiliar with such notations will find References 20 through 25 helpful. The results of an example solved by the proposed method and the accuracy obtained are discussed in Chapter III.

Since the analysis involves some simplifying assumptions, the validity of these assumptions was tested experimentally. A plastic model was built and tested; the test set-up, procedure, and test results are discussed in Chapter IV.

In Chapter V, the proposed method of analysis and the commonly adopted method utilizing the thin isotropic plate theory are compared. Chapter VI provides conclusions and remarks.

The stiffness derivation for the cover plate element based on an assumed stress pattern, and the derivation of the web element stiffness are presented in Appendix I and II.

II. ANALYTICAL SOLUTION

2.1 Idealization of the Structure

The structure is infinitely indeterminate statically. For finite indeterminacy, we will consider the structure as composed of an assembly of plane, cover, and web elements (Figure 1). The lines of intersection of these elements intersect at finite number of points (nodal points).

Conditions of equilibrium, compatibility of deformations, and the boundary conditions must be satisfied at the nodal points.

2.2 Simplifying Assumptions

1. The structure is symmetrical about the middle surface and the application of loads normal to the middle surface only are considered; consequently, only three displacement components, namely, θx, θy, and w, are defined at each web intersection (joint), where:

   θx and θy are the rotations about the x and y axes, respectively, and

   w is the deflection in the z-direction (Figure 1).

2. The middle plane is a neutral plane.

3. The plane section remains plane after bending.

4. Stresses and strains are uniform through the thickness of the cover plates.

5. The stiffness of the cover plates in the z-direction is very small compared with the stiffness of the webs in this direction, and can be neglected.

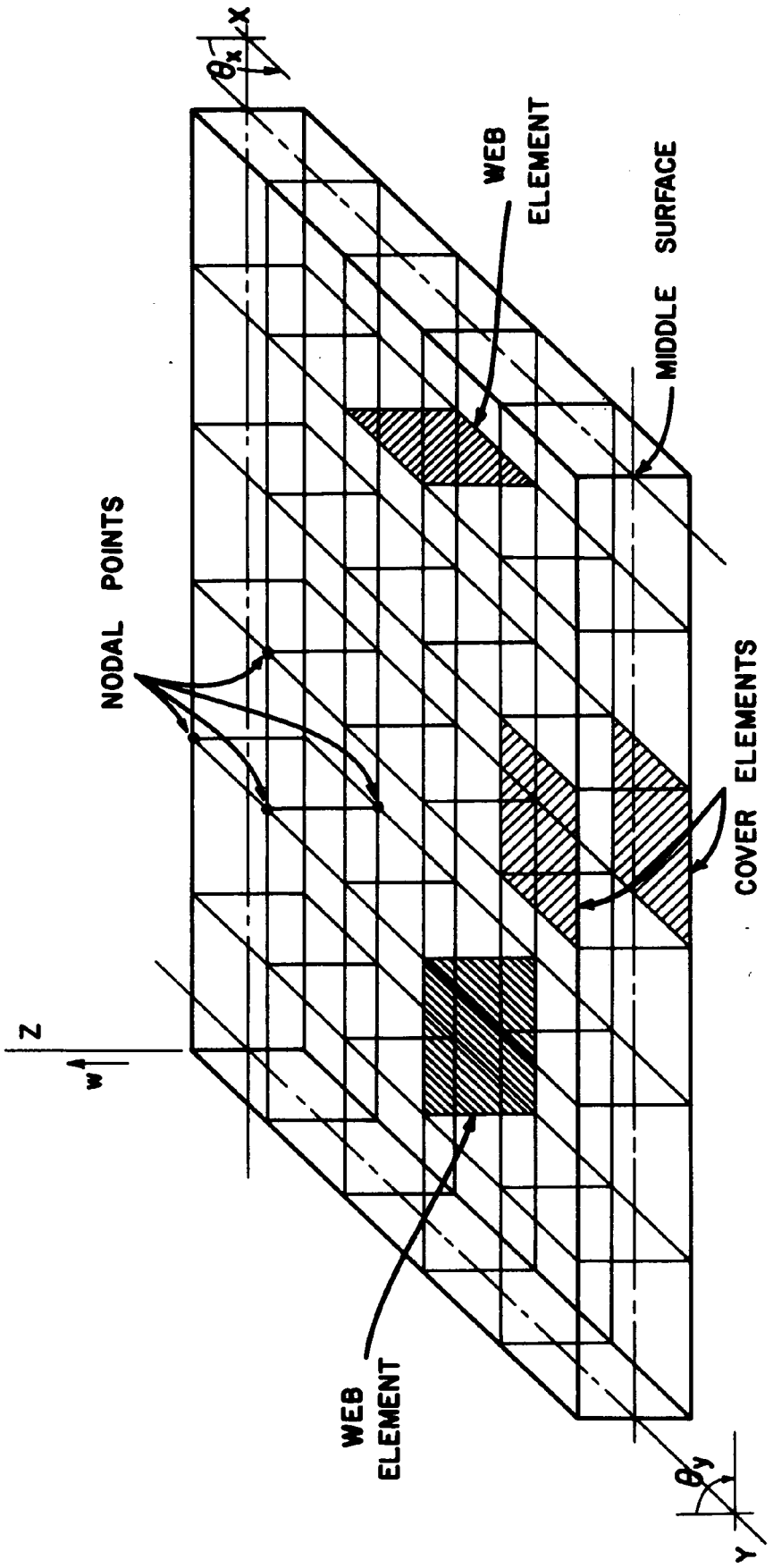


Figure 1. Plane Elements Assembly.

6. The normal stresses σ_{xx}, σ_{yy} (Figure 2a) in the cover plates vary linearly between the nodal points.

7. The shear stresses τ_{xy} (Figure 2a) in the cover plates are uniform between the nodal points.

8. The elementary beam theory, modified to take shear deformations into account, is applicable with respect to the webs.

9. Any load distributed over the area of the structure is replaced by equivalent concentrated loads at the nodal points.

10. The deformations are sufficiently small compared with the over-all dimensions of the structure to consider the changes in the over-all dimensions negligible.

2.3 The Stiffness Matrix of the Individual Elements

2.3.1 Cover Plates -- The stiffness properties of a single cover plate element are obtained by a plane stress analysis, assuming the stress pattern shown in Figure 2a, using the stress-strain relationship of plane linear elasticity and the principle of virtual displacements (see Appendix I). Having these properties one can express the stiffness of a pair of cover plate elements as a stiffness matrix.

The stiffness matrix is arranged to agree with the equation:

$$\begin{vmatrix} Mx_1 \\ Mx_2 \\ Mx_3 \\ Mx_4 \\ My_1 \\ My_2 \\ My_3 \\ My_4 \end{vmatrix} = [Kc] \begin{vmatrix} \theta x_1 \\ \theta x_2 \\ \theta x_3 \\ \theta x_4 \\ \theta y_1 \\ \theta y_2 \\ \theta y_3 \\ \theta y_4 \end{vmatrix} \qquad (2.1)$$

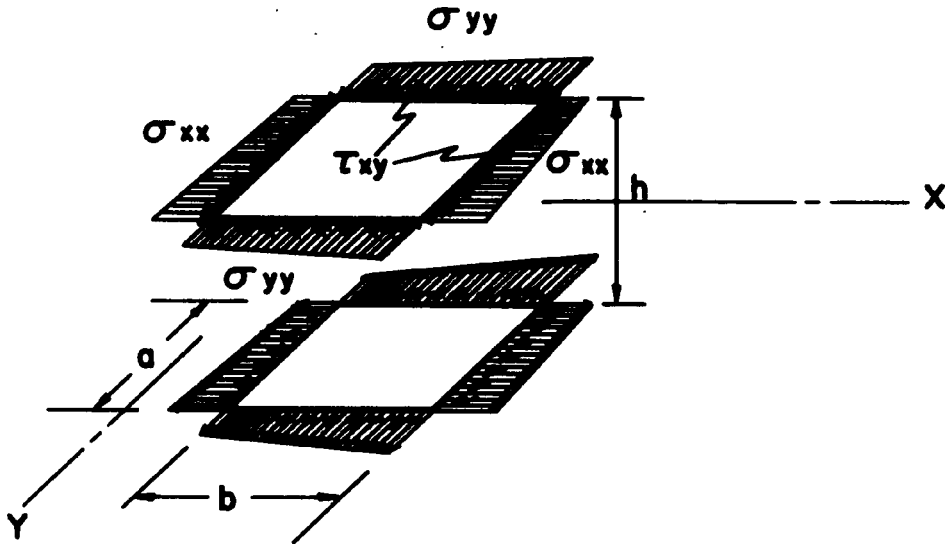


Figure 2a. Assumed Stress Pattern in Cover Plate Element.

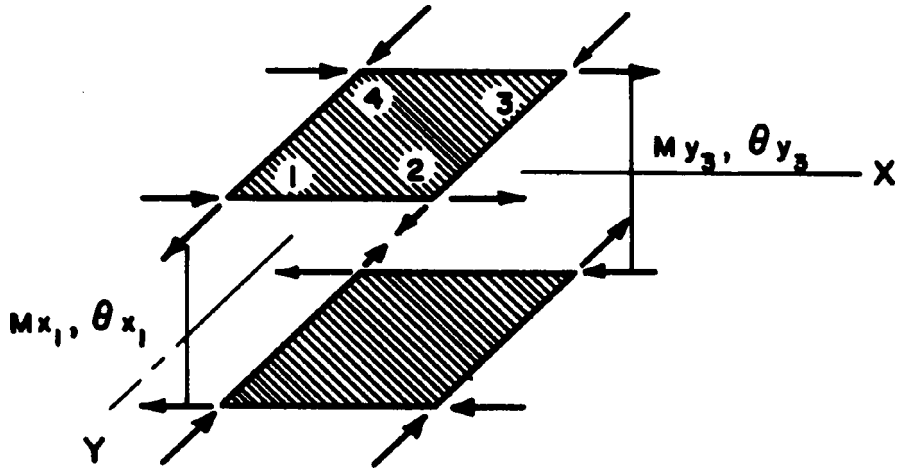


Figure 2b. Joint Moments and Rotations in Cover Plate Element.

in which the M's and the Θ's are the joint moments and rotations, respectively (Figure 2b), where

$$[Kc] = \frac{Et_c h^2}{16(1-\nu^2)} \begin{bmatrix} a_2+b_2 & & & & & & & \\ c_2-a_2 & a_2+b_2 & & & & & & \\ -a_2-c_2 & a_2-b_2 & a_2+b_2 & & & & & \\ a_2-b_2 & -a_2-c_2 & c_2-a_2 & a_2+b_2 & & \text{(symmetric)} & & \\ -1-\nu & 1-3\nu & 1+\nu & 3\nu-1 & a_1+b_1 & & & \\ 3\nu-1 & 1+\nu & 1-3\nu & -1-\nu & a_1-b_1 & a_1+b_1 & & \\ 1+\nu & 3\nu-1 & -1-\nu & 1-3\nu & -a_1-c_1 & c_1-a_1 & a_1+b_1 & \\ 1-3\nu & -1-\nu & 3\nu-1 & 1+\nu & c_1-a_1 & -a_1-c_1 & a_1-b_1 & a_1+b_1 \end{bmatrix} \qquad (2.2)$$

In the above matrix:

$a_1 = m(1-\nu)$, $b_1 = 2(4-\nu^2)/3m$, $c_1 = 2(2+\nu^2)/3m$

$a_2 = (1-\nu)/m$, $b_2 = 2m(4-\nu^2)/3$, $c_2 = 2m(2+\nu^2)/3$

m = b/a, where a and b are the dimensions of the rectangular plate element in the y- and the x-directions, respectively.

ν = Poisson's ratio, and

E = Young's modulus of elasticity

[Kc] is symmetric (i.e., $Kc_{ij} = Kc_{ji}$) according to Maxwell's reciprocal theorem.

From the symmetry of the plate element, and from Maxwell's reciprocal theorem, the 64 stiffness coefficients reduce to only 10 different coefficients, namely:

$$Kc_1 = Et_c h^2(a_2+b_2)/16(1-\nu^2)$$

$$Kc_2 = Et_c h^2(c_2-a_2)/16(1-\nu^2)$$

$$Kc_3 = Et_c h^2(a_2-b_2)/16(1-\nu^2)$$

$$Kc_4 = Et_c h^2(-a_2-c_2)/16(1-\nu^2)$$

$$Kc_5 = Et_c h^2(a_1+b_1)/16(1-\nu^2)$$

$$Kc_6 = Et_c h^2(a_1-b_1)/16(1-\nu^2)$$

$$Kc_7 = Et_c h^2(c_1-a_1)/16(1-\nu^2)$$

$$Kc_8 = Et_c h^2(-a_1-c_1)/16(1-\nu^2)$$

$$Kc_9 = Et_c h^2(-1-\nu)/16(1-\nu^2)$$

$$Kc_{10} = Et_c h^2(1-3\nu)/16(1-\nu^2)$$

The above coefficients are arranged on Figure 3.

2.3.2 Webs -- From elementary beam theory modified to account for shear deformation, one derives a web element stiffness matrix (see Appendix II). The stiffness matrix is arranged to agree with the equation:

$$\begin{vmatrix} M_1 \\ R_1 \\ M_2 \\ R_2 \end{vmatrix} = [Kw] \begin{vmatrix} \theta_1 \\ w_1 \\ \theta_2 \\ w_2 \end{vmatrix} \qquad (2.3)$$

See Figure 4.

In Equation (2.3) the M's and the R's are the moments and the reactions, respectively, while the θ's and the w's are the rotations and deflections, respectively (see Figure 4), and

$$[Kw] = \frac{2EI}{L(1+4n)} \begin{bmatrix} 2(1+n) & & & \\ -3/L & 6/L^2 & (\text{Symmetric}) & \\ 1-2n & -3/L & 2(1+n) & \\ 3/L & -6/L^2 & 3/L & 6/L^2 \end{bmatrix} \qquad (2.4)$$

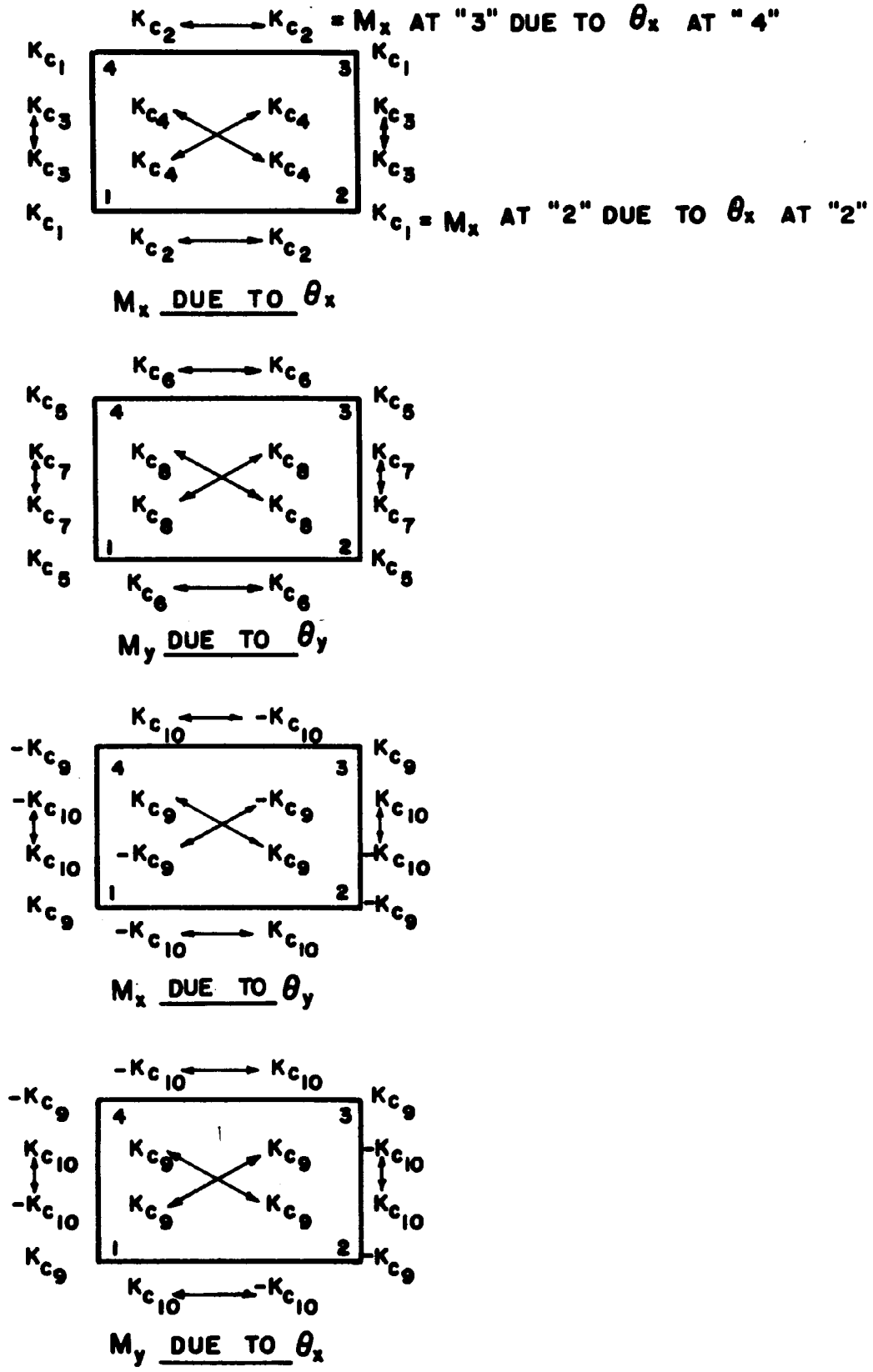


Figure 3. Stiffness Coefficients of the Cover Plates.

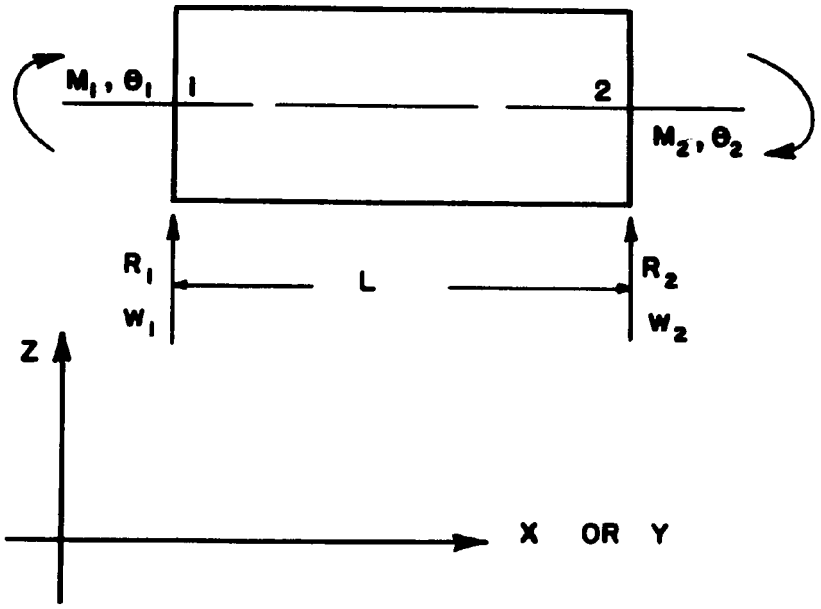


Figure 4. Moments, Reactions, Rotations, and Deflections in a Web Element.

In the above matrix,

$$I = t_w h^3/12$$

$$n = 3EI/Ght_wL^2$$

G = shear modulus (modulus of rigidity)

Notice that "n" represents the contribution of the shear deformation. If shear deformation is neglected, n = 0.

[Kw] is symmetric (i.e., $Kw_{ij} = Kw_{ji}$), according to Maxwell's reciprocal theorem.

From the symmetry in the web element, and from Maxwell's reciprocal theorem, the 16 stiffness coefficients reduce to only 4 different coefficients, namely:

$$Kw_1 = 4EI(1+n)/L(1+4n)$$

$$Kw_2 = 2EI(1-2n)/L(1+4n)$$

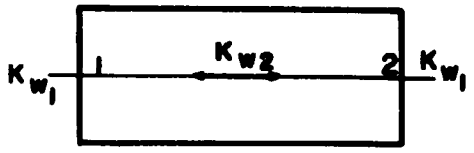
$$Kw_3 = 12EI/L^3(1+4n)$$

$$Kw_4 = 6EI/L^2(1+4n)$$

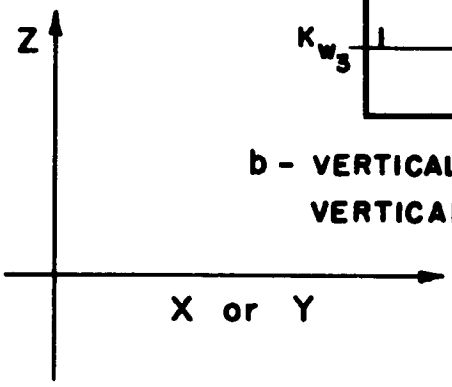
The above coefficients are arranged on Figure 5.

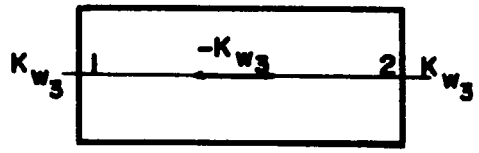
2.4 The Formulation of the Stiffness Matrix

To find the stiffness coefficients for the assembly, one joint is displaced in the z-direction or rotated about the x- or the y-axis, while all other joints are held fixed. The force in the z-direction, the moment about the x-axis, and the moment about the y-axis required to do this and the reactions set up at neighboring joints are then known from the individual element stiffness matrices. These are the coefficients in the stiffness matrix of the complete structure. When all three components of displacements (w, θx, and θy) at all joints have

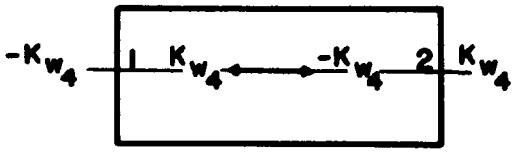


a - MOMENTS DUE TO ROTATIONS.

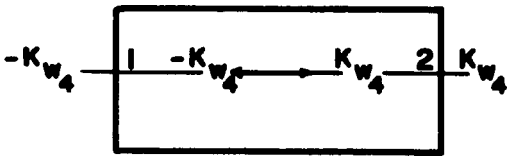




b - VERTICAL FORCES DUE TO VERTICAL DISPLACEMENTS.



c - MOMENTS DUE TO VERTICAL DISPLACEMENTS.



d - VERTICAL FORCES DUE TO ROTATIONS.

Figure 5. Stiffness Coefficients of the Web.

been considered in this manner, the complete stiffness matrix will have been developed. In general this matrix will be of the order 3N x 3N, where

$$N = \text{number of joints}$$

To facilitate the formulation of the stiffness matrix, let us arrange it to agree with the equation:

$$\begin{vmatrix} \overline{R} \\ \hline \overline{Mx} \\ \hline \overline{My} \end{vmatrix} = \left[\begin{array}{c|c|c} [Kzz] & [Kzx] & [Kzy] \\ \hline [Kxz] & [Kxx] & [Kxy] \\ \hline [Kyz] & [Kyx] & [Kyy] \end{array}\right] \begin{vmatrix} \overline{w} \\ \hline \overline{\Theta x} \\ \hline \overline{\Theta y} \end{vmatrix} \qquad (2.5)$$

where $\overline{R}$ = Forces in the z-direction, $R_1 \ldots R_N$

$\overline{Mx}$ = Moments about the x-axis, $Mx_1 \ldots Mx_N$

$\overline{My}$ = Moments about the y-axis, $My_1 \ldots My_N$

$\overline{W}$ = Displacements in the z-direction, $w_1 \ldots w_N$

$\overline{\Theta x}$ = Rotations about the x-axis, $\Theta x_1 \ldots \Theta x_N$

$\overline{\Theta y}$ = Rotations about the y-axis, $\Theta y_1 \ldots \Theta y_N$

Each of the individual sub-matrices, [Kzz] ... [Kyy], is of the order N x N, and from Maxwell's reciprocal theorem,

$$[Kzx] = [Kxz]^T ,$$

$$[Kzy] = [Kyz]^T , \text{ and}$$

$$[Kyx] = [Kxy]^T .$$

Let us now formulate the individual sub-matrices.

2.4.1 The Displacement Stiffness in the z-Direction for Displacements in the z-Direction Only, [Kzz] -- Since the stiffness of the cover plates in the z-direction is assumed to be negligible, only the web plates contribute to this stiffness.

If the force vector $\bar{R}$ is partitioned to a set of vectors, $\bar{r}_1 \ldots \bar{r}_m$, where $\bar{r}_i$ is the force vector at the nodal points of the i-th horizontal grid line (grid line parallel to the x-axis) (see Figure 6), and the displacement vector $\bar{W}$ is partitioned in the same manner, then [Kzz] will be arranged to agree with the equation:

$$\begin{vmatrix} \bar{r}_1 \\ \bar{r}_2 \\ .. \\ .. \\ \bar{r}_m \end{vmatrix} = \begin{bmatrix} [kzz]_{11} & [kzz]_{12} & ..... & [kzz]_{1m} \\ [kzz]_{21} & [kzz]_{22} & ..... & [kzz]_{2m} \\ ..... & ..... & ..... & ..... \\ ..... & ..... & ..... & ..... \\ [kzz]_{m1} & [kzz]_{m2} & ..... & [kzz]_{mm} \end{bmatrix} \begin{vmatrix} \bar{w}_1 \\ \bar{w}_2 \\ .. \\ .. \\ \bar{w}_m \end{vmatrix} \qquad (2.6)$$

Each of the individual sub-matrices $[kzz]_{ij}$ is of the order n x n, where

n = number of the webs parallel to the y-axis, and

m = number of the webs parallel to the x-axis (see Figure 6).

Since the forces which arise due to a unit displacement in the z-direction at any joint O will be limited to the four neighboring joints, N,E,W, and S (see Figure 6), then $[kzz]_{ij} = [0]$, for $i < j - 1$ or $i > j + 1$; moreover, $[kzz]_{ij}$ is a tri-diagonal matrix for $i = j$, and a diagonal matrix for $i = j - 1$, and $i = j + 1$.

Now [Kzz] can be written as

$$[Kzz] = \begin{bmatrix} [kzz]_{11} & [kzz]_{12} & & & \\ [kzz]_{21} & [kzz]_{22} & [kzz]_{23} & & \\ & ..... & ..... & ..... & \\ & & ..... & ..... & ..... \\ & & & [kzz]_{m,m-1} & [kzz]_{mm} \end{bmatrix} \qquad (2.6')$$

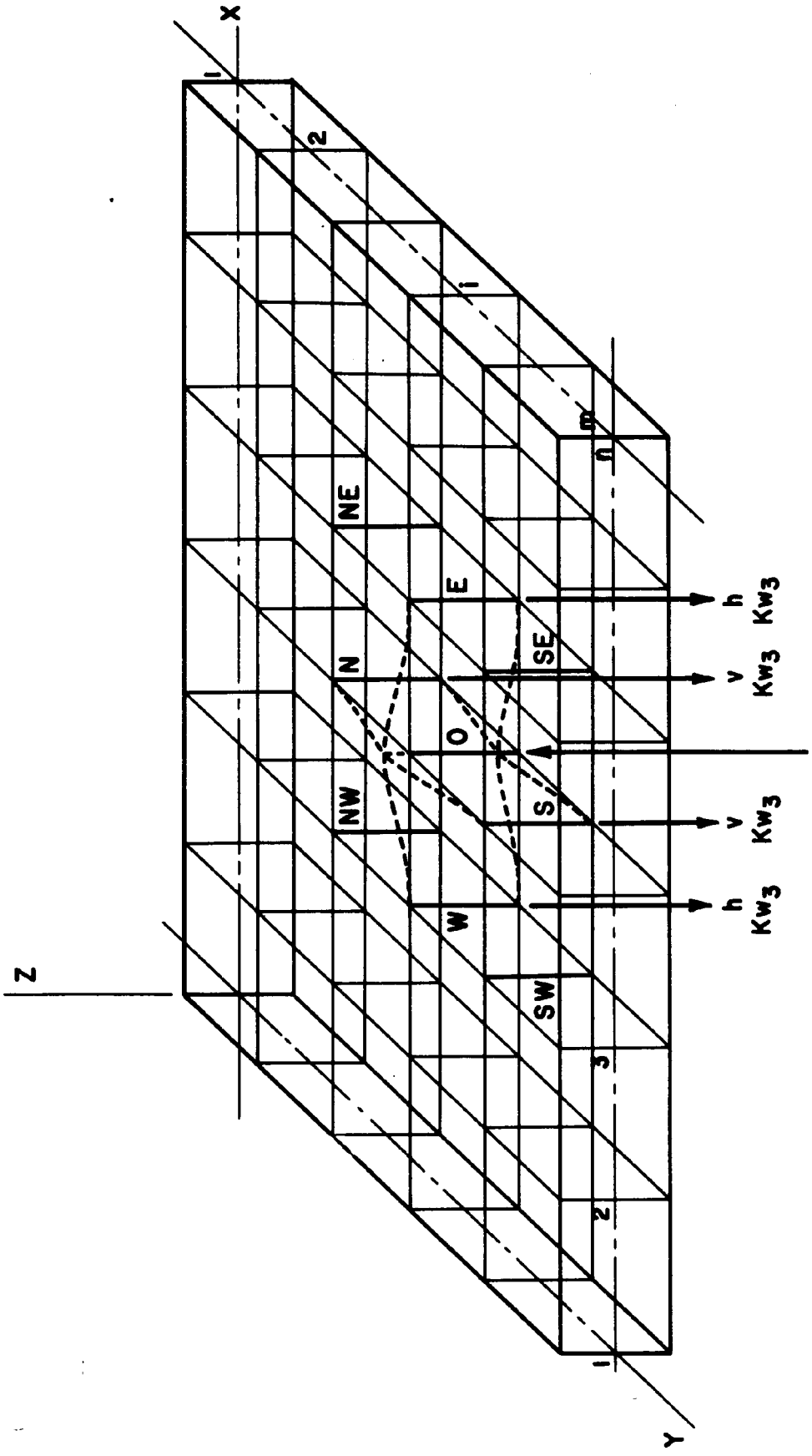


Figure 6. Unit Displacement at Joint O, and the Forces at the Neighboring Joints.

The above matrix is symmetrical from Maxwell's reciprocal theorem. If the horizontal webs (webs parallel to the x-axis) have equal stiffness and are equally spaced, and if the vertical webs (webs parallel to the y-axis) have equal stiffness and are equally spaced, then

$$[Kzz] = \begin{bmatrix} [Azz] & [Bzz] & & & \\ [Bzz]^T & [Czz] & [Bzz] & & \\ & \cdots & \cdots & \cdots & \\ & & \cdots & \cdots & \cdots \\ & & & [Bzz]^T & [Azz] \end{bmatrix}$$

where, from the stiffness matrix of the web element,

$$[Azz] = \begin{bmatrix} (Kw_3^h+Kw_3^v) & (-Kw_3^h) & & \\ (-Kw_3^h) & (2Kw_3^h+Kw_3^v) & (-Kw_3^h) & \\ & \cdots\cdots & \cdots\cdots & \cdots\cdots \\ & & (-Kw_3^h) & (Kw_3^h+Kw_3^v) \end{bmatrix},$$

$$[Bzz] = \begin{bmatrix} (-Kw_3^v) & & & \\ & (-Kw_3^v) & & \\ & & \cdots\cdots & \\ & & & (-Kw_3^v) \end{bmatrix}, \text{ and}$$

$$[Czz] = \begin{bmatrix} (Kw_3^h+2Kw_3^v) & (-Kw_3^h) & & \\ (-Kw_3^h) & (2Kw_3^h+2Kw_3^v) & (-Kw_3^h) & \\ & \cdots\cdots & \cdots\cdots & \cdots\cdots \\ & & (-Kw_3^h) & (Kw_3^h+2Kw_3^v) \end{bmatrix}.$$

In the above matrices the superscripts h and v refer to horizontal (parallel to the x-axis), and vertical (parallel to the y-axis) webs, respectively.

2.4.2 The Rotational Stiffness About the x-Axis for Displacements in the z-Direction Only, [Kxz] -- Since the stiffness of the cover plates in the z-direction is assumed to be negligible, the cover plates will not contribute to this stiffness.

If the moment vector $\overline{Mx}$ is partitioned to a set of vectors, $\overline{mx}_1 \ldots \overline{mx}_m$, where $\overline{mx}_i$ is the moment vector at the nodal points of the i-th horizontal grid line, and the displacement vector $\overline{W}$ is partitioned in the same manner, then [Kxz] will be arranged to agree with the equation:

$$\begin{vmatrix} \overline{mx}_1 \\ \overline{mx}_2 \\ \cdots \\ \cdots \\ \overline{mx}_m \end{vmatrix} = \begin{bmatrix} [kxz]_{11} & [kxz]_{12} & \cdots\cdots & [kxz]_{1m} \\ [kxz]_{21} & [kxz]_{22} & \cdots\cdots & [kxz]_{2m} \\ \cdots\cdots & \cdots\cdots & \cdots\cdots & \cdots\cdots \\ \cdots\cdots & \cdots\cdots & \cdots\cdots & \cdots\cdots \\ [kxz]_{m1} & [kxz]_{m2} & \cdots\cdots & [kxz]_{mm} \end{bmatrix} \begin{vmatrix} \overline{w}_1 \\ \overline{w}_2 \\ \cdots \\ \cdots \\ \overline{w}_m \end{vmatrix} \qquad (2.7)$$

Each of the individual sub-matrices $[kxz]_{ij}$ is of the order n x n, where n and m are as defined before.

Since the moments due to a unit displacement at any joint O will be limited to the two neighboring joints, N and S (see Figure 6), then $[kxz]_{ij} = [0]$, for $i < j - 1$ or $i > j + 1$; moreover, all non-zero matrices are diagonal matrices.

Now [Kxz] can be written as:

$$[Kxz] = \begin{bmatrix} [kxz]_{11} & [kxz]_{12} & & & \\ [kxz]_{21} & [kxz]_{22} & [kxz]_{23} & & \\ & \cdots\cdots & \cdots\cdots & \cdots\cdots & \\ & & \cdots\cdots & \cdots\cdots & \cdots\cdots \\ & & & [kxz]_{m,m-1} & [kxz]_{mm} \end{bmatrix} \qquad (2.7')$$

From the symmetry of the web element, and according to the adopted moment and displacement sign convention, $[kxz]_{ji} = -[kxz]_{ij}$. If the horizontal webs have the same stiffness and are equally spaced, and if the vertical webs have the same stiffness and are equally spaced, then

$$[Kxz] = \begin{bmatrix} -[Bxz] & [Bxz] & & & \\ -[Bxz]^T & [\ 0\ ] & [Bxz] & & \\ & \cdots & \cdots & \cdots & \\ & & \cdots & \cdots & \cdots \\ & & & -[Bxz]^T & [Bxz] \end{bmatrix}$$

where, from the stiffness matrix of the web element,

$$[Bxz] = \begin{bmatrix} \overset{v}{Kw_4} & & & & \\ & \overset{v}{Kw_4} & & & \\ & & \cdots & & \\ & & & \cdots & \\ & & & & \overset{v}{Kw_4} \end{bmatrix}$$

Again the superscript v refers to the vertical webs as mentioned before.

2.4.3 The Rotational Stiffness About the y-Axis for Displacements in the z-Direction Only, [Kyz] -- As mentioned before, the stiffness of the cover plates in the z-direction is assumed to be negligible, and it will not contribute to this stiffness.

If the moment vector $\overline{My}$ is partitioned to a set of vectors, $\overline{my}_1 \ldots \overline{my}_m$, where $\overline{my}_i$ is the moment vector at the nodal points of the i-th horizontal grid line, and the displacement vector $\overline{W}$ is partitioned in the same manner, then [Kyz] will be arranged to agree with the equation:

$$\begin{vmatrix} \overline{my}_1 \\ \overline{my}_2 \\ \cdots \\ \cdots \\ \overline{my}_m \end{vmatrix} = \begin{bmatrix} [kyz]_{11} & [kyz]_{12} & \cdots\cdots & [kyz]_{1m} \\ [kyz]_{21} & [kyz]_{22} & \cdots\cdots & [kyz]_{2m} \\ \cdots\cdots & \cdots\cdots & \cdots\cdots & \cdots\cdots \\ \cdots\cdots & \cdots\cdots & \cdots\cdots & \cdots\cdots \\ [kyz]_{m1} & [kyz]_{m2} & \cdots\cdots & [kyz]_{mm} \end{bmatrix} \begin{vmatrix} \overline{w}_1 \\ \overline{w}_2 \\ \cdots \\ \cdots \\ \overline{w}_m \end{vmatrix} \qquad (2.8)$$

Each of the individual sub-matrices $[kyz]_{ij}$ is of the order n x n, where n and m are as defined before.

Since the moments due to a unit displacement at any joint O will be limited to the two neighboring joints, E and W, then $[kyz]_{ij} = [0]$ for $i \neq j$, and [Kyz] can be written as

$$[Kyz] = \begin{bmatrix} [kyz]_{11} & & & & \\ & [kyz]_{22} & & & \\ & & \cdots\cdots & & \\ & & & \cdots\cdots & \\ & & & & [kyz]_{mm} \end{bmatrix} \qquad (2.8')$$

If the stiffnesses of the horizontal webs are the same, and the vertical webs are equally spaced,

$$[Kyz] = \begin{bmatrix} [Ayz] & & & & \\ & [Ayz] & & & \\ & & \cdots & & \\ & & & \cdots & \\ & & & & [Ayz] \end{bmatrix}$$

where, from the stiffness matrix of the web element,

$$[Ayz] = \begin{bmatrix} {}^{h}Kw_4 & -{}^{h}Kw_4 & & & \\ -{}^{h}Kw_4 & {}^{h}Kw_4 & & & \\ & 0 & {}^{h}Kw_4 & & \\ & \cdots & \cdots & \cdots & \\ & & \cdots & \cdots & \cdots \\ & & & -{}^{h}Kw_4 & {}^{h}Kw_4 \end{bmatrix}$$

The superscript h refers to the horizontal webs as mentioned before.

2.4.4 <u>The Rotational Stiffness About the x-Axis for Rotations About the x-Axis Only, [Kxx]</u> -- The cover plates and the webs parallel to the y-axis contribute to this stiffness, while the webs parallel to the x-axis do not.

If the moment vector $\overline{Mx}$ is partitioned to a set of vectors $\overline{mx}_1 \ldots \overline{mx}_m$, where $\overline{mx}_i$ is the moment vector at the nodal points of the i-th horizontal grid line (see Figure 6), and the rotation vector $\overline{\theta x}$ is partitioned in the same manner, then [Kxx] will be arranged to agree with the equation:

$$\begin{vmatrix} \overline{mx}_1 \\ \overline{mx}_2 \\ \cdots \\ \cdots \\ \overline{mx}_m \end{vmatrix} = \begin{bmatrix} [kxx]_{11} & [kxx]_{12} & \cdots\cdots & [kxx]_{1m} \\ [kxx]_{21} & [kxx]_{22} & \cdots\cdots & [kxx]_{2m} \\ \cdots\cdots & \cdots\cdots & \cdots\cdots & \cdots\cdots \\ \cdots\cdots & \cdots\cdots & \cdots\cdots & \cdots\cdots \\ [kxx]_{m1} & [kxx]_{m2} & \cdots\cdots & [kxx]_{mm} \end{bmatrix} \begin{vmatrix} \overline{\theta x}_1 \\ \overline{\theta x}_2 \\ \cdots \\ \cdots \\ \overline{\theta x}_m \end{vmatrix} \qquad (2.9)$$

Each of the individual sub-matrices $[kxx]_{ij}$ is of the order n x n.

Since the moments due to a unit rotation at any joint O will be limited to the 8 neighboring joints, N,NE,E,SE,S,SW,W, and NW (see Figure 6), then $[kxx]_{ij} = [0]$, for $i < j - 1$ or $i > j + 1$; moreover, all non-zero sub-matrices are tridiagonal matrices. Now [Kxx] can be written as:

$$[Kxx] = \begin{bmatrix} [kxx]_{11} & [kxx]_{12} & & & & \\ [kxx]_{21} & [kxx]_{22} & [kxx]_{23} & & & \\ & \cdots\cdots & \cdots\cdots & \cdots\cdots & & \\ & & \cdots\cdots & \cdots\cdots & \cdots\cdots & \\ & & & [kxx]_{m,m-1} & [kxx]_{mm} \end{bmatrix} \qquad (2.9')$$

[Kxx] is symmetrical from Maxwell's reciprocal theorem. If the horizontal webs are equally spaced, and if the vertical webs have the same stiffness and are equally spaced, and if the thickness of the cover plates is uniform then

$$[Kxx] = \begin{bmatrix} [Axx] & [Bxx] & & & & \\ [Bxx]^T & [Cxx] & [Bxx] & & & \\ & \cdots & \cdots & \cdots & & \\ & & \cdots & \cdots & \cdots & \\ & & & [Bxx]^T & [Axx] \end{bmatrix}$$

where, from the stiffness matrix of the cover plate element, and from the stiffness matrix of the web element,

$$[Axx] = \begin{bmatrix} (K\overset{v}{w}_1+Kc_1) & (Kc_2) & & \\ (Kc_2) & (K\overset{v}{w}_1+2Kc_1) & (Kc_2) & \\ & \cdots\cdots & \cdots\cdots & \cdots\cdots \\ & & (Kc_2) & (K\overset{v}{w}_1+Kc_1) \end{bmatrix},$$

$$[Bxx] = \begin{bmatrix} (K\overset{v}{w}_2+Kc_3) & (Kc_4) & & \\ (Kc_4) & (K\overset{v}{w}_2+2Kc_3) & (Kc_4) & \\ & \cdots\cdots & \cdots\cdots & \cdots\cdots \\ & & (Kc_4) & (K\overset{v}{w}_2+Kc_3) \end{bmatrix}, \text{ and}$$

$$[Cxx] = \begin{bmatrix} (2K\overset{v}{w}_1+2Kc_1) & (2Kc_2) & & \\ (2Kc_2) & (2K\overset{v}{w}_1+4Kc_1) & (2Kc_2) & \\ & \cdots\cdots & \cdots\cdots & \cdots\cdots \\ & & (2Kc_2) & (2K\overset{v}{w}_1+2Kc_1) \end{bmatrix}$$

2.4.5 The Rotational Stiffness About the y-Axis for Rotations About the y-Axis Only, [Kyy] -- The cover plates and the webs parallel to the x-axis contribute to this stiffness, while the webs parallel to the y-axis do not.

If the moment vector $\overline{My}$ is partitioned to a set of vectors $\overline{my}_1 \ldots \overline{my}_m$, where $\overline{my}_i$ is the moment vector at the nodal points of the i-th horizontal grid line (see Figure 6), and the rotation vector $\overline{\Theta y}$ is partitioned in the same manner, then [Kyy] will be arranged to agree with the equation:

$$\begin{vmatrix} \overline{my}_1 \\ \overline{my}_2 \\ \cdots \\ \cdots \\ \overline{my}_m \end{vmatrix} = \begin{bmatrix} [kyy]_{11} & [kyy]_{12} & \cdots\cdots & [kyy]_{1m} \\ [kyy]_{21} & [kyy]_{22} & \cdots\cdots & [kyy]_{2m} \\ \cdots\cdots & \cdots\cdots & \cdots\cdots & \cdots\cdots \\ \cdots\cdots & \cdots\cdots & \cdots\cdots & \cdots\cdots \\ [kyy]_{m1} & [kyy]_{m2} & \cdots\cdots & [kyy]_{mm} \end{bmatrix} \begin{vmatrix} \overline{\theta y}_1 \\ \overline{\theta y}_2 \\ \cdots \\ \cdots \\ \overline{\theta y}_m \end{vmatrix} \qquad (2.10)$$

Each of the individual sub-matrices $[kyy]_{ij}$ is of the order n x n.

Since the moments due to a unit rotation at any joint O will be limited to the 8 neighboring joints N,NE,E,SE,S,SW,W, and NW (see Figure 6), then $[kyy]_{ij} = [0]$, for $i < j - 1$ or $i > j + 1$; moreover, all non-zero sub-matrices are tri-diagonal matrices. Now [Kyy] can be written

$$[Kyy] = \begin{bmatrix} [kyy]_{11} & [kyy]_{12} & & & \\ [kyy]_{21} & [kyy]_{22} & [kyy]_{23} & & \\ & \cdots\cdots & \cdots\cdots & \cdots\cdots & \\ & & \cdots\cdots & \cdots\cdots & \cdots\cdots \\ & & & [kyy]_{m,m-1} & [kyy]_{mm} \end{bmatrix} \qquad (2.10')$$

[Kyy] is symmetrical from Maxwell's reciprocal theorem. If the vertical webs are equally spaced, and the stiffnesses of the horizontal webs are the same, and they are equally spaced, and if the thickness of the cover plates is uniform, then

$$[Kyy] = \begin{bmatrix} [Ayy] & [Byy] & & & \\ [Byy]^T & [Cyy] & [Byy] & & \\ & \cdots & \cdots & \cdots & \\ & & \cdots & \cdots & \cdots \\ & & & [Byy]^T & [Ayy] \end{bmatrix}$$

where, from the stiffness matrix of the cover plate element, and the stiffness matrix of the web element,

$$[Ayy] = \begin{bmatrix} (K\overset{h}{w}_1+Kc_5) & (K\overset{h}{w}_2+Kc_6) & & \\ (K\overset{h}{w}_2+Kc_6) & (2K\overset{h}{w}_1+2Kc_5) & (Kw_2^h+Kc_6) & \\ & \cdots\cdots & \cdots\cdots & \cdots\cdots \\ & & (Kw_2^h+Kc_6) & (Kw_1^h+Kc_5) \end{bmatrix},$$

$$[Byy] = \begin{bmatrix} Kc_7 & Kc_8 & & \\ Kc_8 & 2Kc_7 & Kc_8 & \\ & \cdots & \cdots & \cdots \\ & & Kc_8 & Kc_7 \end{bmatrix} \text{ and}$$

$$[Cyy] = \begin{bmatrix} (K\overset{h}{w}_1+2Kc_5) & (K\overset{h}{w}_2+2Kc_6) & & \\ (K\overset{h}{w}_2+2Kc_6) & (2K\overset{h}{w}_1+4Kc_5) & (Kw_2^h+2Kc_6) & \\ & \cdots\cdots & \cdots\cdots & \cdots\cdots \\ & & (Kw_2^h+2Kc_6) & (Kw_1^h+2Kc_5) \end{bmatrix}$$

2.4.6 The Rotational Stiffness About the x-Axis for Rotations About the y-Axis Only, [Kxy] -- Only the cover plates contribute to this matrix; webs do not.

If the moment vector $\overline{Mx}$, and the rotation vector $\overline{\Theta y}$ are partitioned as before, then [Kxy] will be arranged to agree with the equation:

$$\begin{vmatrix} \overline{mx}_1 \\ \overline{mx}_2 \\ \cdots \\ \cdots \\ \overline{mx}_m \end{vmatrix} = \begin{bmatrix} [kxy]_{11} & [kxy]_{12} & \cdots\cdots & [kxy]_{1m} \\ [kxy]_{21} & [kxy]_{22} & \cdots\cdots & [kxy]_{2m} \\ \cdots\cdots & \cdots\cdots & \cdots\cdots & \cdots\cdots \\ \cdots\cdots & \cdots\cdots & \cdots\cdots & \cdots\cdots \\ [kxy]_{m1} & [kxy]_{m2} & \cdots\cdots & [kxy]_{mm} \end{bmatrix} \begin{vmatrix} \overline{\theta y}_1 \\ \overline{\theta y}_2 \\ \cdots \\ \cdots \\ \overline{\theta y}_m \end{vmatrix} \qquad (2.11)$$

Each of the individual sub-matrices $[kxy]_{ij}$ is of the order n x n.

Since the moments which arise due to a unit rotation at any joint 0 will be limited to the 8 neighboring joints N,NE,E,SE,S,SW,W, and NW (see Figure 6), then [Kxy] is a tri-diagonal matrix, and can be written as:

$$[Kxy] = \begin{bmatrix} [kxy]_{11} & [kxy]_{12} & & & \\ [kxy]_{21} & [kxy]_{22} & [kxy]_{23} & & \\ & \cdots\cdots & \cdots\cdots & \cdots\cdots & \\ & & \cdots\cdots & \cdots\cdots & \cdots\cdots \\ & & & [kxy]_{m,m-1} & [kxy]_{mm} \end{bmatrix} \qquad (2.11')$$

From the symmetry of the cover plate element, and according to the adopted moment and rotation sign convention, $[kxy]_{ij} = -[kxy]^T_{ji}$. If the horizontal webs are equally spaced and the vertical webs are equally spaced also, and if the thickness of the cover plates is uniform, then

$$[Kxy] = \begin{bmatrix} [Axy] & [Bxy] & & & \\ -[Bxy]^T & [\ 0\ ] & [Bxy] & & \\ & \cdots & \cdots & \cdots & \\ & & \cdots & \cdots & \cdots \\ & & & -[Bxy]^T & -[Axy] \end{bmatrix}$$

where, from the stiffness matrix of the cover plate element,

$$[Axy] = \begin{bmatrix} -Kc_9 & Kc_{10} & & & & \\ -Kc_{10} & 0 & Kc_{10} & & & \\ & \cdots & \cdots & \cdots & & \\ & & \cdots & \cdots & \cdots & \\ & & & -Kc_{10} & Kc_9 \end{bmatrix}, \text{ and}$$

$$[Bxy] = \begin{bmatrix} -Kc_{10} & Kc_9 & & & & \\ -Kc_9 & 0 & Kc_9 & & & \\ & \cdots & \cdots & \cdots & & \\ & & \cdots & \cdots & \cdots & \\ & & & -Kc_9 & Kc_{10} \end{bmatrix}$$

2.5 Boundary (Support) Conditions

In the derivation of the stiffness matrix, nothing was mentioned about the support conditions. The stiffness matrix just derived is a singular matrix. The physical significance of this is that rigid-body displacements can occur. In this analysis we are involved with geometrical boundary condition, i.e., the displacements or rotations are prevented at some joints on the boundary. This corresponds to zero displacements and/or rotations at those points. Hence some deformations (displacements and/or rotations) are equal to zero at some boundary joints; we may thus eliminate the columns in the stiffness matrix corresponding to these deformations. Furthermore, the loads (forces and/or moments) corresponding to these deformations are completely dependent on the other quantities, so we

can solve for the other quantities without reference to the loads corresponding to zero deformations. Then, to impose the desired support conditions, we delete columns for which zero deformations have been specified and the corresponding rows in the stiffness matrix. This will reduce the order of the matrix and make it non-singular, if sufficient support to prevent rigid body motion is provided.

In the dock-gate analysis, the support conditions are equivalent to zero deflections (in the z-direction) at the joints on three sides of the boundary (the two sidewalls and the bottom sill).

2.6 The Flexibility Matrix

The stiffness matrix [K] specifies the values of the joint load components (force or moment) which are caused by unit values of joint deformation components (deflection or rotation). Since our problem involves analyses of the effects of given loads rather than given deformations, it would be desirable to have a matrix which specifies the values of the joint deformation components caused by unit values of joint load components. Such a matrix is the "flexibility matrix," the inverse of the stiffness matrix.

The order of the stiffness matrix before imposing the boundary conditions is $(3mn) \times (3mn)$, and after imposing the boundary conditions, it reduces to $[3mn - (2m+n-2)] \times [3mn - (2m+n-2)]$, where $(2m+n-2)$ corresponds to the number of boundary joints with zero

deflections. Now if we have, for example, 20 horizontal webs and 20 vertical webs, then the order of the stiffness matrix is 1142 x 1142. Inverting such a high-order matrix is a major problem, necessitating the use of digital computing equipment. However, difficulties arise with respect to time and memory requirements. Two possible approaches to avoid these difficulties will be outlined here.

2.7 The First Approach

The analysis can be made without inverting the whole matrix, since the applied moments at the joints are zero. If we partition the load vector to force and moment vectors, and the deformation vector to deflection and rotation vectors, then the relation between joint loads and deformations may be written in the form:

$$\begin{vmatrix} \bar{R} \\ \bar{M} \end{vmatrix} = \begin{bmatrix} [k11] & [k12] \\ [k21] & [k22] \end{bmatrix} \begin{vmatrix} \bar{w} \\ \bar{\theta} \end{vmatrix} \tag{2.12}$$

We want the flexibility matrix [F], such that

$$\begin{vmatrix} \bar{w} \\ \theta \end{vmatrix} = \begin{bmatrix} [F11] & [F12] \\ [F21] & [F22] \end{bmatrix} \begin{vmatrix} \bar{R} \\ \bar{M} \end{vmatrix}$$

However, since $\bar{M} = \bar{0}$, we need only to evaluate [F11] and [F21]. Of course $[F12] = [F21]^T$, from Maxwell's reciprocal theorem. We have no need to evaluate [F22].

From Equation (2.12)

$$\bar{R} = [k11]\ \bar{w} + [k12]\ \bar{\theta} \tag{2.12a}$$

$$\bar{M} = [k21]\ \bar{w} + [k22]\ \bar{\theta} \tag{2.12b}$$

From equilibrium considerations,

$\bar{R}$ = Applied lateral loads

$\bar{M} = \bar{0}$ (No applied moments)

From Equation (2.12b) and using $\bar{M} = \bar{0}$, we can express $\bar{\theta}$ in terms of $\bar{w}$, i.e.,

$$\bar{\theta} = -[k22]^{-1}\,[k21]\,\bar{w} \tag{2.13}$$

Now we can express $\bar{R}$ in terms of $\bar{w}$, by substituting for $\bar{\theta}$ from Equation (2.13) into Equation (2.12a), then

$$\bar{R} = [k11]\,\bar{w} - [k12]\,[k22]^{-1}[k21]\,\bar{w}$$

$$= ([k11] - [k12]\,[k22]^{-1}\,[k21]\,)\bar{w}$$

or

$$\bar{R} = [k0]\,\bar{w} \tag{2.14}$$

[k0] expresses the forces caused by unit displacements, so we can invert [k0] to obtain a matrix [F11] which expresses the displacements caused by unit forces, i.e.,

$$\bar{w} = [k0]^{-1}\,\bar{R}$$

$$= [F11]\;\bar{R} \tag{2.15}$$

Now we can substitute $\bar{w}$ from Equation (2.15) into Equation (2.13) to determine $\bar{\theta}$. Then

$$\bar{\theta} = -[k22]^{-1}\,[k21][F11]\bar{R}$$

or

$$\bar{\theta} = [F21]\,\bar{R}$$

where [F21] expresses the rotations caused by unit forces. The procedure just discussed avoids the inversion of a matrix of the order $(3mn-2m-n+2) \times (3mn-2m-n+2)$, it includes two inversions of matrices of the order $2mn \times 2mn$ and $(mn-2m-n+2) \times (mn-2m-n+2)$.

Although the above method was derived for the case where the moment part of the load vector is specified to be zero, it could be applied for the general case (no part of the load vector is specified to be zero) as follows:

1. Divide the joints into two groups.
2. Load the first group of joints only, and determine the deformations at all the joints due to these loads from the above procedure.
3. Load the second group of joints only, and determine the deformations at all the joints due to these loads from the above procedure.
4. Add the deformations from Steps 2 and 3.

Of course this procedure will be very efficient if we divide the joints to two groups which are symmetrical about an axis of symmetry in the structure (if there is one). In such a case Step 3 is not needed, since it can be deduced from Step 2 from the symmetry.

2.8 The Second Approach

If the load (forces and moments) vector $\overline{L}$ is partitioned to a set of vectors $\overline{\ell}_1 \ldots \overline{\ell}_m$, where $\overline{\ell}_i$ is the load vector at the nodal points of the i-th horizontal grid-line, and the deformation vector $\overline{D}$ is partitioned in the same manner, and since the load vector $\overline{\ell}_i$ arising at the nodal points of the i-th horizontal grid-line is caused by the deformation vectors $\overline{d}_{(i-1)}$, $\overline{d}_i$, and $\overline{d}_{(i+1)}$ only, the stiffness matrix is arranged to agree with:

$$\begin{vmatrix} \bar{\ell}_1 \\ \bar{\ell}_2 \\ .. \\ .. \\ \bar{\ell}_m \end{vmatrix} = \begin{bmatrix} [k]_{11} & [k]_{12} & & & & \\ [k]_{21} & [k]_{22} & [k]_{23} & & & \\ & \cdots & \cdots & \cdots & & \\ & & \cdots & \cdots & \cdots & \\ & & & [k]_{m,m-1} & [k]_{mm} & \end{bmatrix} \begin{vmatrix} \bar{d}_1 \\ \bar{d}_2 \\ .. \\ .. \\ \bar{d}_m \end{vmatrix} \qquad (2.16)$$

If the stiffnesses of the horizontal webs are the same, and they are equally spaced, and if the stiffnesses of the vertical webs are the same and they are equally spaced, and if also the cover plates have uniform thickness, Equation (2.16) can be written as:

$$\begin{vmatrix} \bar{\ell}_1 \\ \bar{\ell}_2 \\ .. \\ .. \\ \bar{\ell}_m \end{vmatrix} = \begin{bmatrix} [A] & [B] & & & \\ [B]^T & [C] & [B] & & \\ & \cdot & \cdot & \cdot & \\ & \cdot & \cdot & \cdot & \cdot \\ & & & [B]^T & [D] \end{bmatrix} \begin{vmatrix} \bar{d}_1 \\ \bar{d}_2 \\ .. \\ .. \\ \bar{d}_m \end{vmatrix} \qquad (2.16')$$

where

$$[A] = \begin{bmatrix} [Azz] & -[Bxz]^T & [Ayz]^T \\ [Bxz] & [Axx] & [Axy] \\ [Ayz] & [Axy]^T & [Ayy] \end{bmatrix},$$

$$[B] = \begin{bmatrix} [Bzz] & -[Bxz] & [\ 0\ ] \\ [Bxz] & [Bxx] & [Bxy] \\ [\ 0\ ] & -[Bxy] & [Byy] \end{bmatrix},$$

$$[C] = \begin{bmatrix} [Czz] & [\ 0\ ] & [Ayz]^T \\ [\ 0\ ] & [Cxx] & [\ 0\ ] \\ [Ayz] & [\ 0\ ] & [Cyy] \end{bmatrix}, \text{ and}$$

$$[D] = \begin{bmatrix} [Azz] & [Bxz]^T & [Ayz]^T \\ [Bxz] & [Axx] & -[Axy] \\ [Ayz] & -[Axy]^T & [Ayy] \end{bmatrix} .$$

Imposing the boundary conditions by deleting the columns corresponding to zero deflections and the corresponding rows in the stiffness matrix as mentioned before, Equation (2.16') will be:

$$\begin{Vmatrix} \overline{\ell l}_1 \\ \overline{\ell l}_2 \\ \cdots \\ \cdots \\ \overline{\ell l}_m \end{Vmatrix} = \begin{bmatrix} [A1] & [B1] & & & & \\ [B1]^T & [C1] & [B1] & & & \\ & \cdot\cdot & \cdot\cdot & \cdot\cdot & & \\ & & \cdot\cdot & \cdot\cdot & \cdot\cdot & \\ & & & [B2]^T & [D1] & \end{bmatrix} \begin{Vmatrix} \overline{dl}_1 \\ \overline{dl}_2 \\ \cdots \\ \cdots \\ \overline{dl}_m \end{Vmatrix} \qquad (2.16")$$

where [A1], [B1], [C1] are of the order (3n-2) x (3n-2), [B2] is of the order (3n-2) x (2n), and [D1] is of the order 2n x 2n. Equation (2.16") is equivalent to a set of linear algebraic equations in which only the diagonal coefficients immediately adjacent to the diagonal are non-zero. From Equation (2.16"),

$$\begin{aligned}
\overline{\ell l}_1 &= [A1]\,\overline{dl}_1 + [B1]\,\overline{dl}_2 && (1) \\
\overline{\ell l}_2 &= [B1]^T\overline{dl}_1 + [C1]\,\overline{dl}_2 + [B1]\,\overline{dl}_3 && (2) \\
\cdots &\quad \cdots\cdots\cdots\cdots\cdots\cdots\cdots\cdots\cdots\cdots && \\
\overline{\ell l}_i &= [B1]^T\overline{dl}_{i-1} + [C1]\,\overline{dl}_i + [B1]\,\overline{dl}_{i+1} && (i) \qquad (2.17) \\
\cdots &\quad \cdots\cdots\cdots\cdots\cdots\cdots\cdots\cdots\cdots\cdots && \\
\overline{\ell l}_{m-1} &= [B1]^T\overline{dl}_{m-2} + [C1]\,\overline{dl}_{m-1} + [B2]\,\overline{dl}_m && (m-1) \\
\overline{\ell l}_m &= [B2]^T\overline{dl}_{m-1} + [D1]\,\overline{dl}_m && (m)
\end{aligned}$$

The above set of equations is m equations in m unknowns, $\overline{dl}_1 \ldots \overline{dl}_m$. Let us rewrite the above set of equations in the following form:

$$
\begin{aligned}
\overline{dl}_1 &= -[A1]^{-1}[B1]\,\overline{dl}_2 + [A1]^{-1}\,\overline{\ell l}_1 && (1)\\
\overline{dl}_2 &= -[C1]^{-1}[B1]\,\overline{dl}_3 - [C1]^{-1}[B1]^T\,\overline{dl}_1 + [C1]^{-1}\,\overline{\ell l}_2 && (2)\\
\cdots &\quad \cdots\cdots\cdots\cdots \quad \cdots\cdots\cdots\cdots\cdots \quad \cdots\cdots\cdots\cdots && \\
\overline{dl}_i &= -[C1]^{-1}[B1]\,\overline{dl}_{i+1} - [C1]^{-1}[B1]^T\,\overline{dl}_{i-1} + [C1]^{-1}\,\overline{\ell l}_i && (i) \qquad (2.17')\\
\cdots &\quad \cdots\cdots\cdots\cdots \quad \cdots\cdots\cdots\cdots\cdots \quad \cdots\cdots\cdots\cdots && \\
\overline{dl}_{m-1} &= -[C1]^{-1}[B2]\,\overline{dl}_m - [C1]^{-1}[B1]^T\,dl_{m-2} + [C1]^{-1}\,\overline{\ell l}_{m-1} && (m-1)\\
\overline{dl}_m &= - [D1]^{-1}[B2]^T\,dl_{m-1} + [D1]^{-1}\,\overline{\ell l}_m && (m)
\end{aligned}
$$

Now let us use Equation (1) in the above set to eliminate $\overline{dl}_1$ from Equation (2), and then use Equation (2) to eliminate $\overline{dl}_2$ from Equation (3). If we proceed down the set, eliminating one equation from the next, we shall end with one equation in one unknown, namely, $\overline{dl}_m$. Now if we work backward, we get $\overline{dl}_{m-1}$ from $\overline{dl}_m$, and $\overline{dl}_{m-2}$ from $\overline{dl}_{m-1}$, and so on until we get $\overline{dl}_1$. To express this mathematically, let us define

$$
\begin{aligned}
\overline{U}_1 &= [A1]^{-1}\overline{\ell l}_1\\
[W_1] &= -[A1]^{-1}[B1]\\
[V_1] &= [C1] + [B1]^T[W_1]
\end{aligned}
$$

$$
\begin{aligned}
\overline{U}_2 &= [V_1]^{-1}\left|\ell l_2 - [B1]^T\,\overline{U}_1\right|\\
[W_2] &= -[V_1]^{-1}[B1]\\
[V_2] &= [C1] + [B1]^T[W_2]
\end{aligned}
$$

$$
\begin{aligned}
\overline{U}_i &= [V_{i-1}]^{-1}\left|\overline{\ell l}_i - [B1]^{-1}\overline{U}_{i-1}\right|\\
[W_i] &= -[V_{i-1}]^{-1}[B1]\\
[V_i] &= [C1] + [B1]^T[W_i]
\end{aligned}
$$

$$
\begin{aligned}
\overline{U}_{m-1} &= [V_{m-2}]^{-1}\left|\ell l_{m-1} - [B1]^T\,\overline{U}_{m-2}\right|\\
[W_{m-1}] &= -[V_{m-2}]^{-1}[B2].
\end{aligned}
$$

The above vectors and matrices can be determined successively. Now Equation (2.17') can be rewritten as:

$$\begin{aligned}
\overline{dl}_1 &= [W_1]\ \overline{dl}_2 + \overline{U}_1 \\
\overline{dl}_2 &= [W_2]\ \overline{dl}_3 + \overline{U}_2 \\
&\cdots \qquad \cdots\cdots\cdots\cdots\cdots \\
\overline{dl}_i &= [W_i]\ \overline{dl}_{i+1} + \overline{U}_i \qquad (2.17'') \\
&\cdots \qquad \cdots\cdots\cdots\cdots\cdots \\
\overline{dl}_{m-1} &= [W_{m-1}]\ \overline{dl}_m + \overline{U}_{m-1}
\end{aligned}$$

Substitute $\overline{dl}_{m-1}$ in the last equation of (2.17'), and notice that $\overline{\ell l}_m = \overline{0}$ (no applied moments). Then

$$\overline{dl}_m = -\left[[B2]^T[W_{m-1}] + [D1]\right]^{-1} [B2]^T\, \overline{U}_{m-1} \qquad (2.18)$$

Equation (2.18) gives $\overline{dl}_m$. Knowing the deformations at the bottom grid line (rotations about the x- and the y-axes), we can go backward in Equation (2.17") to determine $\overline{dl}_{m-1} \cdots \overline{dl}_1$, respectively.

It has to be noticed that this approach does not produce the flexibility matrix, it only solves the equations.

2.9 Stress Calculations

2.9.1 The Covers -- From $\overline{\theta x}$, $\overline{\theta y}$ known from the previous calculations,

$$\begin{aligned}
\overline{rx} &= \overline{\theta y}\ h/2 \\
\overline{ry} &= \overline{\theta x}\ h/2
\end{aligned}$$

where $\overline{rx}$, $\overline{ry}$ are the displacements in the x- and the y-directions, respectively. From the derivation of the stiffness matrix of the plane stress plate element (see Appendix I),

$$\bar{\sigma} = [B][A]^{-1}\bar{V} \qquad \text{(see Appendix I, Equation (A-4))}$$

and $\bar{V} = [a]\bar{r}$.

Then

$$\bar{\sigma} = [B][A]^{-1}[a]\bar{r}$$

If we invert [A], and do the multiplications, we get

$$\bar{\sigma} = [T]\bar{r}$$

where

$$[T] = E\begin{bmatrix} -(t_1+t_5) & t_3 & (t_1+t_5) & t_3 & (t_1-t_5) & -t_3 & -(t_1-t_5) & -t_3 \\ -t_4 & (t_2-t_6) & t_4 & (t_2+t_6) & t_4 & -(t_2+t_6) & -t_4 & -(t_2-t_6) \\ t_8 & -t_7 & t_8 & t_7 & -t_8 & t_7 & -t_8 & -t_7 \end{bmatrix}$$

where

$$t_1 = 1/2b(1-\nu^2), \quad t_3 = \nu/2a(1-\nu^2), \quad t_5 = y/ba$$

$$t_2 = 1/2a(1-\nu^2), \quad t_4 = \nu/2b(1-\nu^2), \quad t_6 = x/ba$$

$$t_7 = 1/2b\lambda, \quad t_8 = 1/2a\lambda$$

$$\lambda = 2(1+\nu)$$

or

$$\sigma_x = \sum_{i=1}^{8} T_{1i}\, r_i ,$$

$$\sigma_y = \sum_{i=1}^{8} T_{2i}\, r_i , \quad \text{and}$$

$$\tau = \sum_{i=1}^{8} T_{3i}\, r_i .$$

2.9.2 Shear Stresses in the Webs -- The average shear stress

$$\tau = R/t_w h$$

where $R = -6EI(\theta_1+\theta_2)/L^2(1+4n) + 12EI(w_1-w_2)/L^3(1+4n)$.

III. ANALYSIS OF A SPECIFIC CASE

The finite-element analysis which has been explained in the previous chapter was applied to a dock gate with dimensions as shown in Figure 7, 160 feet wide, 50 feet deep, and 10 feet thick. Between the two cover plates, 11 horizontal webs spaced at 5 feet and 17 vertical webs spaced 10 feet apart are provided. The thickness of the cover plates as well as the webs is 0.5 inch.

To avoid buckling of the cover plates and the webs, stiffeners may have to be provided between the joints. The additional stiffness of these stiffeners is generally very small compared to the stiffness of the cover plates and the webs, so that it can be neglected. However, if it is not sufficiently small, they can be included.

The gate is made of steel; the modulus of elasticity is 29,000,000 psi, and Poisson's ratio is 0.3.

It is assumed that the side-walls and the bottom sill provide a simple support for three sides of the gate, i.e., the displacements in the z-direction are equal to zero on these three sides, and the fourth side is free.

Deformations at the joints, and stresses in the cover plates and the webs, due to water pressure on the full height of the gate, were calculated. The computations were done on the IBM 7090 electronic computer. The solution would involve the inversion of a matrix of the order 524 x 524; however, the second approach proposed in the previous

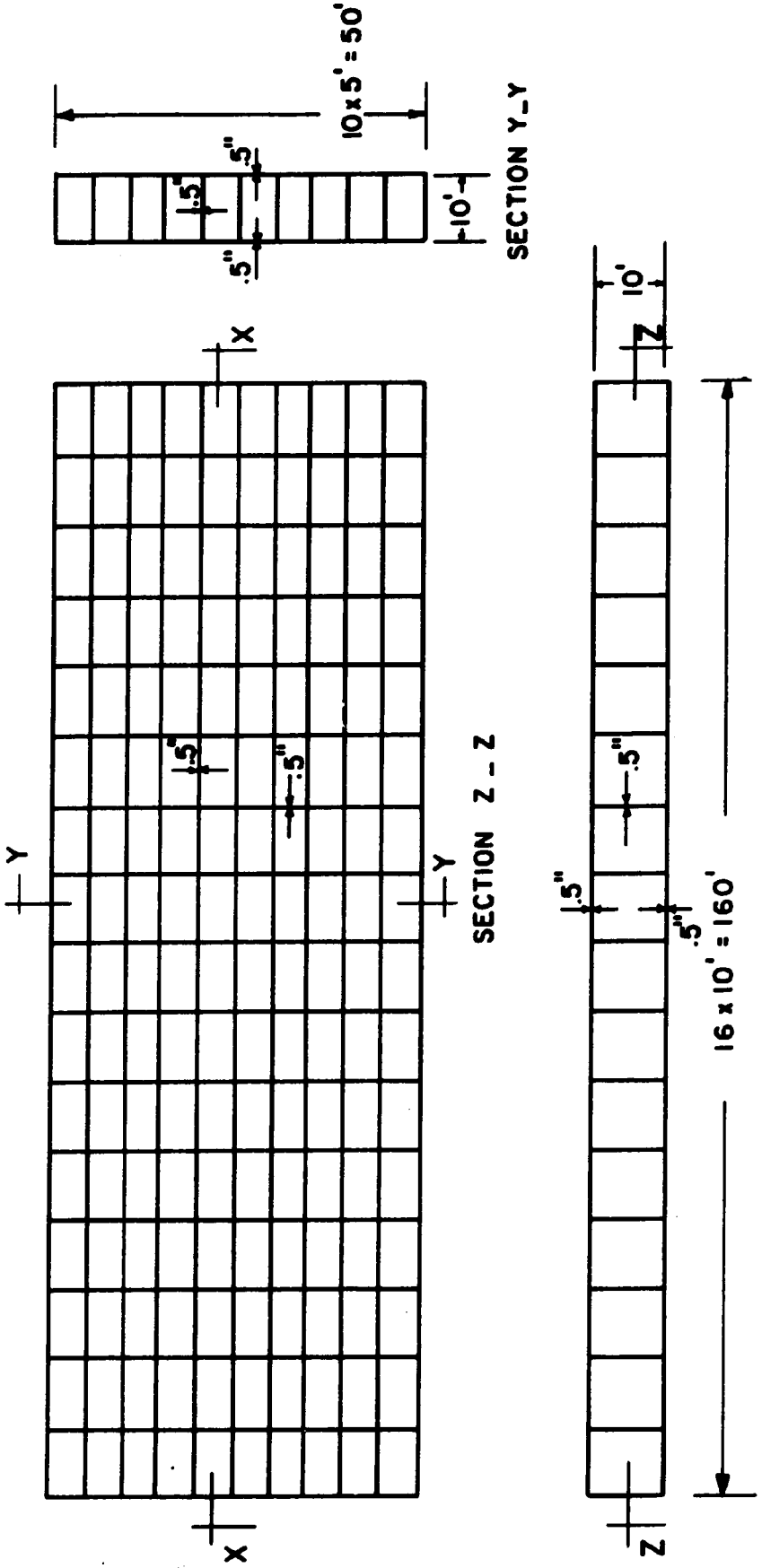


Figure 7. Dock-Gate Example Dimensions.

chapter was applied, and the highest order of a matrix inverted was 49 x 49. The bordering method[26] was used in the inversion. The results of the analysis are shown in Figures 8 through 14. The results shown represent two cases. In the first case, shear deformations of the webs were considered by substituting the appropriate value for "n"; however, in the second case, shear deformations of the webs were neglected by substituting zero for "n".

Since our structure is symmetrical and symmetrically loaded, only the results on half the structure are shown. The deflection curves considering shear deformations and neglecting it are shown by the solid and the dashed curves, respectively, in Figure 8. The error in the deflections because of neglecting shear deformations of the webs is more appreciable toward the support, as it should be.

The normal stresses σ_x (in the x-direction) in the cover plates are shown in Figure 9. Since σ_x are assumed not to vary in the x-direction within the element of the cover plate, it is assumed that these calculated values are representative of conditions along mid-sections of the elements as shown.

The stress discontinuities between elements is a natural result, since each element is stressed independently of its neighbors, and the gross continuity requirements which are satisfied only insure a general similarity of stresses in adjacent elements. However, the straight-line segments give very reasonable approximation of a smooth stress curve.

1 CM. = 5"

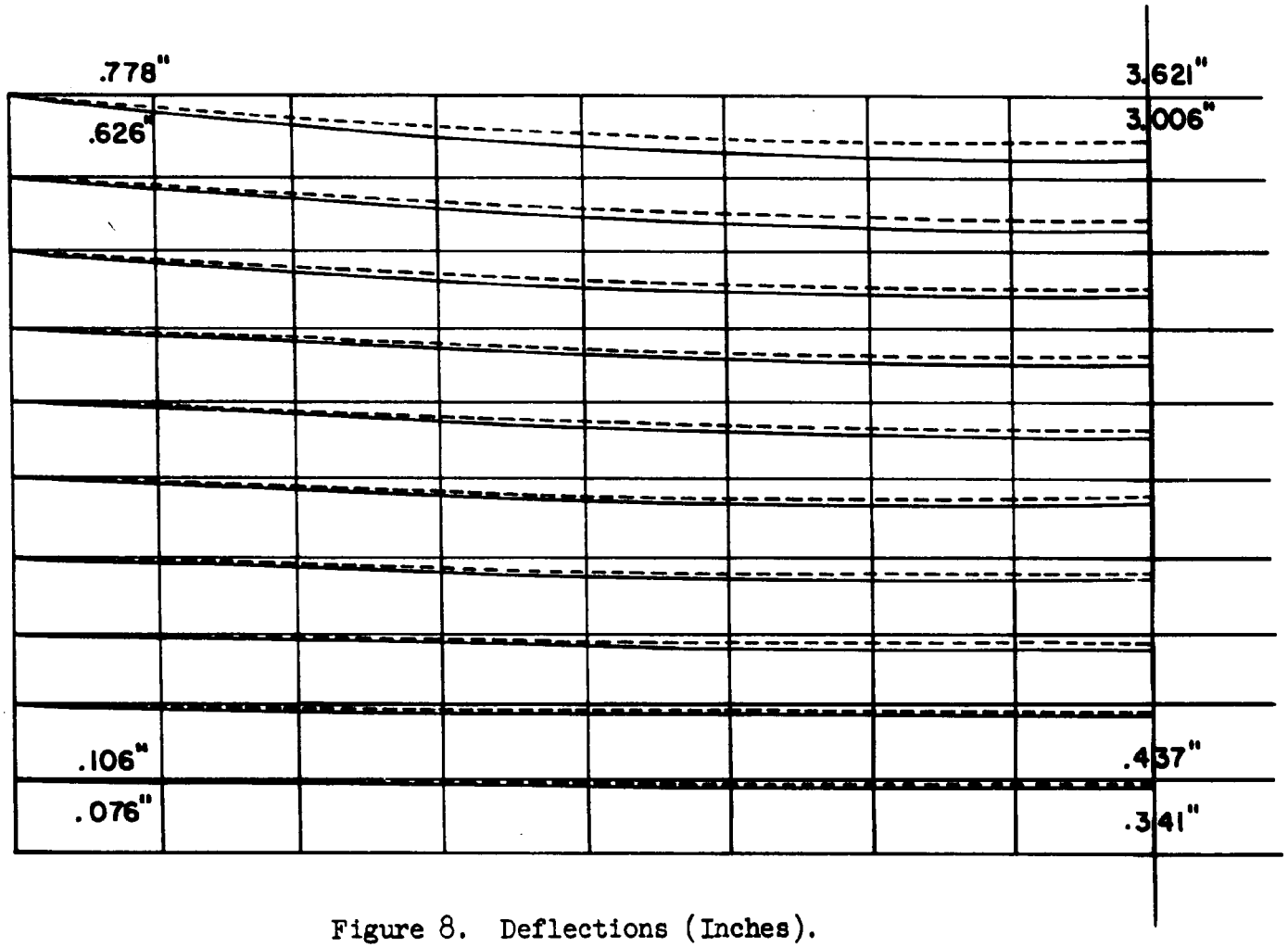


Figure 8. Deflections (Inches).

(Considering and Neglecting Shear Deformations).

—— Considering Shear Deformations of the Webs.
--- Neglecting Shear Deformations of the Webs.

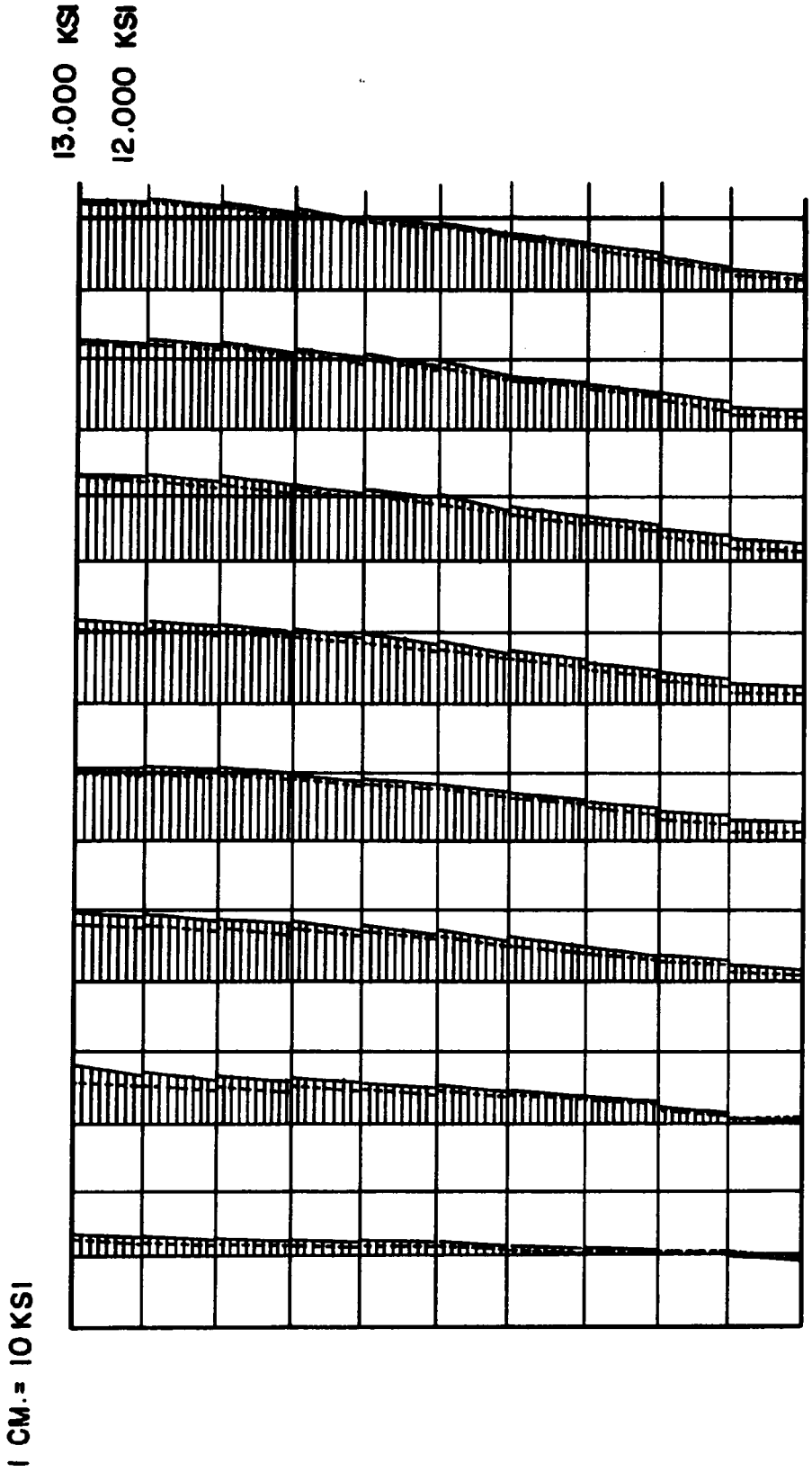


Figure 9. Normal Stresses in the Cover-Plate in the x-Direction KSI. (Considering and Neglecting Shear Deformations).

The normal stresses σ_y (in the y-direction) in the cover plates are shown in Figure 10. Again, since σ_y are assumed not to vary in the y-direction within the element of the cover plate, it is assumed that these calculated values are representative of conditions along mid-sections of the elements as shown. Stress discontinuities between elements are again not serious; the reason for these discontinuities as mentioned before, and the straight-line segments give a very reasonable approximation of a smooth stress curve.

Shear stresses τ_{yx} in the cover plates are shown in Figure 11. The shear stress was assumed to be constant within the element, so the calculated values are representative of conditions along mid-sections of the elements as mentioned before. Shear stresses τ_{xy} are equal to τ_{yx} and could be drawn as horizontal line segments through mid-sections of the elements.

Shear stresses in the web elements τ_{xz} and τ_{yz} which are constant within each web element are shown in Figures 12 and 13 respectively. The reactions at the boundary joints calculated both ways (considering and neglecting shear deformations of the webs) are shown in Figure 14.

The steps in the actual machine computation will not be detailed here. However, for the previous example the amount of time required by the IBM 7090 to carry out such computations was about 24 minutes.

To check the accuracy of the computations, the sum of the reactions was compared with the sum of the applied loads; the two sums are identical.

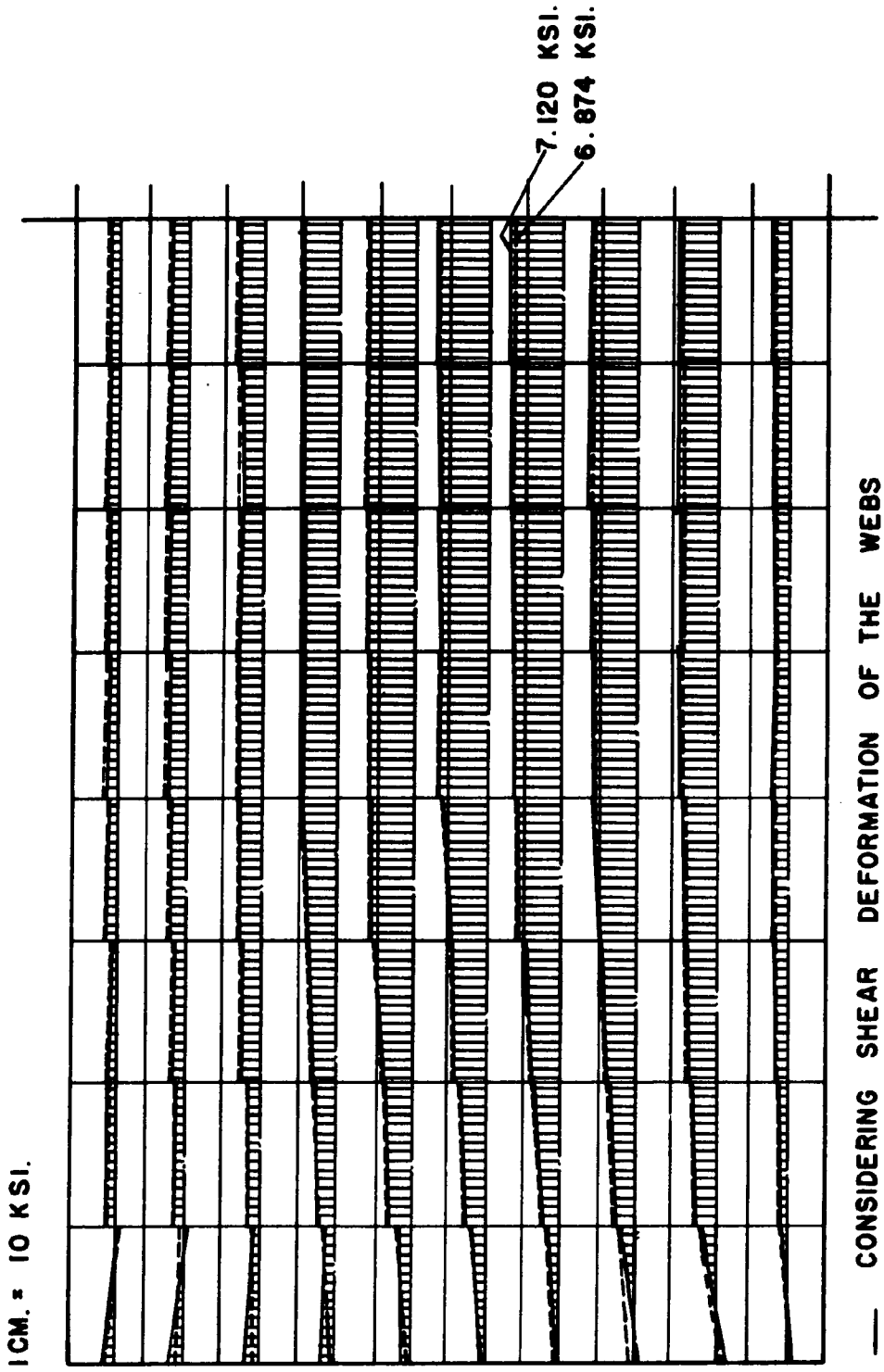


Figure 10. Normal Stresses in the Cover Plate in the y-Direction KSI.

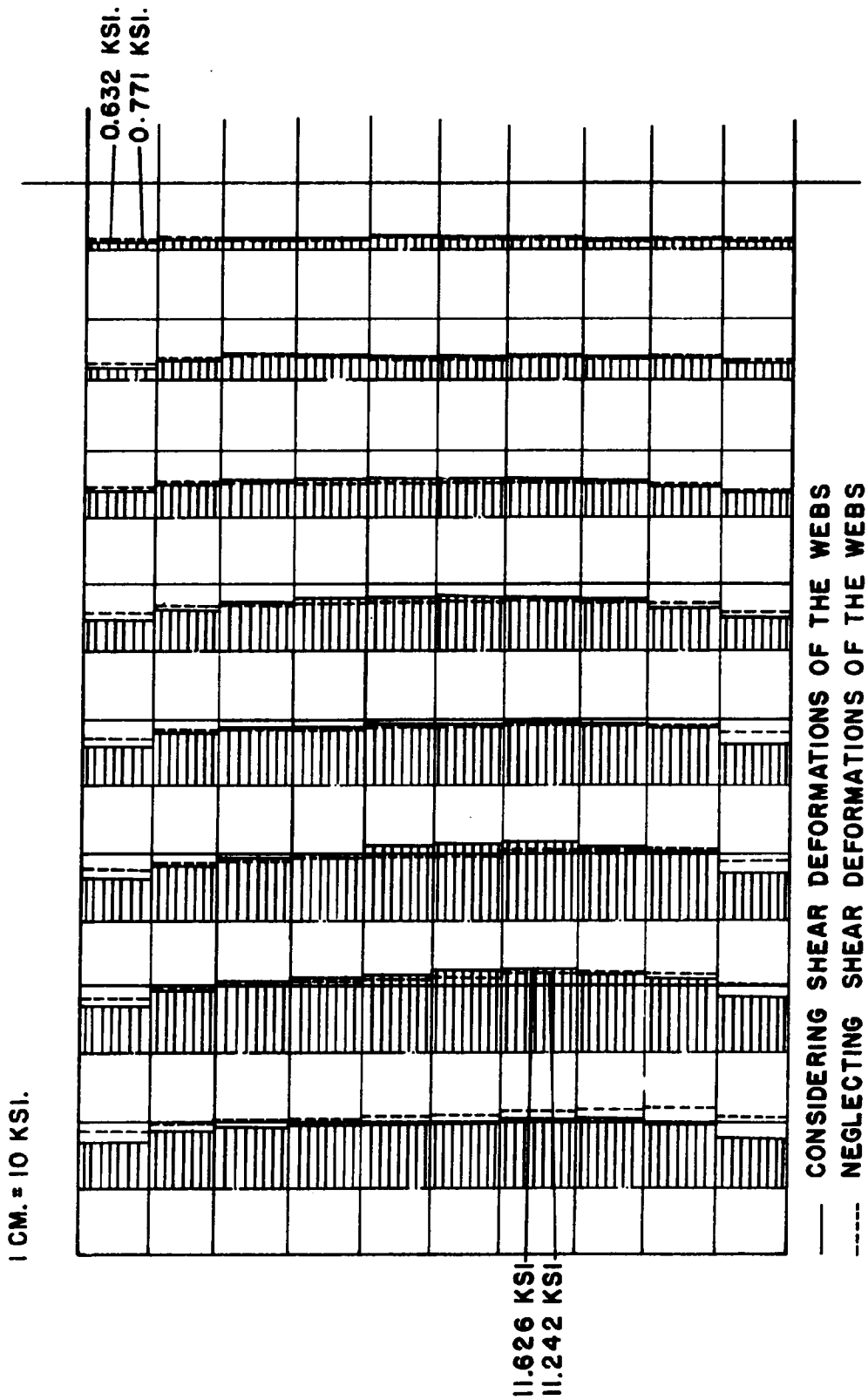


Figure 11. Shear Stresses in the Cover Plate τ_{yx} KSI.
(Considering and Neglecting Shear Deformations).

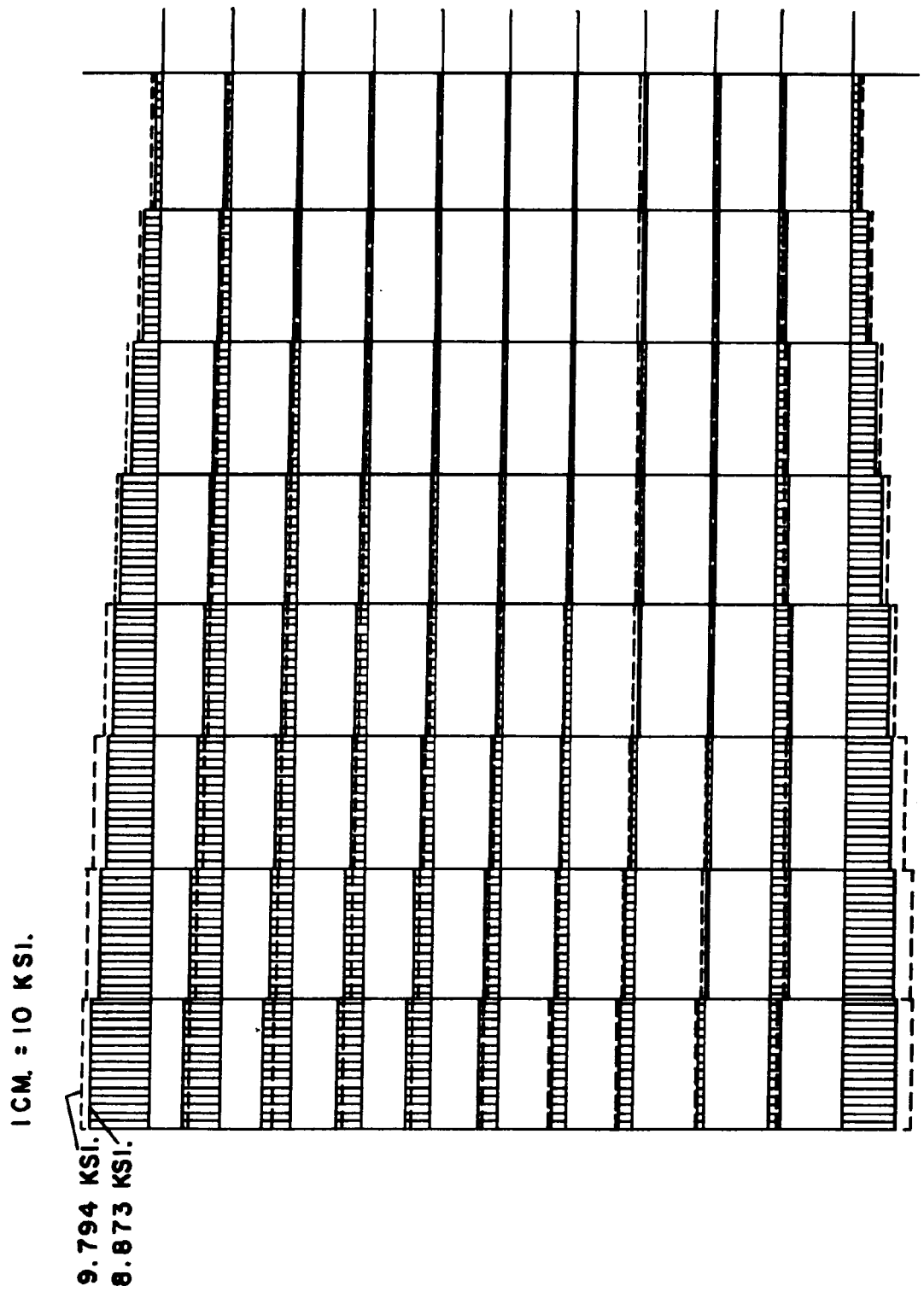


Figure 12. Shear Stresses in the Horizontal Webs, τ_{xz} KSI.

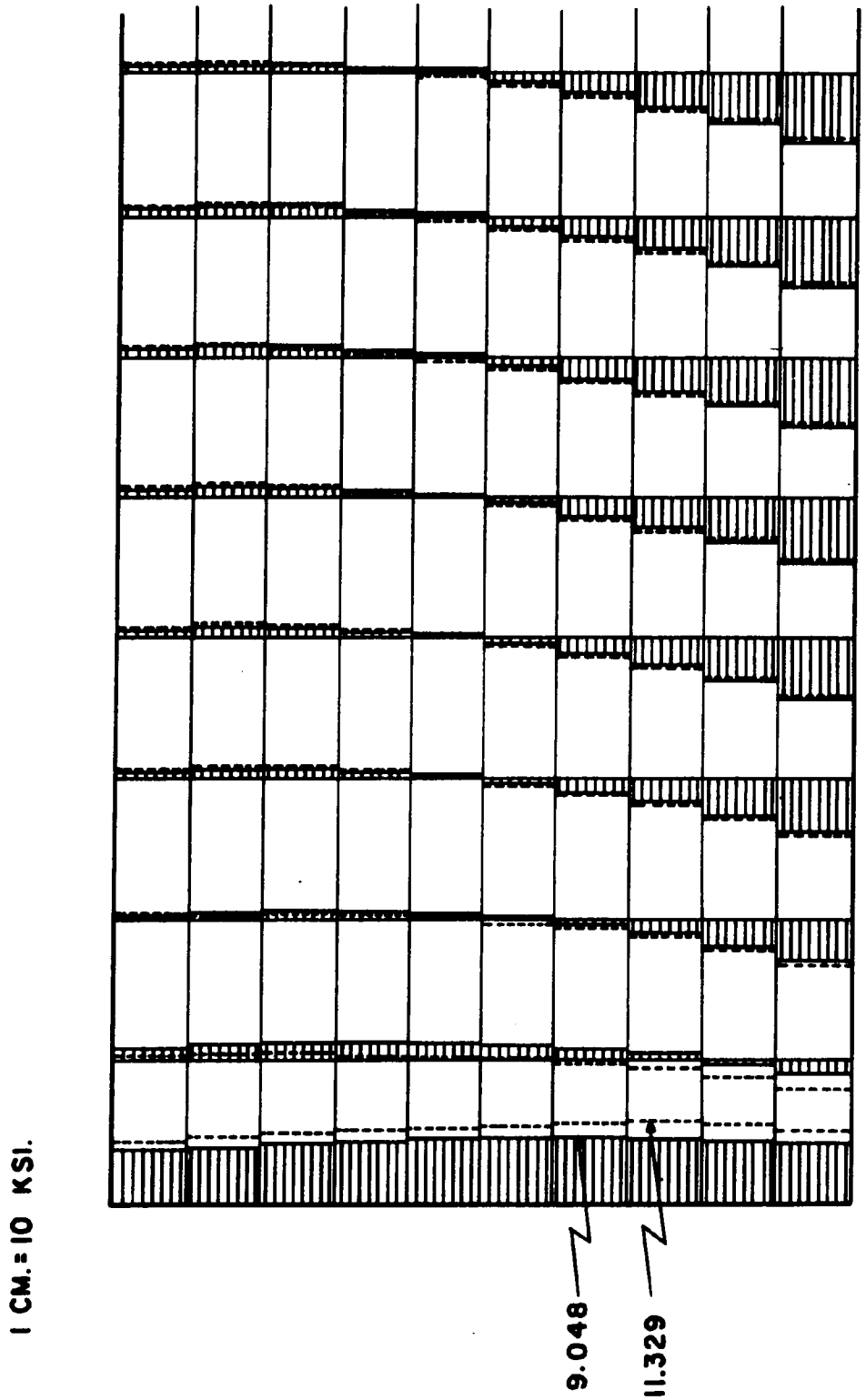


Figure 13. Shear Stresses in the Vertical Webs, τ_{yz} KSI.
(Considering and Neglecting Shear Deformations).

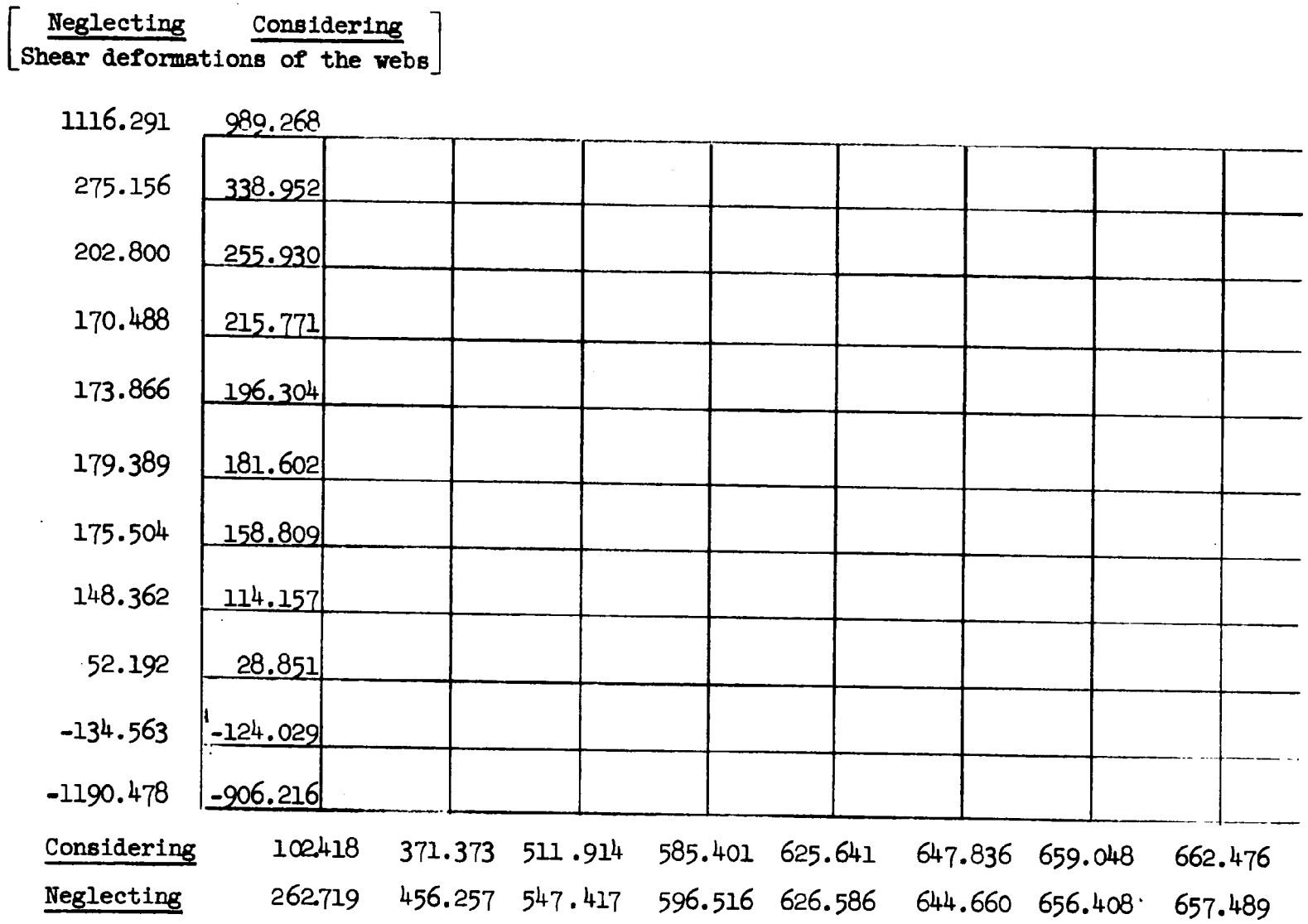


Figure 14. Reactions in Kips.

(Considering and Neglecting Shear Deformations)

In general, the results which we obtain are exact as long as our assumptions are valid.

All the assumptions except 6 and 7 in Chapter II are widely accepted in theory of structures. Assumptions 6 and 7 stated that the normal stresses σ_{xx} and σ_{yy} in the cover plates are varied linearly between the nodal points and that the shear stresses are uniform between the nodal points. So the results obtained will be accurate as long as the stress patterns assumed in the cover plates is reasonably representative of the actual stress patterns. However, in this method we calculate deflections from an approximated stress pattern. This in general gives better results than the ones from a method in which we calculate stresses from an approximated deflection pattern, since the first is in general an intergration process while the second is a differentiation process.

The size of the mesh provided by the actual spacing of the webs seems to be adequate for accurate answers in the previous example. However, if the webs are too widely spaced and too few, we can introduce further grid lines intermediate between the actual webs.

IV. EXPERIMENTAL ANALYSIS

As several simplifying assumptions were necessarily involved in the analytical solution, it seemed desirable to check the validity of these simplifying assumptions by experimental work on a small-scale celluloid model. The model, test procedure, and results will now be discussed.

4.1 Material Used

The use of plastic models is an attractive approach for the determination of deflections and stresses. Not only are such models inexpensive, but they can also be constructed quickly and tested with relatively simple experimental equipment. Although this saving in time and cost is probably obtained with some sacrifice of accuracy of results, it is believed that these disadvantages can be minimized by proper and careful testing.

Transparent cellulose acetate sheets of uniform thickness were used. They are available in sizes 20" x 50" in various gages.

4.2 Properties of the Material

The mechanical properties of the cellulose acetate sheets have been described by Celanese Corporation of America -- Plastics Division in their bulletin B-19 (September 15, 1959). Some useful information about fabricating the sheets was given in their bulletin B-11 (March 30, 1959). However, a simple tension test is necessary to determine the required information which is not available in the bulletin and to check the available information. A 24 inch long and

2 inch wide rectangular specimen was cut out of one of the four 50" x 20" x .06" sheets used to build the model. The specimen was reinforced with four 2" x 2" x .06" plates from the same material, which were cemented to it one on each side at both ends. A 1/4-inch hole was drilled with its center on the centerline of the specimen and at one inch from the end, for a 1/4-inch pin at one end; 1/8-inch hole was drilled at the similar location on the other end, for a 1/8-inch steel cable. The cable was passed over a pulley, and a hanger with a loading platform screwed to its end was suspended from the other end of the cable. The specimen was horizontal during the test. The test set-up was held by a 3/4-inch plywood platform which was attached to a rigid steel frame.

Two SR4-A7 strain gages were attached to one side of the specimen at the middle, one to measure the longitudinal strain and the other to measure the transverse strain. Figure 15 shows the test set-up.

The specimen was loaded gradually in tension by hanging about 140 lb., in seven nearly equal increments, from the cable. The specimen was loaded and unloaded three times. The longitudinal and transverse strains were recorded each time (see Figure 16). The specimen was tested also in an inverted position. The results did not show any appreciable change. The stress-strain curve shows a linear relation over the test range of loading, which corresponds to a maximum stress in the specimen of approximately 1350 psi. Care was taken not to exceed 1000 psi as a maximum normal stress when testing the model.

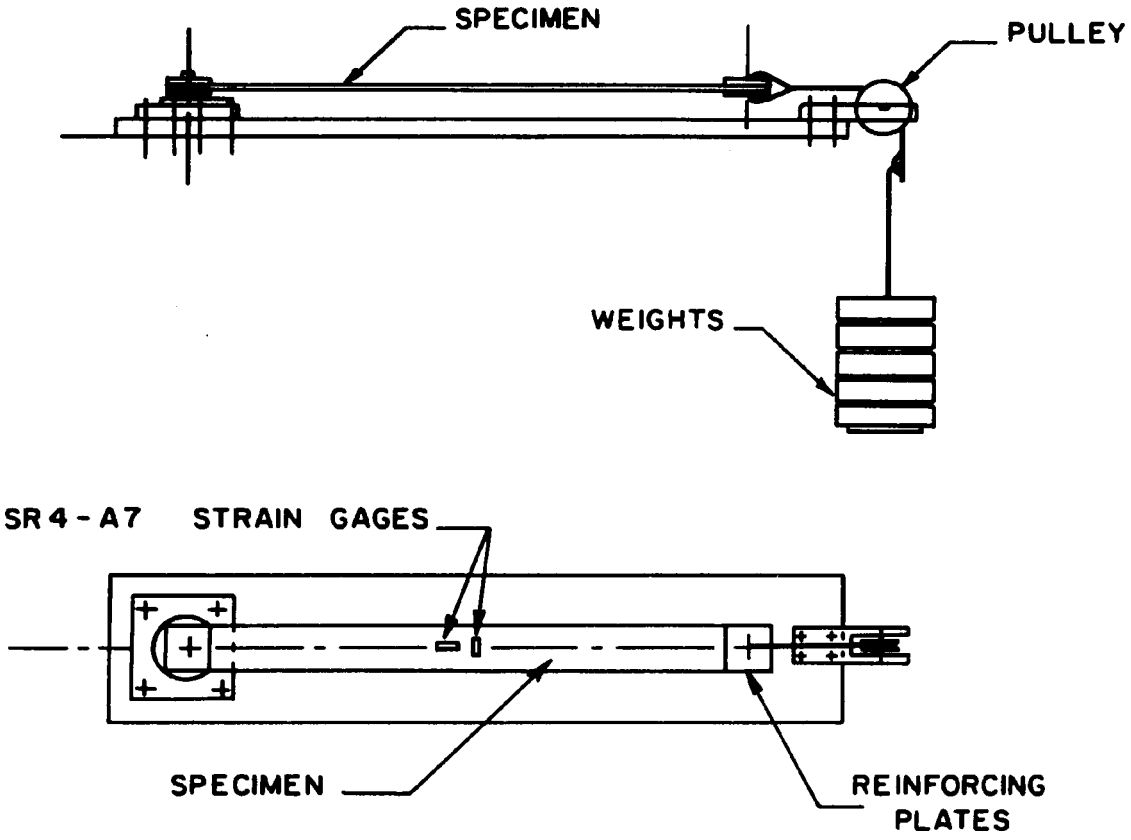


Figure 15. Arrangements for the Tensile Test.

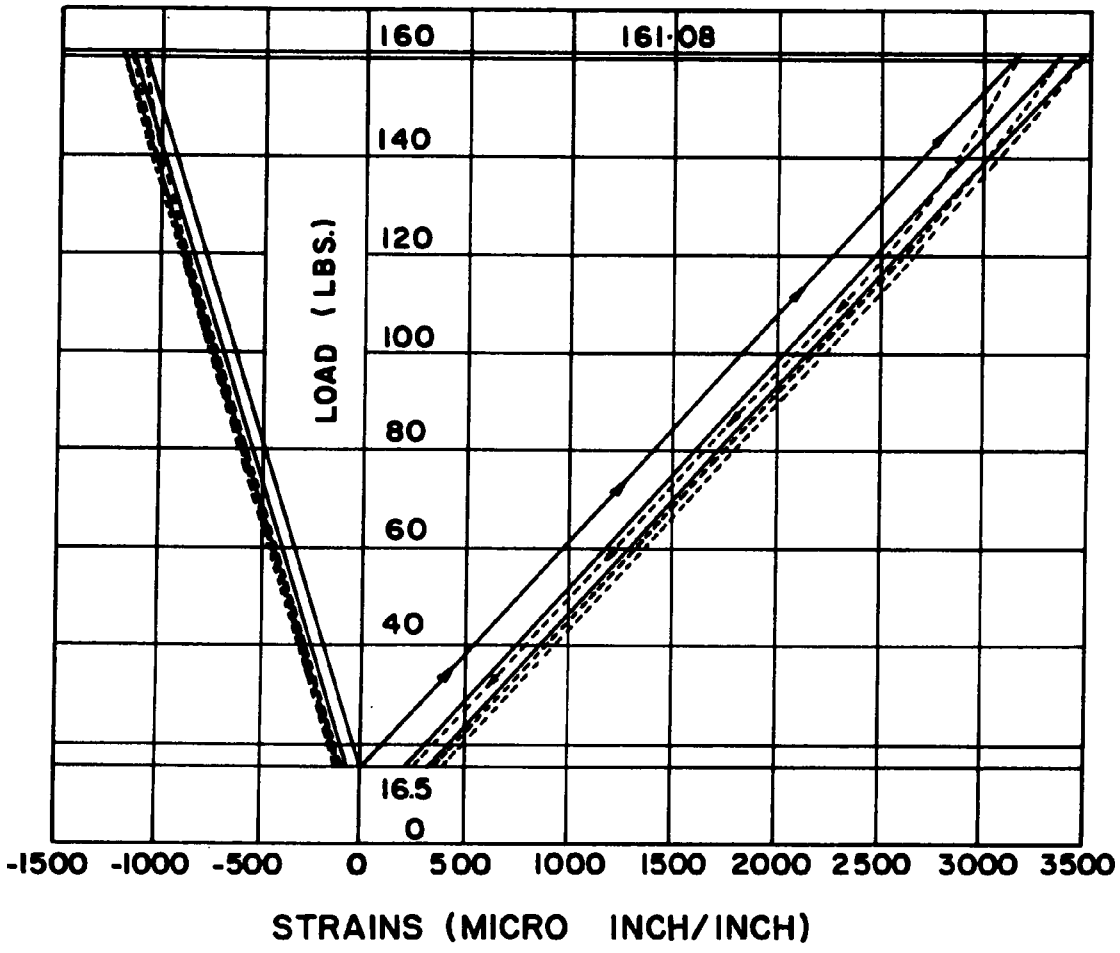


Figure 16. Load Strain Curve.

The ratio between the transverse strain and the longitudinal strain (Poisson's ratio) was found to be 0.35. The ratio between the stress calculated by dividing the applied load by the cross-sectional area of the specimen (2" x .06"), and the strain recorded for that load (Young's modulus of elasticity), was found to be 380,000 psi. The room temperature was 70°F, and the relative humidity was 15%. The material is isotropic, and it was assumed that the modulus of elasticity is the same for tension and compression.

It should be noticed that the properties of the celluloid vary with temperature and humidity, although it remains linearly elastic for a wide range. The modulus of elasticity in flexure and the tensible strength at 73°F and at various degrees of relative humidity, are tabulated below as taken from the Celanese Plastics Company's Technical Bulletin B-19, to show the effect of humidity:

TABLE I

EFFECT OF HUMIDITY ON CELLULOID PROPERTIES

R. Humidity	Tensile Strength, Psi	Mod. of Elasticity, Psi
0%	9000	380,000
50%	7500	300,000
90%	5500	250,000

Care was taken during the test course to record the temperature as well as the relative humidity in the test room, and to correct for these effects.

Similar to all other plastic materials, if a constant load is applied, the model will continue to deform under this load. This is a time effect manifesting itself as "creep" The effect of creep must be taken into consideration when comparing the experimental results with analytical solutions.

4.3 The Model

The model was proportioned similar to the actual gates. As shown in Figure 17, the length of the model is 49 inches, the depth is 15 inches, and the thickness is 3.5 inches. Six horizontal webs spaced 3 inches apart and seven vertical webs spaced 7 inches apart are provided between the two cover plates. The thickness of the webs as well as the cover plates is .06 inch. The parts of the model were first sawed a little oversize from the original 50" x 20" x .06" sheets, and then the exact dimensions were obtained by using a fine sander. The parts were attached together with "Duco Cement", which was tested and proved its adequateness.

4.4 The Supporting Frame

A rigid wooden U-frame supported directly on the floor, on which 2" x 3" bearing plates were fastened at spacing corresponding to the web spacing (see Plates 1 and 2), was made. Ball bearings of 5/16-inch diameter were seated in circular holes which had been drilled in the bearing plates. Circular steel posts 4 inches in height and of 1/2-inch diameter were fixed upright perpendicular to the bearing plates, which are used as a guide for another plate with

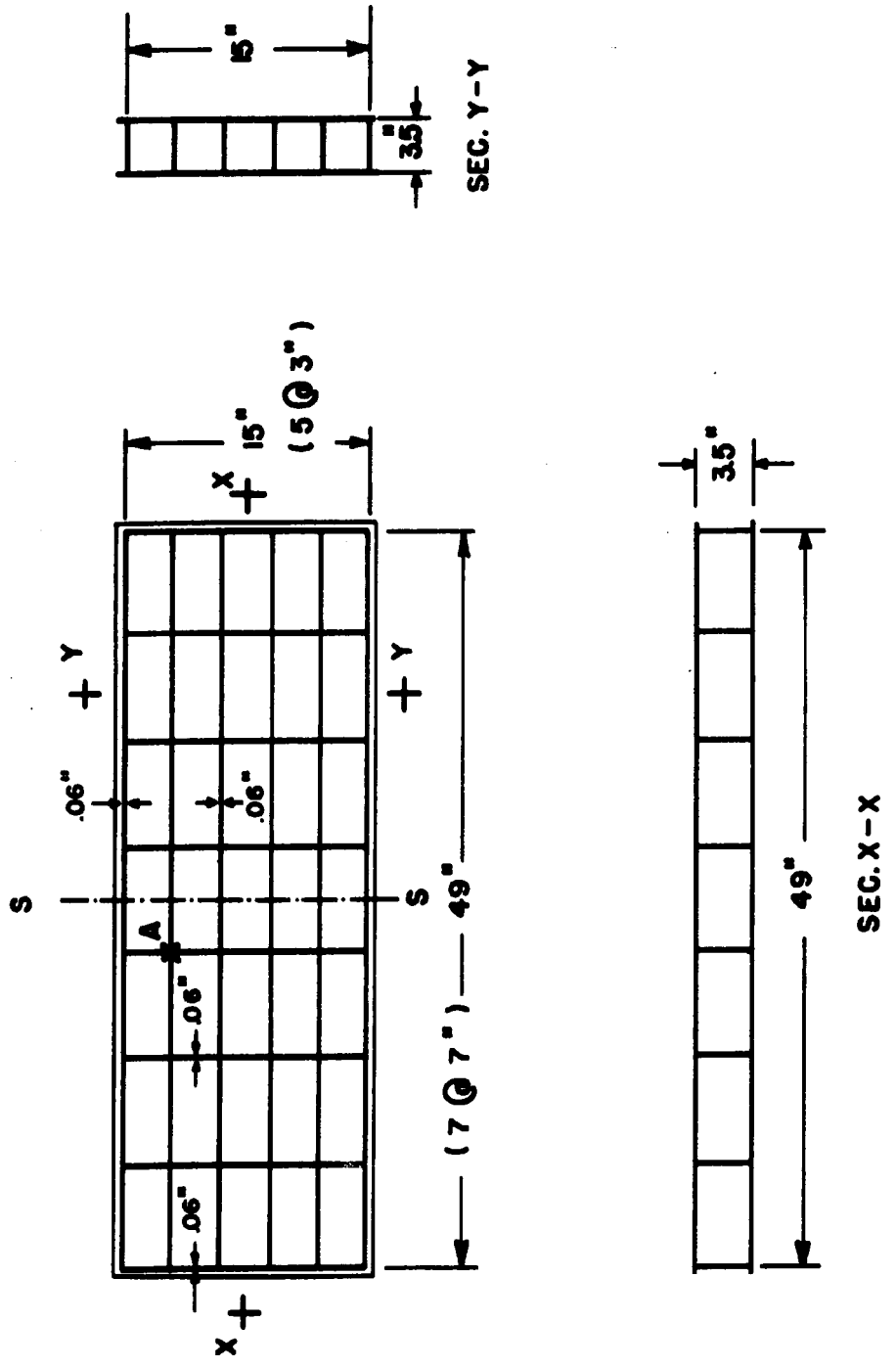


Figure 17. Dimensions of the Model.



Plate 1. The Test Set-Up.

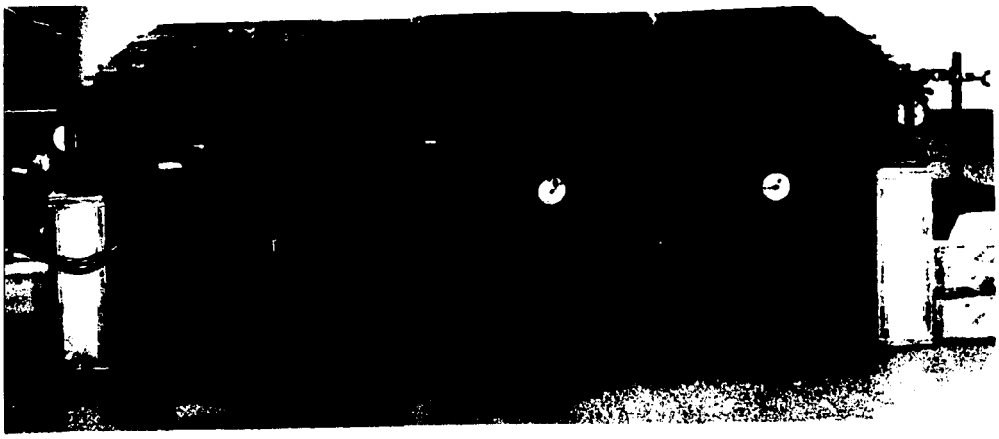


Plate 2. The Loaded Model.

a circular hole drilled exactly concentric with the hole in the bearing plate (drilled while the two plates are clamped together), holding another 5/16-inch ball bearing. The model is supported between the two ball bearings, whose centers are on the same vertical axis through the web intersection (see Plate 3).

The smooth ball bearings are free to move in their seats and the top and bottom surfaces of the model are very smooth, so it is felt that this kind of support will prevent only lateral (perpendicular to the middle plane between the cover plates) displacements at the boundary nodal points. This agrees with the boundary condtions assumed in the analytical solution, where the lateral displacements "w" were assumed to be zero at the boundary nodal points.

4.5 The Test Load

The test load applied to the model was limited to about 510 lbs which corresponds to about 100 lbs/ft^2. This limit was set to be sure that the maximum stress will be within the linearly elastic region, to avoid buckling of the top surface of the model, and to keep deformations in the model within the scope of reading of the measuring instruments. The test load consisted of steel blocks of about 2.3 lbs each, resting directly on the top surface of the model, and uniformly distributed. The load was applied in five increments of about 100 lbs each.

4.6 The Measuring Instruments

Calibrated Ames dial deflectometers, reading .001 inch per division, were used to measure deflections. SR4-A7 strain gages were

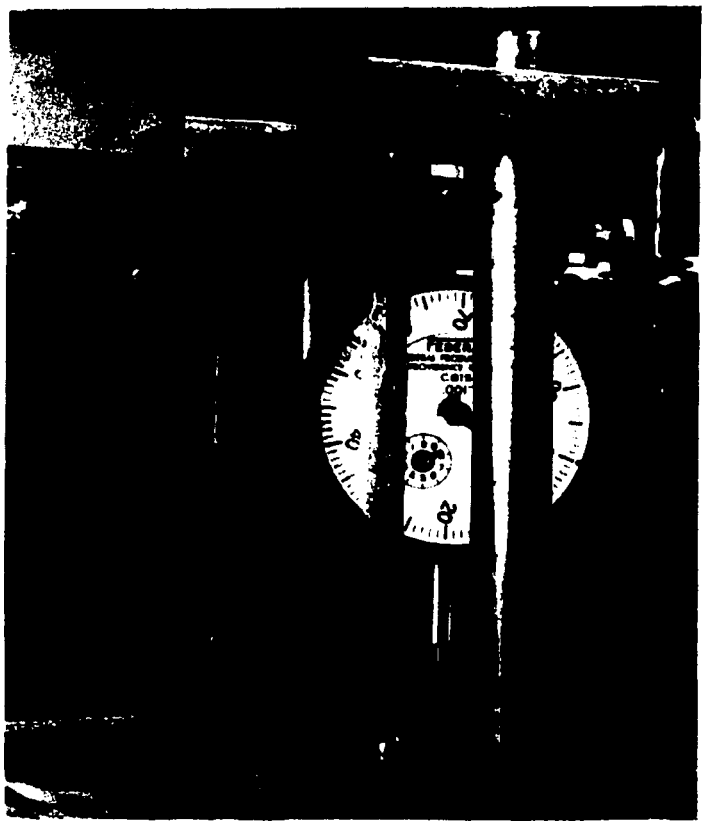


Plate 3. Support Details.

attached to the model to measure the strain. The accuracy in reading the strain is one micro inch/inch. Duco Cement was used to attach the strain gages to the model, taking care to follow the instructions for attaching such gages available in the technical bulletins.

4.7 Preliminary Tests

To measure ϵ_x (strain in the longitudinal direction), and ϵ_y (strain in the transverse direction), top and bottom, four SR4-A7 strain gages were attached to the model at point A (see Figure 17), two on each side.

The strains measured top and bottom were almost equal and opposite. So it was decided that for convenience and to have room for the loads on the top surface of the model, strain gages had to be attached only to the bottom surface of the model, and it was assumed that the strains in the top surface are of the same magnitude and in the opposite direction.

The strain resulting from the increase in temperature (due to the heat from the electric current in the gage) was appreciable, because the coefficient of thermal expansion of the cellulose sheets is relatively high (coefficient of linear thermal expansion = .00014 per degree Fahrenheit). It was therefore decided to use a compensating dummy gage, attached to a similarly restrained structure constructed from the same material mainly for this purpose. This was placed just under the model (see Plates 1 and 2). Preliminary tests showed that more than one compensating dummy gage was needed, so that they can be connected with the active gages in a pattern allowing the active and the dummy to be at the same temperature whenever an active gage is read, provided that the

active gages are read in the appropriate order. Deflectometers were placed at various bearing plates to measure the settlements of the supports (Plate 3). Very small settlements were measured at the supports, which were about 1% of the maximum deflection in the model. Since it was practically impossible to eliminate such settlements, it was decided to correct for them. Symmetry about the S-S axis in the model (see Figure 17) was checked by measuring deflections at symmetrical points; the model was found to be perfectly symmetrical, so it was decided to measure deflections and strains only on one side of the axis of symmetry S-S.

4.8 The Test

Forty-eight SR4-A7 strain gages were attached to the bottom nodal points on one side of the model, as shown in Figure 18. Also, six gages were attached to the boundary webs on the neutral axis to measure the strain in the direction parallel to the covers which is assumed to be zero (the middle surface is a neutral surface). Six compensating gages were connected with the 54 active ones to balance for the temperature strain from the heat due to the electric current in the gage, mentioned before.

The gages were connected in series to three switch boxes, and then to the indicator, to switch, balance, and read one gage at a time. The time to balance and read each gage was about 90 seconds. Also, two deflectometers were inserted upright under two nodal points on the other side of the model as shown in Plates 1 and 2, and as indicated in Figure 18.

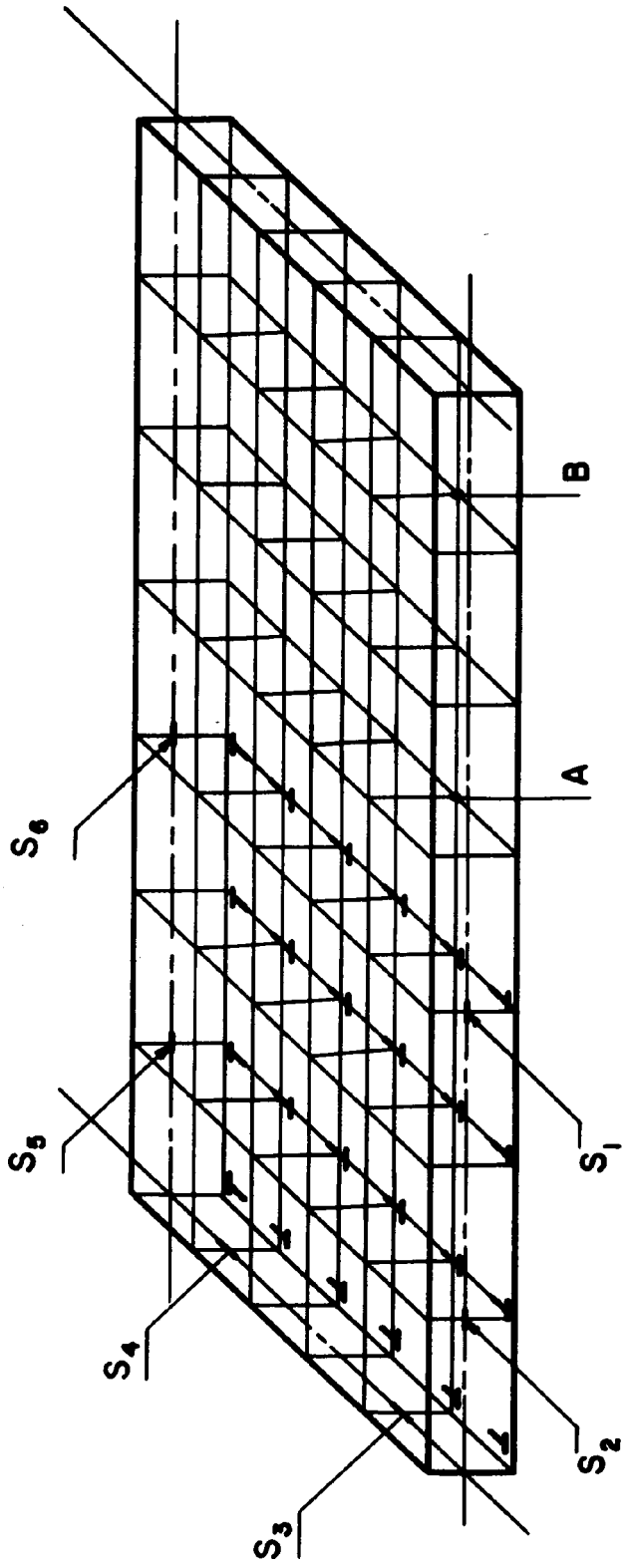


Figure 18. Locations of Strain Gages.

The 510-lb load was applied in five nearly equal increments, as mentioned before. Deflections and strains were read before and after applying each increment of load. The difference between the two readings is the deflection or strain due to the applied increment.

The temperature and the relative humidity in the test room were measured before and after the test; the average temperature was 81°F, and the average relative humidity was 29% so the corresponding value for Young's modulus of elasticity is 300,000 psi.

4.9 Test Results and Comparison with Analytical Answers

The average strains (ϵ_x's and ϵ_y's) in the cover from the test are plotted on Figures 19 and 20.

From the stresses calculated analytically and using the stress-strain relationships,

$$\epsilon_x = (\sigma_x - \nu\sigma_y)/E \quad , \quad \text{and}$$

$$\epsilon_y = (\sigma_y - \nu\sigma_x)/E \quad ,$$

the analytical strains were computed and plotted on the same figures for comparison.

The deflections at points A and B are shown on Figure 19. The numbers between parentheses are the average measured experimentally, and the other numbers are calculated analytically.

The strain measured on the webs was very small, especially the strain at s1 and s2, whereas the strain at s3, s4, s5, and s6 was more appreciable.

As shown in Figures 19 and 20 the experimental results agree reasonably with the analytical answers, and the scatter of the results

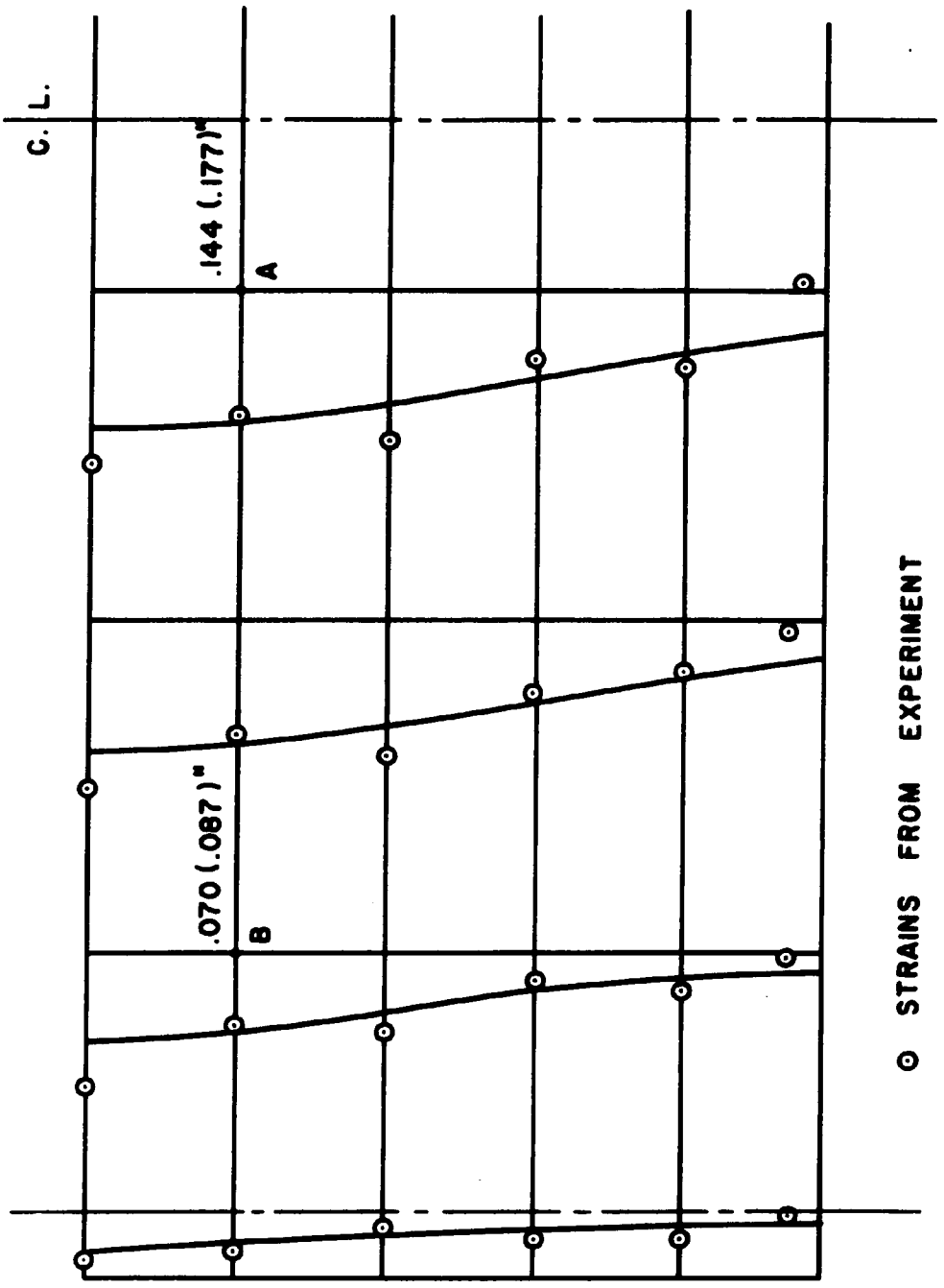


Figure 19. Strains in the Horizontal Direction.

-The curves shown are for the strains calculated.
-The numbers between parentheses at points A and B are the average deflections at those points measured experimentally, and the other numbers are the corresponding deflections calculated.

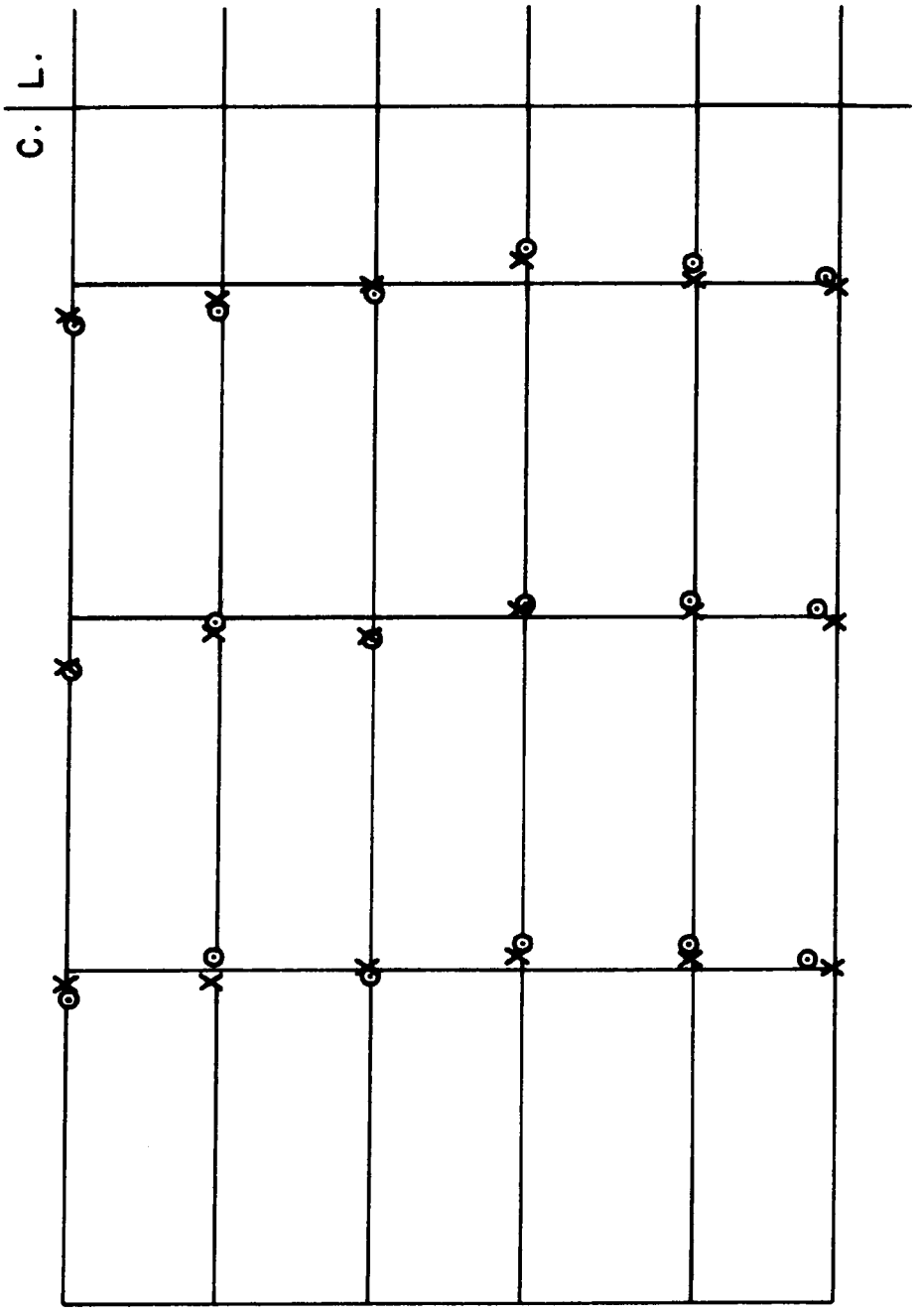


Figure 20. Strains in the Vertical Direction.

seen is within the range that has to be expected. Values measured are in general bigger than the calculated values, as predicted. This is due to the effect of creep. Better results might be obtained from an aluminum model; however, it is felt that using the plastic model is adequate for our purpose.

If all the possible influences on test results are considered, the correspondence between theoretical and experimental results is quite satisfactory.

V. THIN ISOTROPIC PLATE SOLUTION VS. FINITE ELEMENT SOLUTION

If we assume that the two parallel cover plates supply all of the bending resistance and if we neglect web shear deformation, then the structure consisting of two cover plates each of thickness t_c and separated by a distance h, where $h \gg t_c$, will behave like an isotropic plate which has a flexural rigidity $D = Eh^2 t_c/2(1-\nu^2)$, provided that the webs are close enough to ensure that the plating is fully effective.

Such idealization has been checked by Jaeger[8] experimentally. His observations were made for deflections only. The idealized plate solution and the finite element solution are compared in this chapter.

5.1 Thin Isotropic Plate Solution

Consider a plate with three edges simply supported and the fourth edge free, and subjected to a hydrostatic pressure, as shown in Figure 21. The boundary conditions are:

$$w = 0, \quad \frac{\partial^2 w}{\partial x^2} = 0 \quad , \quad \text{at } x = -\frac{b}{2} \quad \text{and } x = \frac{b}{2}$$

$$\frac{\partial^2 w}{\partial y^2} + \frac{\nu \partial^2 w}{\partial x^2} = 0$$

$$\frac{\partial^3 w}{\partial y^3} + (2-\nu)\frac{\partial^3 w}{\partial y \partial x^2} = 0 \qquad , \text{ at } y = 0$$

$$w = 0, \quad \frac{\partial^2 w}{\partial y^2} = 0 \quad , \quad \text{at } y = a$$

and the plate bending equation is:

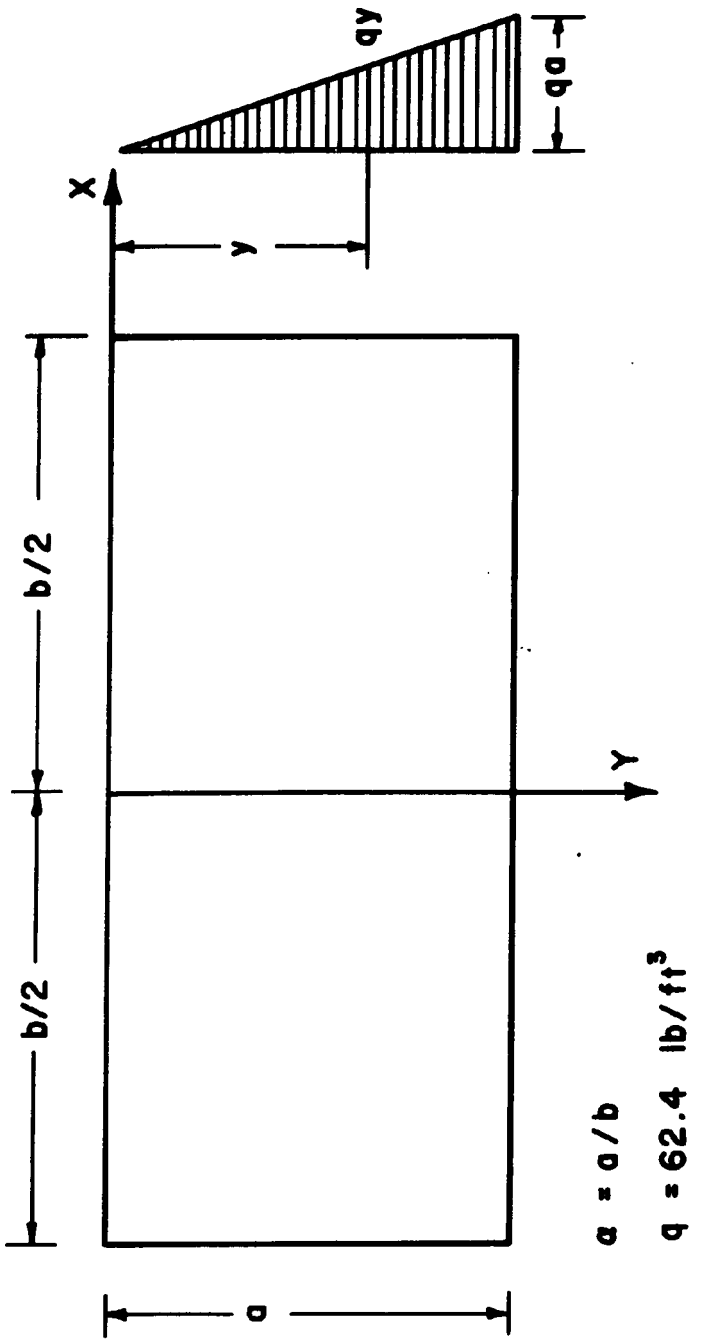


Figure 21. Plate Simply Supported on Three Sides and Subjected to a Hydrostatic Pressure.

$$\frac{\partial^4 w}{\partial x^4} + \frac{2\partial^4 w}{\partial x^2 \partial y^2} + \frac{\partial^4 w}{\partial y^4} = q/D \quad .$$

The deflection surface equation can be derived using M. Levy's method, and is given in the form:

Deflections:

$$w = \frac{4qb^4}{\pi^5 D} y \sum_{n=1,3,..}^{\infty} \frac{1}{n^5} (-1)^{(n-1)/2} \cos \frac{n\pi x}{b} + \sum_{n=1,3,..}^{\infty} (A_n \cosh \frac{n\pi y}{b} +$$

$$B_n \sinh \frac{n\pi y}{b} + C_n \frac{n\pi y}{b} \sinh \frac{n\pi y}{b} + D_n \frac{n\pi y}{b} \cosh \frac{n\pi y}{b})$$

$$\cos \frac{n\pi x}{b} \quad ..... \qquad (5.1)$$

where

$$A_n = \frac{-2}{1-\nu} C_n$$

$$D_n = \frac{aN_n}{2 \sinh n\pi\alpha} - C_n \operatorname{cotgh} n\pi\alpha$$

$$B_n = \frac{aN_n}{1-\nu} \left(\frac{1+\nu}{2 \sinh n\pi\alpha} - \frac{2-\nu}{n\pi\alpha} \right) - \frac{1+\nu}{1-\nu} C_n \operatorname{cotgh} n\pi\alpha$$

$$C_n = aN_n \left[\frac{3-\nu}{2(1-\nu)} + \frac{n\pi\alpha}{2} \operatorname{cotgh} n\pi\alpha - \frac{(2-\nu)}{(1-\nu)} \frac{\sinh n\pi\alpha}{n\pi\alpha} \right] \div$$

$$\left[\frac{n\pi\alpha}{\sinh n\pi\alpha} + \frac{3+\nu}{1-\nu} \cosh n\pi\alpha \right]$$

$$N_n = \frac{4qb^4}{n^5 \pi^5 D} (-1)^{(n-1)/2}$$

From the deflection surface equation moments, shears, and reactions are derivable, namely,

Moments

$$Mx = -\left[\frac{\partial^2 w}{\partial x^2} + \nu \frac{\partial^2 w}{\partial y^2}\right] D$$

$$Mx = D \sum_{n=1,3,..}^{\infty} \left(\frac{n\pi}{b}\right)^2 (1-\nu) \left[\frac{N_n}{1-\nu} y + B_n \sinh \frac{n\pi y}{b} + C_n \left(\frac{n\pi y}{b} \sinh \frac{n\pi y}{b} - \frac{2(1+\nu)}{1-\nu} \cosh \frac{n\pi y}{b}\right) + D_n \left(\frac{n\pi y}{b} \cosh \frac{n\pi y}{b} - \frac{2\nu}{1-\nu} \sinh \frac{n\pi y}{b}\right)\right] \cos \frac{n\pi x}{b} \quad .... \quad (5.2)$$

where Mx is the bending moment per unit length about the y-axis

$$My = -\left[\frac{\partial^2 w}{\partial y^2} + \nu \frac{\partial^2 w}{\partial x^2}\right] D$$

$$My = D \sum_{n=1,3,..}^{\infty} (1-\nu) \left(\frac{n\pi}{b}\right)^2 \left[\frac{\nu N_n}{1-\nu} y - B_n \sinh \frac{n\pi y}{b} - C_n \frac{n\pi y}{b} \sinh \frac{n\pi y}{b} - D_n \left(\frac{2}{1-\nu} \sinh \frac{n\pi y}{b} + \frac{n\pi y}{b} \cosh \frac{n\pi y}{b}\right)\right] \cos \frac{n\pi x}{b} \quad ..... \quad (5.3)$$

where My is the bending moment per unit length about the x-axis

$$Mxy = (1-\nu) \frac{\partial^2 w}{\partial x \partial y} D$$

$$Mxy = -Myx = -D \sum_{n=1,3,..}^{\infty} (1-\nu) \left(\frac{n\pi}{b}\right)^2 \left[\frac{b}{n\pi} N_n + B_n \cosh \frac{n\pi y}{b} + C_n \left(\frac{n\pi y}{b} \cosh \frac{n\pi y}{b} - \frac{1+\nu}{1-\nu} \sinh \frac{n\pi y}{b}\right) + D_n \left(\cosh \frac{n\pi y}{b} + \frac{n\pi y}{b} \sinh \frac{n\pi y}{b}\right)\right] \sin \frac{n\pi x}{b} \quad ..... \quad (5.4)$$

where Mxy is the twisting moment per unit length.

Shears

$$Vx = -\left(\frac{\partial^3 w}{\partial x^3} + \frac{\partial^3 w}{\partial x \partial y^2}\right) D$$

$$Vx = D \sum_{n=1,3,..}^{\infty} \left(\frac{n\pi y}{b}\right)^3 \left[- N_n y + 2\, C_n \cosh \frac{n\pi y}{b} + 2\, D_n \sinh \frac{n\pi y}{b} \right] \sin \frac{n\pi x}{b} \quad ..... \qquad (5.5)$$

where Vx is the shearing force in the y-z plane per unit length

$$Vy = -\left(\frac{\partial^3 w}{\partial y^3} + \frac{\partial^3 w}{\partial x^2 \partial y}\right) D$$

$$Vy = D \sum_{n=1,3,..}^{\infty} \left(\frac{n\pi y}{b}\right)^3 \left[\frac{b}{n\pi} N_n - 2\, C_n \sinh \frac{n\pi y}{b} - 2\, D_n \cosh \frac{n\pi y}{b} \right] \cos \frac{n\pi y}{b} \quad ..... \qquad (5.6)$$

where Vy is the shearing force in the x-z plane per unit length

Reactions

$$Rx = \left[Vx - \frac{\partial Mxy}{\partial y} \right] = -\left[\frac{\partial^3 w}{\partial y^3} + (2-\nu) \frac{\partial^3 w}{\partial x \partial y^2} \right] D$$

$$R\left(x = \frac{b}{2}\right) = D \sum_{n=1,3,..}^{\infty} \left(\frac{n\pi}{b}\right)^3 \sin \frac{n\pi}{2} \left[-N_n y + (1-\nu)\left[B_n \sinh \frac{n\pi y}{b} + C_n \left(2 \cosh \frac{n\pi y}{b} + \frac{n\pi y}{b} \sinh \frac{n\pi y}{b}\right) + D_n \left(\frac{2(2-\nu)}{1-\nu} \sinh \frac{n\pi y}{b} + \frac{n\pi y}{b} \cosh \frac{n\pi y}{b}\right)\right]\right] ..... \qquad (5.7)$$

where Rx is the reaction per unit length at the sides $\left(x = \pm \frac{b}{2}\right)$

$$Ry = \left[Vy + \frac{\partial Myx}{\partial x}\right] = - \left[\frac{\partial^3 w}{\partial y^3} + (2-\nu)\frac{\partial^3 w}{\partial x^2 \partial y}\right] D$$

$$R(y = a) = D \sum_{n=1,3,..}^{\infty} \left(\frac{n\pi}{b}\right)^3 (1-\nu)\left[\frac{2-\nu}{1-\nu}\frac{b}{n\pi} N_n + B_n \cosh n\pi\alpha + C_n (n\pi\alpha \cosh n\pi\alpha - \frac{3+\nu}{1-\nu}\sinh n\pi\alpha) + D_n (n\pi\alpha \sinh n\pi\alpha - \frac{1+\nu}{1-\nu}\cosh n\pi\alpha)\right] \cos\frac{n\pi x}{b} \ldots\ldots \quad (5.8)$$

where Ry is the reaction per unit length at the bottom (y = a).

The moments and the shears are considered positive when they are directed as shown in Figure 22.

5.2 Stresses

5.2.1 Stresses Due to the Bending Moments Mx and My -- Since the contribution of the webs to the flexural rigidity is neglected, the bending moments will be resisted by the two cover plates. Then:

$$\sigma_x t_c h = Mx$$

$$\sigma_y t_c h = My$$

or

$$\sigma_x = \pm \frac{Mx}{t_c h}$$

$$\sigma_y = \pm \frac{My}{t_c h}$$

where σ_x and σ_y are the normal stresses in the cover plates in the x- and the y-directions, respectively.

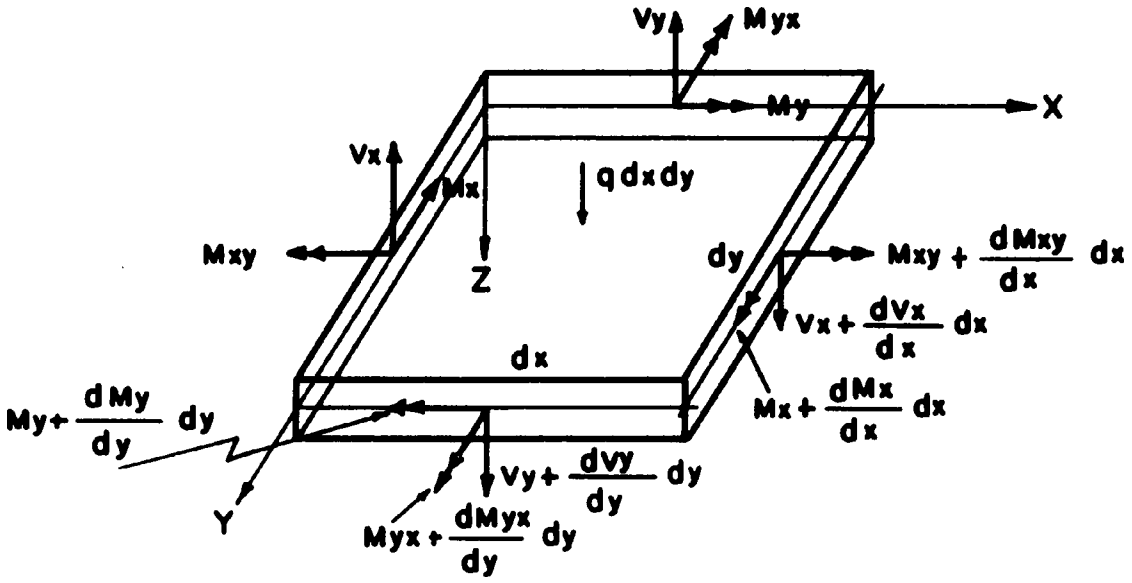


Figure 22. Directions of Positive Load, Moments, and Shears.

5.2.2 Stresses Due to the Twisting Moments Mxy and Myx -- The twisting moments will give rise to horizontal shear stresses τ_{xy}, and τ_{yx} in the cover plates, where

$$\tau_{xy} = \frac{Mxy}{t_c\ h}\ , \quad \text{and}$$

$$\tau_{yx} = \frac{Myx}{t_c\ h}\ .$$

Due to the variation in Mxy and Myx, we have vertically distributed shearing forces $\partial Mxy/\partial y$ (acting along any cross section parallel to the y-axis), and $\partial Myx/\partial x$ (acting along any cross section parallel to the x-axis), respectively. Also, we have concentrated shearing forces which are equal to Mxy and Myx, acting at the short side edges of the cross sections parallel to the y- and the x-axes, respectively.

For the cellular structure (see Figure 23), the vertical shear stresses in the webs will be:

$$\tau_{xz_I} = -\frac{Mxy_1}{t_w\ h}$$

$$\tau_{xz_{II}} = -\frac{(Mxy_4 - Mxy_3)}{t_w\ h}$$

$$\tau_{xz_V} = \frac{Mxy_8}{t_w\ h}$$

$$\tau_{yz_{III}} = \frac{(Myx_6 - Myx_5)}{t_w\ h}$$

$$\tau_{yz_{IV}} = -\frac{Myx_7}{t_w\ h}$$

In the previous τ_{xz} and τ_{yz} stresses, notice that Mxy and Myx are moments per unit length, so they have the dimensions of force. The sign convention follows that in Figure 22.

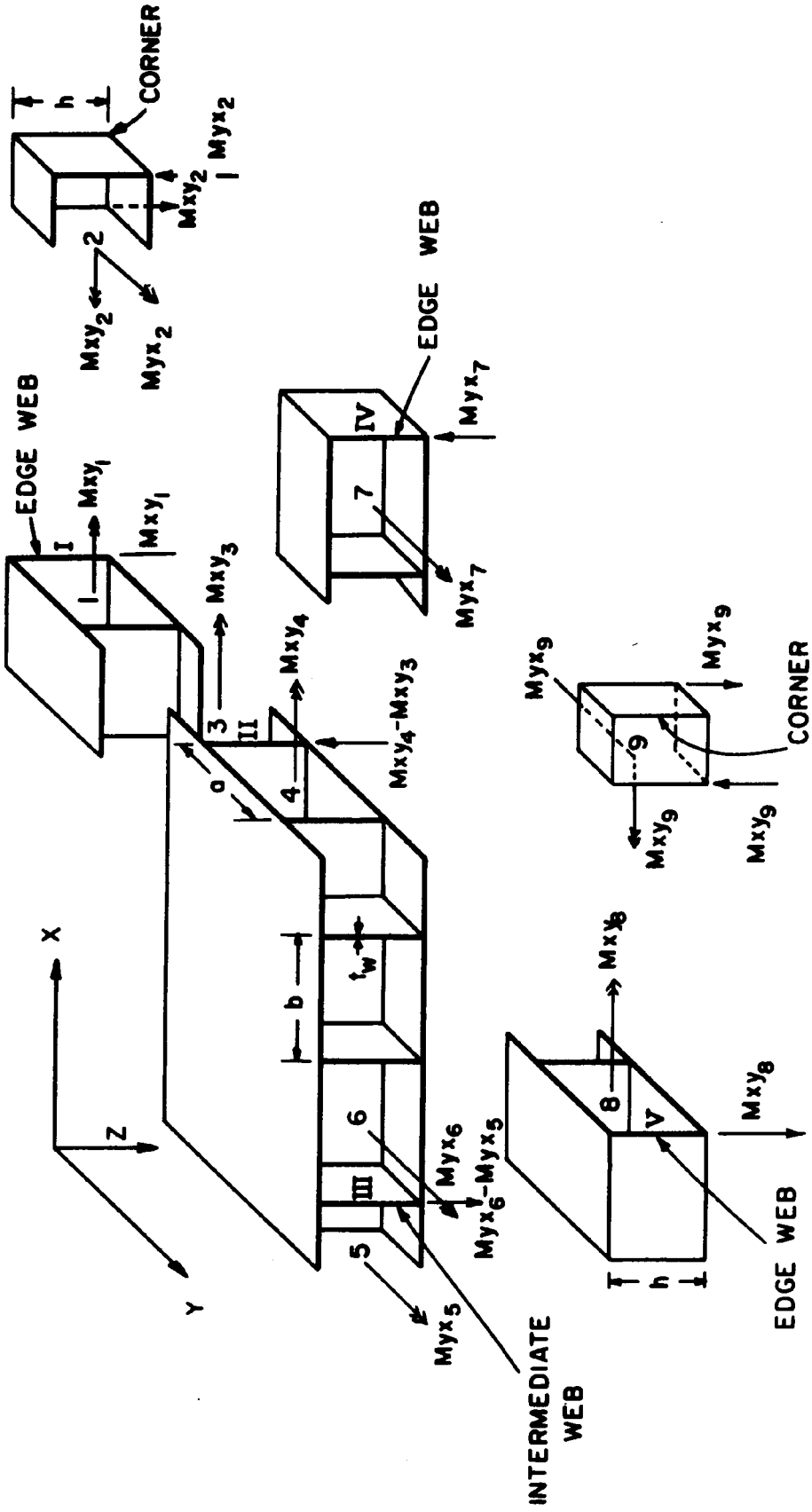


Figure 23. Vertical Shears Due to Twisting Moments.

5.2.3 Stresses Due to the Vertical Shearing Forces Vx and Vy -- The shearing forces Vx and Vy will give rise to vertical shear stresses τ_{xz} and τ_{yz}, respectively.

For the cellular structure (see Figure 23), the vertical shear stresses in the webs will be:

$$\tau_{xz_I} = Vx_I \, a/(2t_w \, h)$$

$$\tau_{xz_{II}} = Vx_{II} a/(t_w \, h)$$

$$\tau_{xz_V} = Vx_V \, a/(2t_w \, h)$$

$$\tau_{yz_{III}} = Vy_{III} b/(t_w \, h)$$

$$\tau_{yz_{IV}} = Vy_{IV} \, b/(2t_w h)$$

The total shearing stresses in the webs are the algebraic sum of the shearing stresses due to the twisting moments and the ones due to the shearing forces.

5.3 Evaluation of the Plate Solution

Deflections are calculated at the web intersections. Bending moments Mx and shearing forces Vx are calculated at the middle of the horizontal webs between web intersections. Bending moments My and shearing forces Vy are calculated at the middle of the vertical webs between web intersections. Twisting moments Mxy are calculated at the centers of the panels (see Figure 24).

Using the stress formulae given before, normal stresses σ_x, and σ_y, and shearing stresses τ_{xy}, τ_{xz}, and τ_{yz} are calculated at the

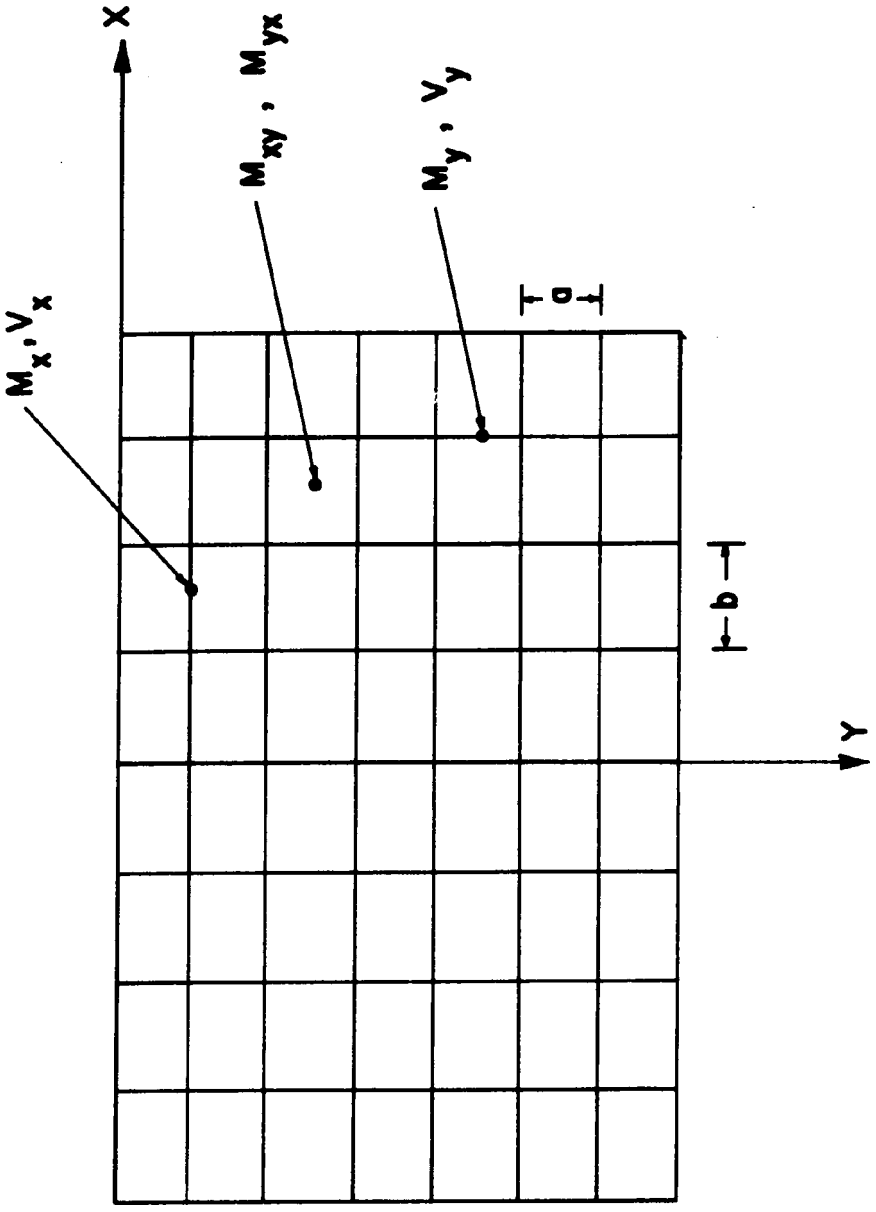


Figure 24. Locations Where Moments and Shears are Calculated.

corresponding points. Reactions are calculated at the web intersections on the three supported boundaries using Equations (5.7) and (5.8); these reactions are uniformly distributed, so to calculate the concentrated reactions we multiply by the corresponding web spacing. The twisting moments at the corners are calculated and the corresponding concentrated reactions are calculated from them (2Mxy).

A computer program evaluates deflections, moments, shears, reactions, and stresses by considering ten terms of the series. The steps in the actual machine computation are omitted here.

5.4 Comparison Between the Finite Element Solution and the Plate Solution

The same gate example solved in Chapter III, using the finite-element method, is solved again using the plate idealization. For comparison, the results from the two different solutions are given in Figures 25-31. Deflections at the web intersections calculated by the finite-element method considering and neglecting web shear deformation are listed in the two top lines, respectively, and the deflections calculated by the plate method are listed in the third line. As one can see, the deflections calculated by the finite-element method, neglecting web shear deformations, are identical with the deflections calculated using the plate idealization. Normal stresses in the cover plates σ_x, and σ_y are shown in Figures 26 and 27. The difference between the results of the two methods is small, and it is tolerable for practical design. Shear stresses in the cover plates are shown in Figure 28. The difference between the results of the two methods is more appreciable in the plate elements of the cover near the boundary;

*	1.486	2.642	3.373	3.621
x	1.218	2.209	2.831	3.006
+	1.217	2.204	2.831	3.046
*	1.219	2.171	2.765	2.967
x	0.997	1.801	2.312	2.487
+	0.997	1.800	2.307	2.480
*	0.962	1.703	2.160	2.314
x	0.776	1.393	1.782	1.914
+	0.778	1.395	1.782	1.913
*	0.688	1.202	1.515	1.620
x	0.542	0.963	1.226	1.315
+	0.543	0.965	1.227	1.316
*	0.373	0.640	0.800	0.853
x	0.283	0.498	0.630	0.675
+	0.283	0.498	0.631	0.676

* Finite element considering web shear deformation.
x Finite element neglecting web shear deformation.
+ Plate solution.

Figure 25

Deflections (inches)
(Finite Element vs. Idealized Plate)

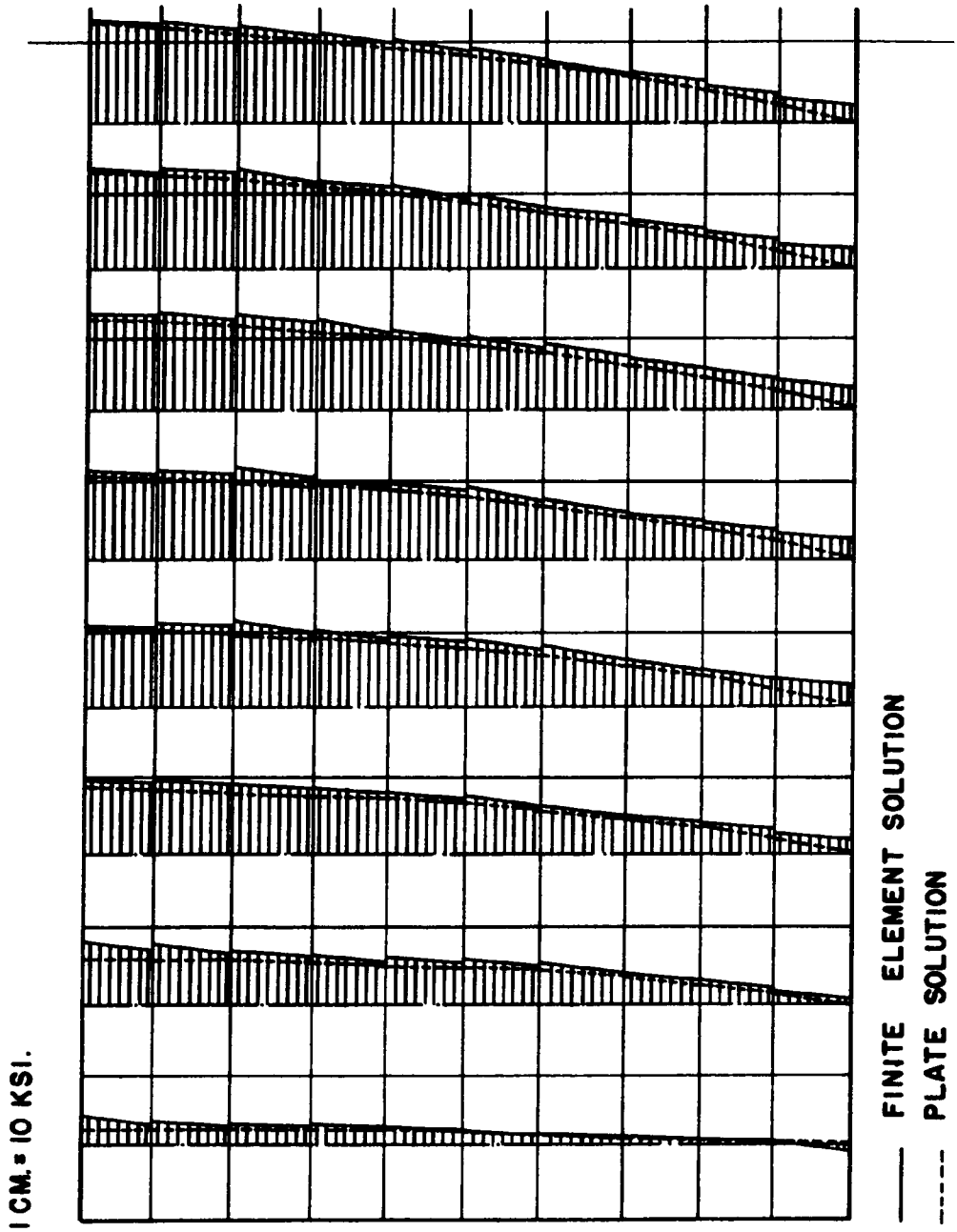


Figure 26. Normal Stresses in the Cover-Plate in the x-Direction KSI.
(Finite Element vs. Idealized Plate).

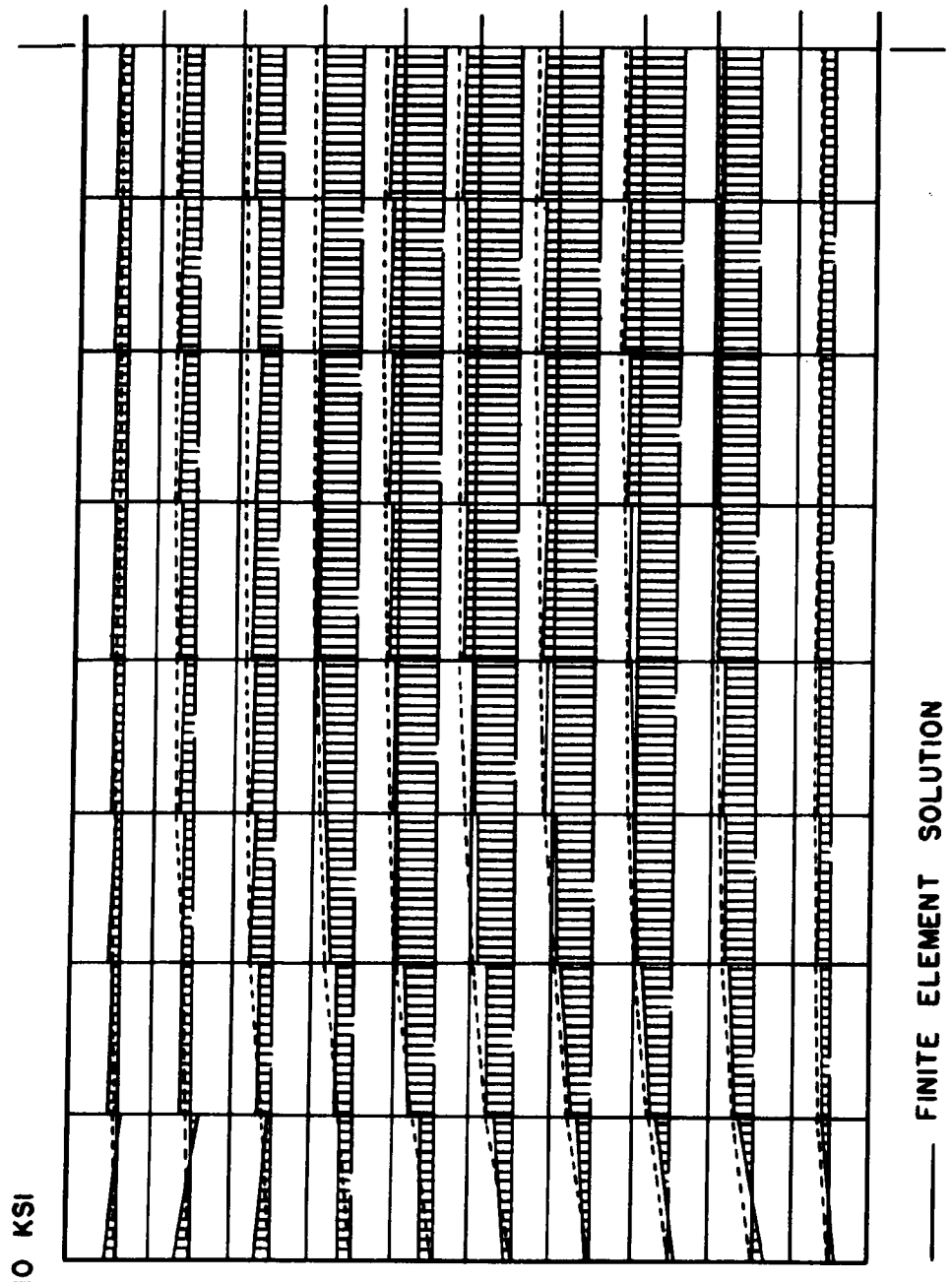


Figure 27. Normal Stresses in the Cover-Plate in the y-Direction KSI.
(Finite Element vs. Idealized Plate).

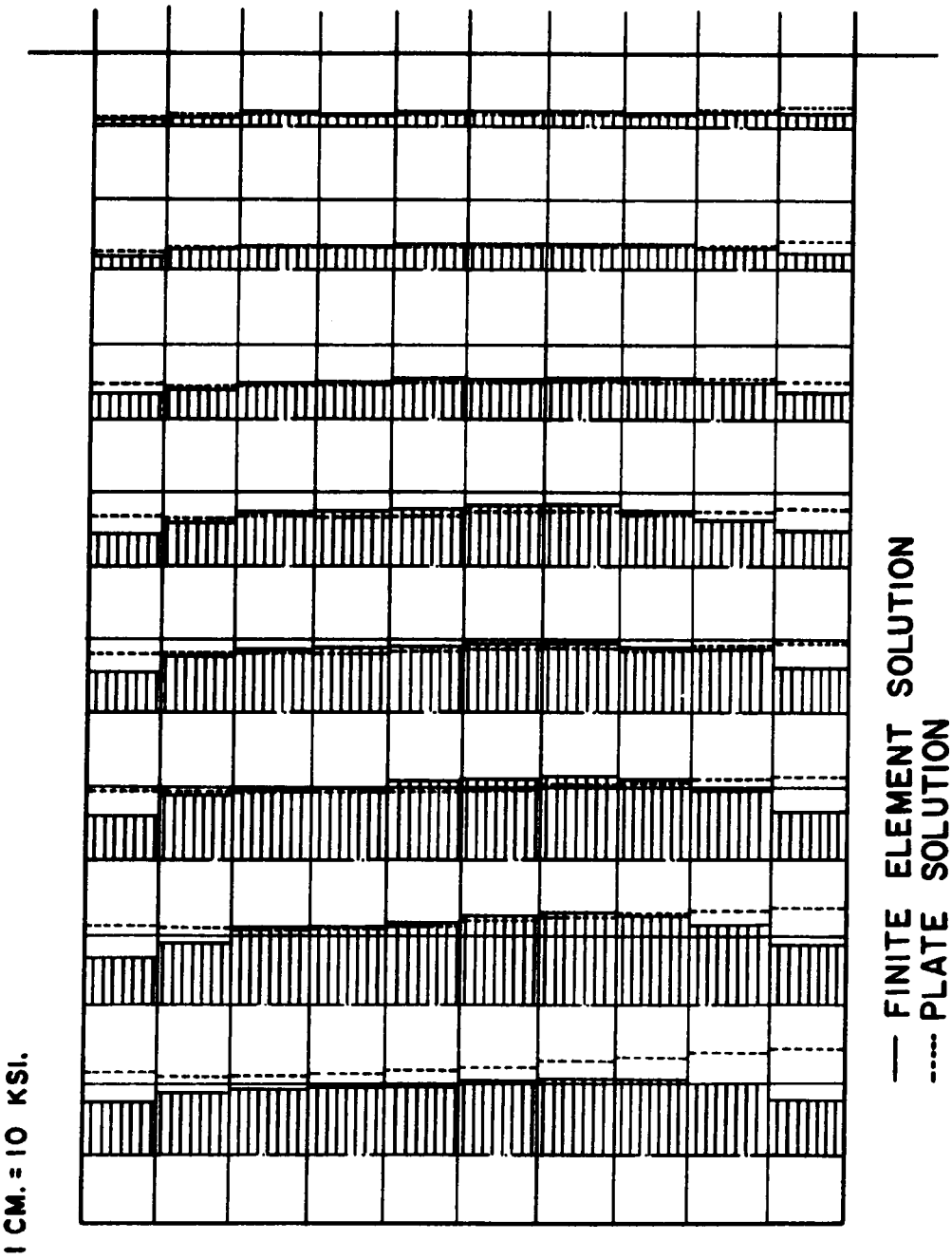


Figure 28. Shear Stresses in the Cover Plate τ_{yx} ksi.
(Finite Element vs. Idealized Plate)

however, the difference elsewhere is not much and can be considered tolerable for practical design. There is disagreement between the shear stresses in the webs calculated by the finite element method and those calculated from the idealized plate, as one can see in Figures 29 and 30.

The reactions listed in Figure 31 indicate considerable deviation between the two methods near the corners of the structure. However, this difference is less away from the corners. One should notice that, in the finite-element solution, we lumped the water-pressure distribution as concentrated loads acting at the web intersections; however, this was not done in the plate solution and we consider the actual water-pressure distribution all over the area of the gate. Reactions shown in italics are obtained by adding to the reactions from the finite-element method the corresponding concentrated loads at the corresponding web intersections on the boundary.

To be able to arrive at general conclusions, the following examples have been solved using the finite-element solution and the plate solution, (Table II).

In Figure 32 deflections in gates "1", "2", and "3" are compared. In gate "3" we have thin cover plates (.375") and thick web plates (.75"), while gate "2" has thick cover plates (.75") and thin web plates (.375"), and gate "1" has cover plates as thick as the web plates (.5").

According to the idealized plate solution, since the width, the depth, and the distance between the cover plates are the same for

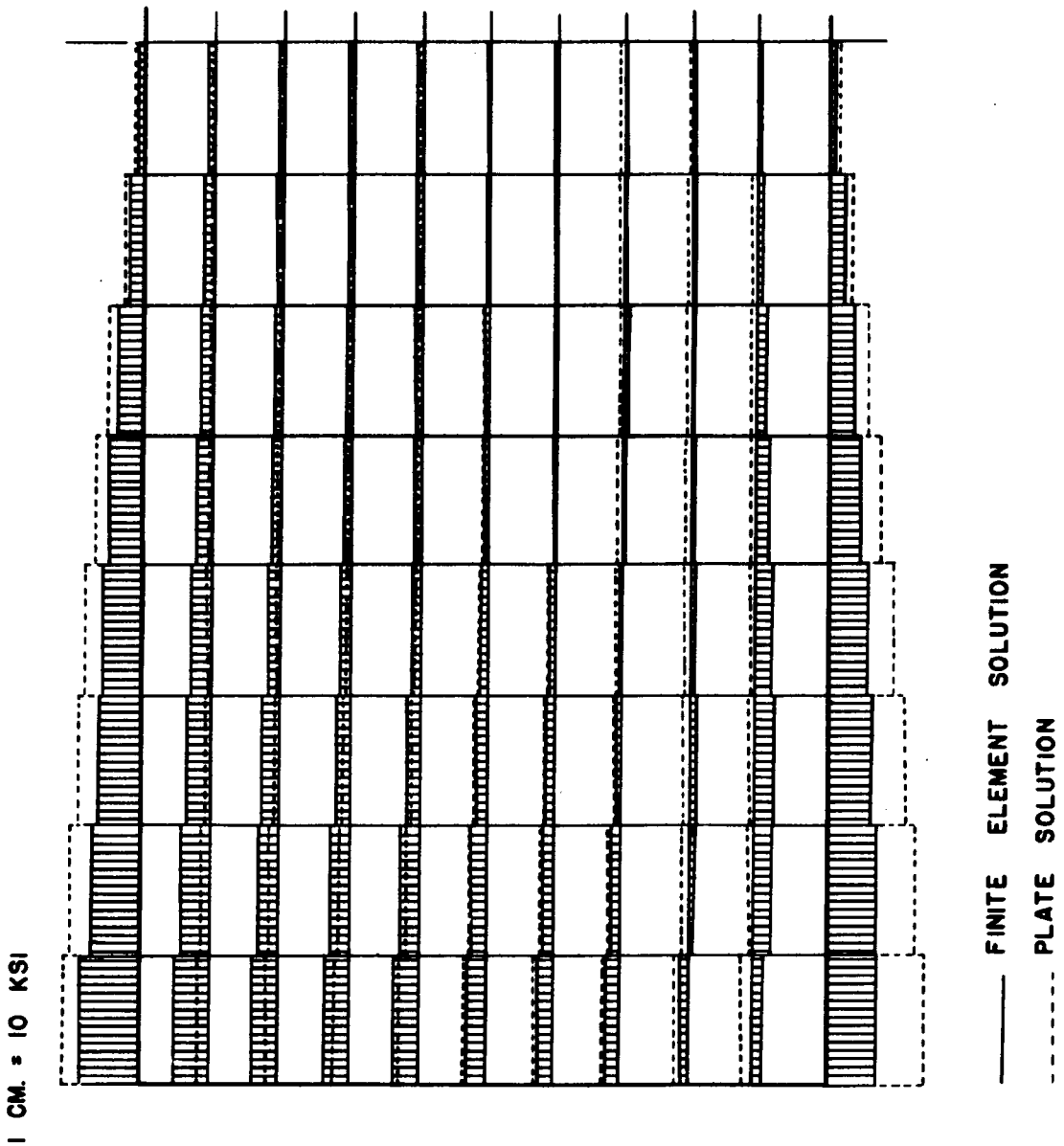


Figure 29. Shear Stresses in the Horizontal Webs τ_{xz} KSI.
(Finite Element vs. Idealized Plate).

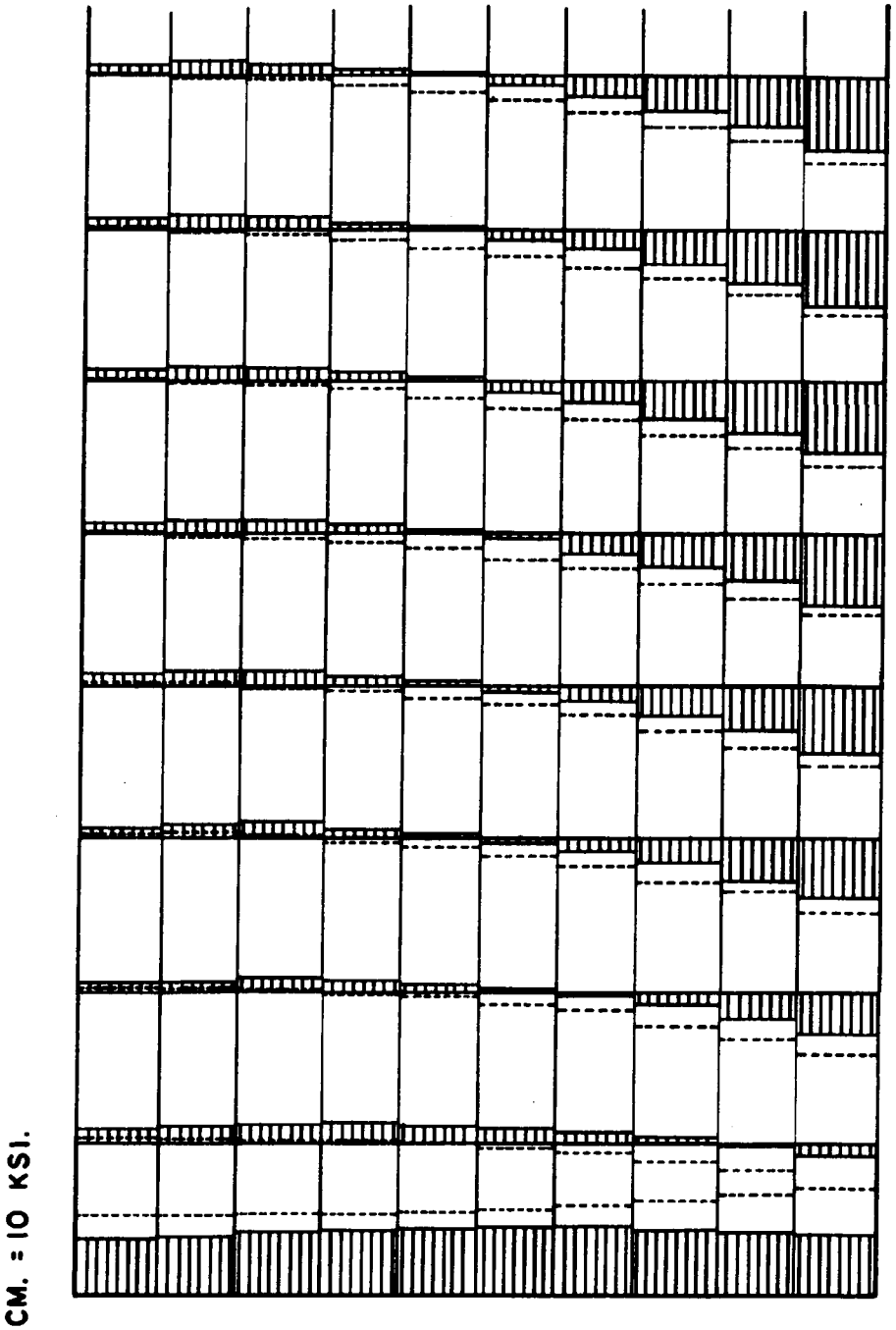


Figure 30. Shear Stresses in the Vertical Webs τ_{yz} KSI.
(Finite Element vs. Idealized Plate).

P.	F.E.								
1335.197	989.268 990.568								
95.592	338.952 346.752								
125.507	255.930 271.530								
155.323	215.771 239.171								
181.733	196.304 227.504								
201.725	181.602 220.602								
211.958	158.809 205.609								
208.098	114.157 168.757								
183.495	28.851 91.251								
125.210	-124.029 -53.829								
-1724.255	-906.216 -868.516								

F.E.	102.418 177.818	371.373 446.773	511.914 587.314	585.401 640.801	625.641 701.041	647.836 723.236	659.048 734.448	662.476 737.876
P.	440.914	571.788	645.377	699.786	718.939	739.105	749.687	747.033

Figure 31. Reactions in Kips.

(Finite Element vs. Idealized Plate)

#3	:	1.652	2.976	3.824	4.114
#1 x 4/3*	:	1.981	3.523	4.397	4.828
#2 x 2 **	:	2.458	4.294	5.438	5.826
Plate	:	1.623	2.939	3.775	4.061
#3	:	1.354	2.437	3.123	3.358
#1 x 4/3	:	1.625	2.895	3.687	3.956
#2 x 2	:	1.018	3.546	4.484	4.800
Plate	:	1.330	2.400	3.077	3.307
#3	:	1.062	1.898	2.422	2.600
#1 x 4/3	:	1.283	2.271	2.880	3.085
#2 x 2	:	1.608	2.810	3.538	3.782
Plate	:	1.037	1.860	2.376	2.551
#3	:	0.750	1.326	1.682	1.802
#1 x 4/3	:	0.917	1.603	2.020	2.160
#2 x 2	:	1.168	2.014	2.518	2.684
Plate	:	0.724	1.287	1.637	1.755
#3	:	0.400	0.695	0.876	0.937
#1 x 4/3	:	0.497	0.853	1.067	1.137
#2 x 2	:	0.650	1.092	1.354	1.440
Plate	:	0.377	0.664	0.841	0.901

*Ratio between plate thicknesses in gate 1 and gate 3.
**Ratio between plate thicknesses in gate 2 and gate 3.

Figure 32

Comparison Between the Deflections in Three Gates with Different Cover and Web Thicknesses.

TABLE II

DIMENSIONS OF SOLVED EXAMPLES

Gate	1*	2	3	4	5	6	7
Width (feet)	160	160	160	160	160	160	160
Depth (feet)	50	50	50	50	50	50	50
Distance between cover plates (feet)	10	10	10	10	10	5	15
Spacing of hl. webs (feet)	5	5	5	2.5	10	5	5
Spacing of vl. webs (feet)	10	10	10	20	20/3	10	10
Thickness of cover plates (inches)	.5	.75	.375	.5	.5	.5	.5
Thickness of hl. webs (inches)	.5	.375	.75	.5	.5	.5	.5
Thickness of vl. webs (inches)	.5	.375	.75	.5	.5	.5	.5

*Two finite-element solutions, considering and neglecting web shear deformations, respectively.

all three gates, the ratio of the deflections will be proportional to the corresponding ratio of the thickness of the cover plates. For comparison, let us multiply the finite-element solution deflections for gate "1" by the ratio of the thickness of cover plate "1" (of gate 1) to the thickness of cover plates "3" (of gate 3), namely .5/.375, and similarly for gate "2" multiply by the ratio of the thickness of cover plate "2" to the thickness of cover plate "3", namely .75/.375. The modification of the deflections for gates "1" and "2" will not affect the comparison between the finite element solution and the plate solution, since we multiply both solutions

by the same factor, and it will enable us to compare the deflections from the finite element solution for the three gates with only one set of deflections from the plate solution, namely, that of gate "3". The deflections in gate "3" and the modified deflections in gates "1" and "2" are shown in Figure 32 as well as the deflections calculated using the plate idealization. The deflections from the finite-element solution in gate "3" can be considered nearly identical with those from the plate solution. Meanwhile there is a considerable difference between the results of the two solutions in gate "1", and this difference is still greater in gate "2". Gates "1", "4", and "5" have the same width, depth, and distance between cover plates, cover plate thickness, and web thickness. However, they have different web spacings as indicated in Table II. The deflections calculated in the three gates using the plate method should naturally be the same. The deflections for the three gates using the finite-element method and the plate method are listed in Figure 33. As one can see, the difference between the deflections in the three gates calculated using the finite-element method is not appreciable.

Finally, gates "6", "1", and "7" have the same width, depth, spacing of webs, thickness of cover plates, and thickness of webs. However, the distance between the cover plates are 5 feet, 10 feet, and 15 feet, respectively. In the idealized plate solution, since the contribution of the webs to the flexural rigidity of the structure is neglected and no regard is given to web shear deformations, the deflections of the gates will be proportional to the square of the

#1:	1.486	2.642	3.373	3.621
#4:	1.410	2.537	3.257	3.504
#5:	1.594	2.803	3.560	3.817
Plate:	1.217	2.204	2.831	3.046
#1:	1.219	2.171	2.765	2.967
#4:	1.168	2.105	2.699	2.901
#5:	1.304	2.295	2.909	3.116
Plate:	0.997	1.800	2.307	2.480
#1:	0.962	1.703	2.160	2.314
#4:	0.941	1.684	2.147	2.304
#5:	1.023	1.778	2.257	2.414
Plate:	0.778	1.395	1.782	1.913
#1:	0.688	1.202	1.515	1.620
#4:	0.692	1.220	1.543	1.651
#5:	0.724	1.250	1.568	1.674
Plate:	0.543	0.965	1.227	1.316
#1:	0.373	0.640	0.800	0.853
#4:	0.390	0.671	0.839	0.895
#5:	0.387	0.657	0.818	0.872
Plate:	0.283	0.498	0.631	0.676

Figure 33

Comparison Between the Deflections
in Three Gates with Different Web Spacings.

corresponding distance between the cover plates. For comparison, the deflections of the three gates calculated using the finite-element method are listed in Figure 34 in which the deflections of gate "1" and "7" are modified by multiplying by the square of the corresponding ratio between the spacings of the cover plates. Again, as mentioned before, this modification will not affect the comparison. The results shown in Figure 34 indicate that the difference between the modified deflections of gates "1" and "7" and the deflections of gate "6", all calculated using the finite-element method, is very small.

Conclusions from the comparison between the stresses in the various elements of the above examples calculated using the finite-element method and the plate method are included in the next section. However, the values of these stresses are not shown. One more example in which the width-to-depth ratio is 2:1 is solved using both methods. The dimensions of this example are given below

Width (feet)	100
Depth (feet)	50
Distance between skin (feet)	8
Spacing of hl. webs (feet)	5
Spacing of vl. webs (feet)	25/3
Thickness of skin (inches)	.5
Thickness of hl. webs (inches)	.5
Thickness of vl. webs (inches)	.5

The results for this example are omitted; however, the conclusions from the comparison between the two solutions are included below.

#6 :	5.914	10.547	13.472	14.468
#1 x 4* :	5.944	10.568	13.492	14.484
#7 x 9** :	6.102	10.809	13.779	14.796
Plate	4.870	8.816	11.326	12.182
#6 :	4.844	8.633	11.004	11.808
#1 x 4 :	4.876	8.684	11.060	11.868
#7 x 9 :	5.013	8.910	11.340	12.159
Plate :	3.990	7.199	7.230	9.921
#6 :	3.803	6.733	8.547	9.159
#1 x 4 :	3.848	6.812	8.640	9.256
#7 x 9 :	3.978	7.029	8.910	9.540
Plate :	3.111	5.579	7.127	7.652
#6 :	2.694	4.715	5.949	6.364
#1 x 4 :	2.752	4.808	6.060	6.480
#7 x 9 :	2.880	4.994	6.300	6.732
Plate :	2.171	3.860	4.910	5.264
#6 :	1.441	2.481	3.109	3.318
#1 x 4 :	1.492	2.560	3.200	3.412
#7 x 9 :	1.584	2.700	3.357	3.582
Plate :	1.130	1.993	2.524	2.702

*Square the ratio between cover plates spacing in gate 1 and gate 6.
**Square the ratio between cover plates spacing in gate 7 and gate 6.

Figure 34

Comparison Between the Deflections
in Three Gates with Different Cover Plates Spacings.

5.5 Concluding Remarks

The conclusions from the previous studies of the comparison between the finite element solutions and the plate solutions are as follows:

1. The contribution of the cover plates to the flexural rigidity of the structure greatly exceeds the contribution of the webs.

2. The anisotropy due to unequal web spacings in both directions has a small effect on the deflections, and on the stresses in the cover plates.

3. Shear deformations of the webs are appreciable, especially for relatively thin webs, and they are more appreciable toward the supports.

4. The plate method furnishes sufficiently good information regarding the distribution of the normal stresses in the cover plates, and the error in the maximum stress is within $\pm$ 10% as an average in the above examples.

5. Except for a zone around the edges, the plate method furnishes sufficiently good information regarding the distribution of the shear stresses in the cover plates.

6. The plate method fails to furnish sufficiently good information regarding the distribution of the shear stresses in the webs or the reactions at the supports.

7. In both methods, the cover plates were assumed to be completely effective between the webs. However, as the web spacing gets larger, the distribution of normal stresses in the cover plates

will be remarkably higher at the cover-web juncture than at the middle between webs, and the cover plates cannot be assumed to be fully effective between the webs. This is referred to as "Shear Lag," since, due to the localized manner in which the shear stresses are transmitted to the cover plates, the strips of the cover plates more remote from the cover-web juncture will lag farther back than those near the webs.

8. If buckling of the cover plates in compression occur its width between the webs would not be fully effective. It is assumed that no buckling will take place.

VI. SUMMARY AND CONCLUSIONS

The advantageous statical properties of cellular structures as well as the economy which can be achieved by their use make them useful for many kinds of civil engineering structures, one of which is the dock flap gate.

The work done on structural analysis of dock flap gates and similar structures was studied. Although dock gates are large and expensive structures, very little attention appears to have been devoted to the investigation of the stress distribution in them. The conventional method of design used in practice nowadays is based on the thin isotropic plate theory. Plate theory may give us a very good approximation for the stresses in the cover plates, but it cannot furnish a reasonable approximation for shear stresses in the web elements. The absence of an accurate analysis may lead to a wasteful disposition of material in the gate.

Fortunately, much attention has been given to similar aircraft structures. A structural idealization which has been used before in similar aircraft structures has been adopted to the problem of the dock gate. This idealization is based on treating the structure as an assembly of plane elements, whose lines of intersection intersect at a finite number of points, at which the conditions of equilibrium and the compatibility of deformations must be satisfied. The analysis involves the derivation of the stiffness matrix of the individual elements and using it to formulate the stiffness matrix of the total structure.

In Chapter II, a method was presented to formulate the stiffness matrix of the structure and arrange it in a pattern that simplifies its formulation and facilitates the computations. Also, two different schemes have been presented to minimize the amount of computation and to cut down the time and the storage required by the machine. They render the application of the idealization possible with respect to the gate structure which has relatively large number of elements.

Several examples for dock gates have been solved using the newly adopted method. In Chapter III, the results obtained for one of these examples have been presented and their accuracy has been discussed.

Although the assumptions involved in the method presented in this study are widely adopted in the structural theory, an experimental check was carried out. The test results (deflections and strains) verified the applicability of these assumptions and proved that they do not impose any considerable errors.

A complete comparison between the proposed method of analysis and the conventional method adopted in practice (hypothetical thin isotropic plate) was presented in Chapter V. It showed the errors involved in the conventional method.

Although the method presented here was directly applied to gates with solid webs, it can as well be easily applied when the webs are in the form of trusses. The truss element stiffness matrix can be easily derived using the basic concepts of the theory of structures.

Although the web spacing has shown to have little effect on the horizontal stress distribution σ_x , σ_y , and τ_{xy}; it obviously affects the vertical stress distribution τ_{xz} , and τ_{yz} . The writer recommends, as implied from the results of the investigation conducted in the course of this study the use of webs which are spaced closer near the supported edges to take care of the high shears there. This does not invalidate the analysis presented in this dissertation, nor does it introduce any serious complications.

As a step toward an optimum design, the writer suggests the use of elements (cover elements and web elements) with different thicknesses according to the stress distribution in the structure. This can be achieved using the method outlined here.

When the dock cross section has some shape other than that of a rectangle, the method presented here, together with a stiffness matrix for a triangular plate element which can be derived similarly to deriving the rectangular element stiffness matrix,[19] can take care of any irregular shape of the boundary.

It is thus hoped that this study contributes to a better understanding of the structural behavior of cellular structures in general and of dock flap gates in particular.

APPENDIX I

STIFFNESS MATRIX OF THE PLANE STRESS PLATE ELEMENT

The general form of the rectangular plate element is shown in Figure A1. The deformations of the element can be described only with respect to some specific system, which is provided arbitrarily by the three reactions shown in Figure A1. The five degrees of freedom due to the remaining five nodal displacement components will be expressed by five independent stress patterns shown in Figure A1, which are associated with a characteristic nodal deformation patterns shown in Figure A1.

The linear relationship between nodal displacements and the deformation patterns can be expressed in matrix form as follows:

$$\begin{vmatrix} u_2 \\ u_4 \\ v_4 \\ u_3 \\ v_3 \end{vmatrix} = \frac{1}{E} \begin{bmatrix} b & b & -\nu b & 0 & 0 \\ 0 & b & 0 & -\frac{a^2}{b} & -a\lambda \\ \nu a & 0 & -a & a & 0 \\ b & 0 & -\nu b & -\frac{a^2}{b} & -a\lambda \\ \nu a & 0 & -a & -a & 0 \end{bmatrix} \begin{vmatrix} m \\ n \\ p \\ q \\ r \end{vmatrix}$$

or

$$\bar{V} = [A]\,\bar{\alpha} \,. \qquad \text{(A-1)}$$

Then:

$$\bar{\alpha} = [A]^{-1}\,\bar{V} \,. \qquad \text{(A-2)}$$

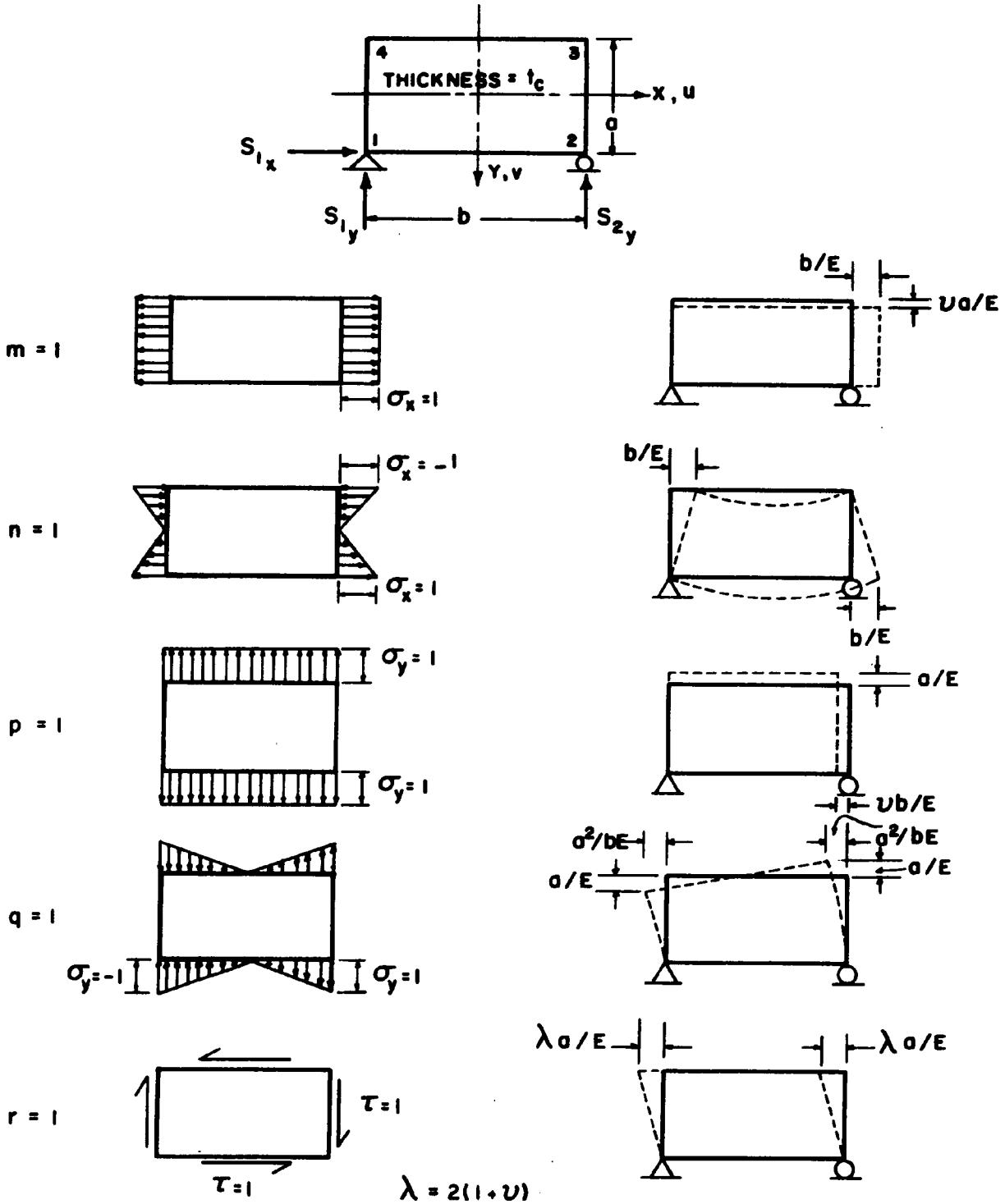


Figure A1. Assumed Stress and Corresponding Deformation Patterns.

The stress at any point in the plate may be expressed in terms of the stress patterns as follows:

$$\begin{vmatrix} \sigma_x \\ \sigma_y \\ \tau \end{vmatrix} = \begin{bmatrix} 1 & \frac{2y}{a} & 0 & 0 & 0 \\ 0 & 0 & 1 & \frac{2x}{b} & 0 \\ 0 & 0 & 0 & 0 & +1 \end{bmatrix} \begin{vmatrix} m \\ n \\ p \\ q \\ r \end{vmatrix}$$

or

$$\bar{\sigma} = [B]\,\bar{\alpha} \,. \tag{A-3}$$

Introduce (A-2) into (A-3); then

$$\bar{\sigma} = [B]\,[A]^{-1}\,\bar{V} \,. \tag{A-4}$$

The stress-strain relationship of plane elasticity

$$\begin{vmatrix} \epsilon_x \\ \epsilon_y \\ \gamma \end{vmatrix} = \frac{1}{E} \begin{bmatrix} 1 & -\nu & 0 \\ -\nu & 1 & 0 \\ 0 & 0 & \lambda \end{bmatrix} \begin{vmatrix} \sigma_x \\ \sigma_y \\ \tau \end{vmatrix}$$

or

$$\bar{\epsilon} = [C]\,\bar{\sigma} \,. \tag{A-5}$$

Introduce (A-4) into (A-5); then

$$\bar{\epsilon} = [C][B][A]^{-1}\,\bar{V} \tag{A-6}$$

If the plate is subjected to a set of external nodal forces $\bar{S}$, where

$$\bar{S} = \begin{vmatrix} S_2^x \\ S_4^x \\ S_4^y \\ S_3^x \\ S_3^y \end{vmatrix}$$

then $\bar{S}$ is in equilibrium with a system of internal stresses $\bar{\sigma}$. Let the element be subjected successively to arbitrary virtual nodal displacements $\hat{V}$, which is compatible with the internal virtual strains $\hat{\bar{\epsilon}}$; then the external work

$$(We) = \hat{\bar{V}}^T \bar{S}$$

and the internal work

$$(W_i) = t \iint \hat{\bar{\epsilon}}^T \bar{\sigma} \, dxdy .$$

From (A-6)

$$\hat{\bar{\epsilon}}^T = \hat{\bar{V}}^T [A^{-1}]^T [B]^T [C] .$$

Then:

$$W_i = t \iint \hat{\bar{V}}^T [A^{-1}]^T [B]^T [C][B][A]^{-1} \bar{V} \, dxdy .$$

From the theorem of virtual displacements

$$W_i = W_e$$

or

$$\hat{\bar{V}}^T \bar{S} = t\iint \hat{\bar{V}}^T [A^{-1}]^T[B]^T[C][B][A]^{-1} \bar{V}\, dxdy .$$

And since $\hat{\bar{V}}$ is arbitrary, then

$$\bar{S} = t\iint [A^{-1}]^T[B]^T[C][B][A]^{-1} \bar{V}\, dxdy .$$

And since $\bar{V}$ are not functions of x or y, then

$$\bar{S} = \left[t\iint [A^{-1}]^T[B]^T[C][B][A]^{-1} dxdy \right] \bar{V}$$

or

$$\bar{S} = [K]\, \bar{V}$$

where $[K] = t\iint [A^{-1}]^T[B]^T[C][B][A]^{-1} dxdy$.

If the matrix inversion and multiplications are performed, and the resulting matrix is integrated term by term between the limits $-\frac{b}{2}$ and $+\frac{b}{2}$; and $-\frac{a}{2}$ and $+\frac{a}{2}$ in the x and y directions, respectively, the final result is:

$$[K] = \frac{Et_c}{8(1-\nu^2)} \begin{bmatrix} (a_1+b_1) & (-c_1-a_1) & (-1-\nu) & (c_1-a_1) & (1-3\nu) \\ (-c_1-a_1) & (a_1+b_1) & (1+\nu) & (-b_1+a_1) & (3\nu-1) \\ (-1-\nu) & (1+\nu) & (a_2+b_2) & (1-3\nu) & (c_2-a_2) \\ (c_1-a_1) & (-b_1+a_1) & (1-3\nu) & (a_1+b_1) & (-1-\nu) \\ (1-3\nu) & (3\nu-1) & (c_2-a_2) & (-1-\nu) & (a_2+b_2) \end{bmatrix}$$

where $a_1 = m(1-\nu)$, $b_1 = 2(4-\nu^2)/3m$, $c_1 = 2(2+\nu^2)/3m$

$a_2 = (1-\nu)/m$, $b_2 = 2m(4-\nu^2)/3$, $c_2 = 2m(2+\nu^2)/3$

and $m = \frac{b}{a}$.

From the kinematics of the element (Figure A2), one can relate the 8 nodal displacement vector $\bar{r}$ to the displacement vector $\bar{v}$ such that

$$\bar{v} = [a]\,\bar{r} ,$$

where

$$[a] = \begin{bmatrix} -1 & 0 & 1 & 0 & 0 & 0 & 0 & 0 \\ -1 & \frac{1}{m} & 0 & -\frac{1}{m} & 0 & 0 & 1 & 0 \\ 0 & -1 & 0 & 0 & 0 & 0 & 0 & 1 \\ -1 & \frac{1}{m} & 0 & -\frac{1}{m} & 1 & 0 & 0 & 0 \\ 0 & 0 & 0 & -1 & 0 & 1 & 0 & 0 \end{bmatrix}$$

where $\bar{r}$ is arranged to agree with

$$\bar{r} = \begin{vmatrix} r_1^x \\ r_1^y \\ r_2^x \\ r_2^y \\ r_3^x \\ r_3^y \\ r_4^x \\ r_4^y \end{vmatrix}$$

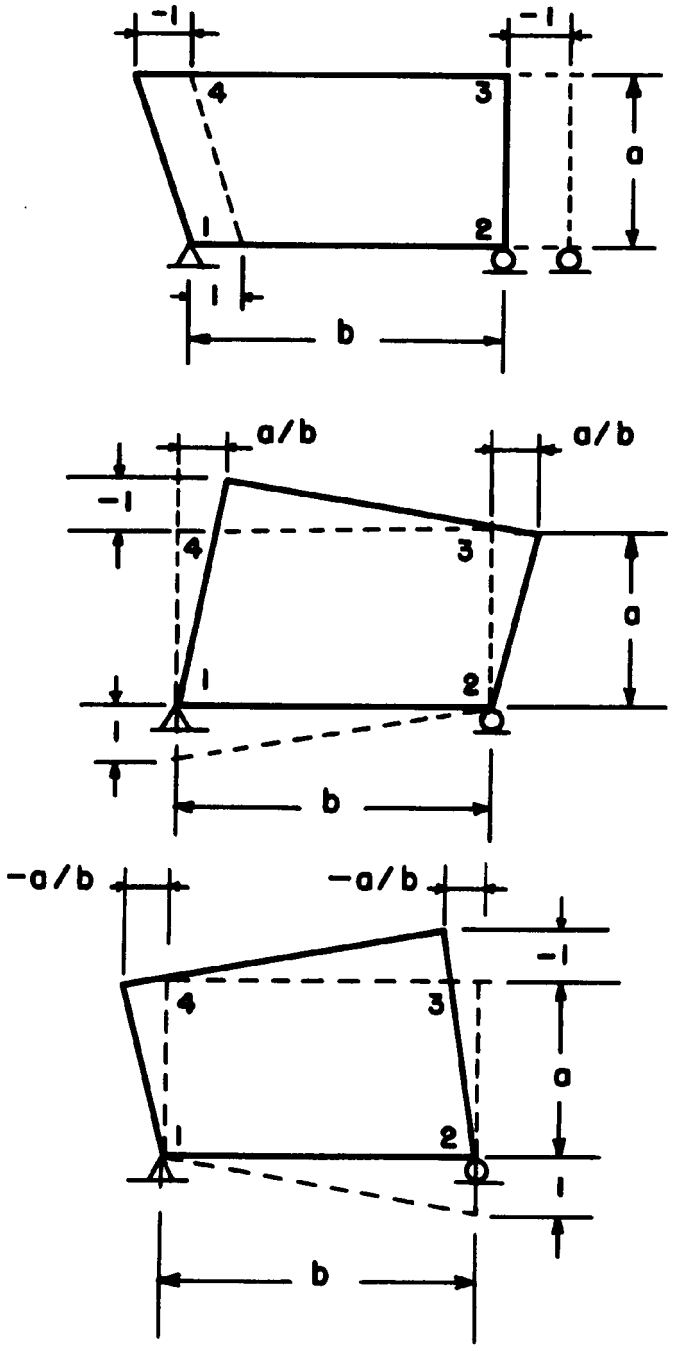


Figure A2. Plate Distortions for Support Displacements.

Using the principle of virtual work,*

$$\bar{R} = [a]^T \bar{S}$$

where $\bar{R}$ is an 8 nodal force vector, and is arranged to agree with

$$\bar{R} = \begin{vmatrix} R_1^x \\ R_1^y \\ R_2^x \\ R_2^y \\ R_3^x \\ R_3^y \\ R_4^x \\ R_4^y \end{vmatrix} .$$

---

* If we impose two compatible sets of displacements $\delta\bar{v}$, and $\delta\bar{r}$, then

$$\delta\bar{v} = [a] \ \delta\bar{r} \qquad \text{(i)}$$

from the principle of virtual work

$$\bar{R}^T \ \delta\bar{r} = \bar{S}^T \ \delta\bar{v} \qquad \text{(ii)}$$

from i, and ii

$$\bar{R}^T \ \delta\bar{r} = \bar{S}^T \ [a] \ \delta\bar{r} .$$

Since $\delta\bar{r}$ is arbitrary, then

$$\bar{R}^T = \bar{S}^T \ [a]$$

or

$$\bar{R} = [a]^T \ \bar{S} .$$

But

$$\bar{S} = [K]\,\bar{V} \ .$$

Then

$$\bar{R} = [a]^T[K][a]\,\bar{r}$$

or

$$\bar{R} = [K]\,\bar{r} \ .$$

Doing the multiplication,

$$[K]=\frac{Et_c}{8(1-\nu^2)}\begin{bmatrix}
a_1+b_1 & -1-\nu & a_1-b_1 & 1-3\nu & -a_1-c_1 & 1+\nu & c_1-a_1 & 3\nu-1 \\
-1-\nu & a_2+b_2 & 3\nu-1 & c_2-a_2 & 1+\nu & -a_2-c_2 & 1-3\nu & a_2-b_2 \\
a_1-b_1 & 3\nu-1 & a_1+b_1 & 1+\nu & c_1-a_1 & 1-3\nu & -c_1-a_1 & -1-\nu \\
1-3\nu & c_2-a_2 & 1+\nu & a_2+b_2 & 3\nu-1 & a_2-b_2 & -1-\nu & -a_2-c_2 \\
-a_1-c_1 & 1+\nu & c_1-a_1 & 3\nu-1 & a_1+b_1 & -1-\nu & a_1-b_1 & 1-3\nu \\
1+\nu & -a_2-c_2 & 1-3\nu & a_2-b_2 & -1-\nu & a_2+b_2 & 3\nu-1 & c_2-a_2 \\
c_1-a_1 & 1-3\nu & -c_1-a_1 & -1-\nu & a_1-b_1 & 3\nu-1 & a_1+b_1 & 1+\nu \\
3\nu-1 & a_2-b_2 & -1-\nu & -a_2-c_2 & 1-3\nu & c_2-a_2 & 1+\nu & a_2+b_2
\end{bmatrix}$$

APPENDIX II

WEB ELEMENT STIFFNESS MATRIX

Let us define,

I = moment of inertia of web section about the neutral axis (x or y).

t_w = thickness of web.

E = modulus of elasticity.

G = modulus of rigidity (shear modulus) = $\frac{E}{2(1+\nu)}$.

ν = Poisson's ratio.

Let us first give end (1) a unit positive rotation without displacement while end (2) is fixed. The deflected element and necessary forces are showing in (Figure A3-a). From energy principles,

$$W_1 = \frac{M_1 L^2}{2EI} + \frac{R_1 L^3}{3EI} \quad (1+n)$$

$$\theta_1 = \frac{M_1 L}{EI} + \frac{R_1 L^2}{2EI}$$

where $n = 3EI/Ght_w L^2$

and W_1 , θ_1 are the vertical displacement and the rotation respectively at end 1. But from the boundary conditions

$$W_1 = 0 \ , \quad \theta_1 = 1 \ .$$

Then

$$\frac{M_1 L^2}{2EI} + \frac{R_1 L^3 (1+n)}{3EI} = 0$$

$$\frac{M_1 L}{EI} + \frac{R_1 L^2}{2EI} = 1 \ .$$

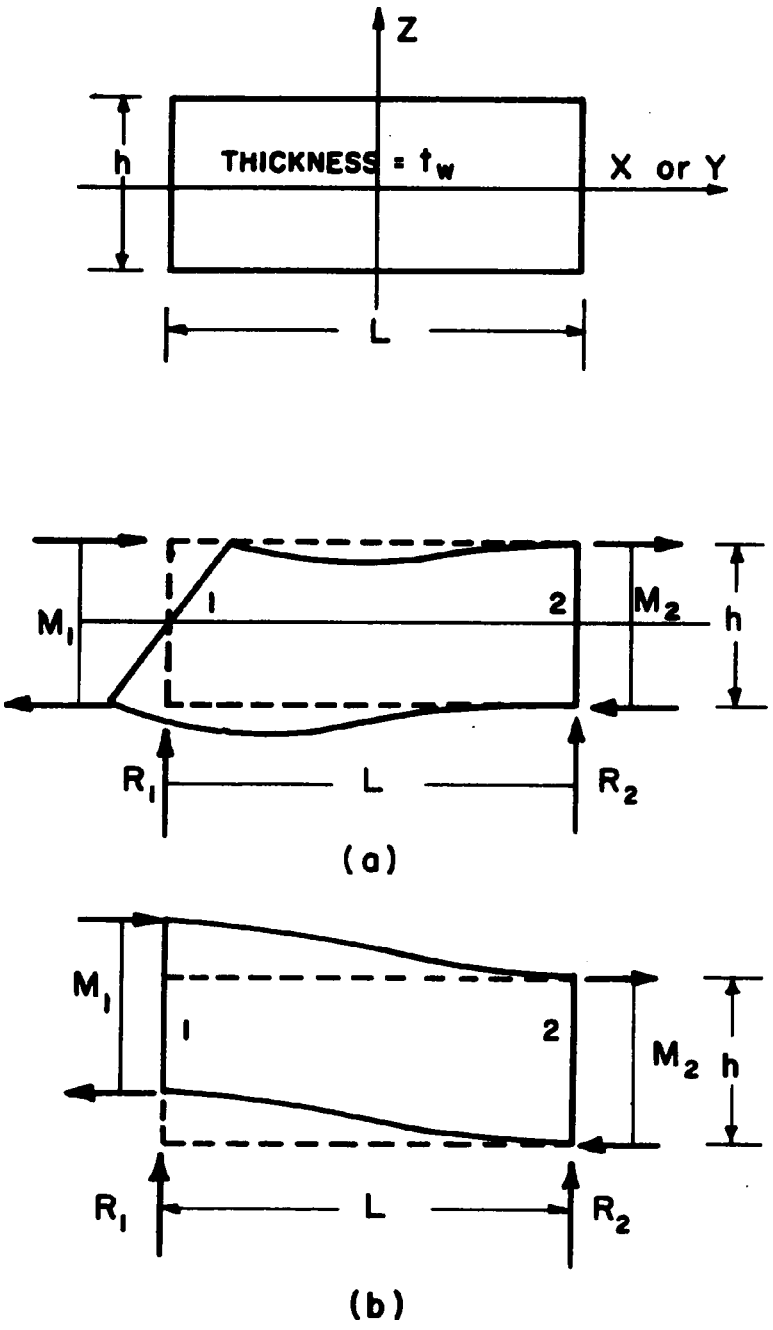


Figure A3. Web Displacements Required in Developing the Web Stiffness Matrix.

Solving for M_1, R_1, then

$$M_1 = \frac{4EI(1+n)}{L(1+4n)} \qquad \text{(i)}$$

$$R_1 = \frac{-6EI}{L^2(1+4n)} \quad . \qquad \text{(ii)}$$

From equilibrium considerations,

$$R_2 = -R_1 = \frac{6EI}{L^2(1+4n)} \qquad \text{(iii)}$$

and by taking moments about 2

$$M_2 = -R_1 L - M_1$$

$$= \frac{2EI(1-2n)}{L(1+4n)} \qquad \text{(iv)}$$

(i), (ii), (iii), and (iv) are the first column in the web element stiffness matrix. Let us give end (1) a unit positive displacement without rotation while end (2) is fixed. The deflected element and necessary forces are shown in (Figure A3-b).

From energy principles,

$$W_1 = \frac{M_1 L^2}{2EI} + \frac{R_1 L^3(1+n)}{3EI}$$

$$\theta_1 = \frac{M_1 L}{EI} + \frac{R_1 L^2}{2EI}$$

where W_1 , θ_1 are as defined before.

From the boundary conditions

$$W_1 = 1 \ , \ \theta_1 = 0 \ .$$

Then

$$\frac{M_1 L^2}{2EI} + \frac{R_1 L^3(1+n)}{3EI} = 1$$

$$\frac{M_1 L}{EI} + \frac{R_1 L^2}{2EI} = 0 .$$

Solving for M_1 , R_1 , then

$$M_1 = - \frac{6EI}{L^2(1+4n)} \qquad \text{(v)}$$

$$R_1 = \frac{12EI}{L^3(1+4n)} . \qquad \text{(vi)}$$

From equilibrium considerations,

$$R_2 = -R_1 = \frac{-12EI}{L^3(1+4n)} \qquad \text{(vii)}$$

and by taking moments about 2

$$M_2 = -R_1 L - M_1$$

$$= - \frac{6EI}{L^2(1+4n)} \qquad \text{(viii)}$$

(v), (vi), (vii), and (viii) are the second column in the web element stiffness matrix. From symmetry one can write the third and the fourth columns directly. In the above analysis n represent the contribution of the shear deformation; for rigid shear webs $n = 0$.

REFERENCES

1. Sott, P. F., "Modern Dry Docks; Design, Construction, and Equipment. (Dock Gates)," Dock and Harbour Authority, (Feb., 1958), p. 286.

2. Stoner, A., "New Dry Dock at Wallsend," Dock and Harbour Authority, (Nov., 1957), p. 237.

3. "Box Gate for Falmouth Dry Dock," Dock and Harbour Authouity, (Oct., 1958), p. 198.

4. Underwood, A. E., Norfolk, J. D., and Eathorne, J. N., "The Design and Construction of the Queen Elizabeth Graving Dock at Falmouth," Inst. of Civil Engineers, Proc., (Jan., 1960), p. 49.

5. Nadai, A., Die elastischen Platten, (Berlin:Julius Springer, 1925), p. 135.

6. Amirikian, A., "New Developments in the Design and Construction of Closure Gates for Dry Docks," 14th International Navigation Congress, London, 1957.

7. Jaeger, L. G., "The Bending Moments in a Dock Gate," Civil Engineering and Public Works Review, (Oct., 1957), p. 1124.

8. Jaeger, L. G., A Theoretical and Experimental Investigation of the Deflection Forms of Certain Grid Frames and Plated Structures, Ph.D. Thesis, University of London, 1955.

9. Williams, D., "Recent Developments in the Structural Approach to Aeroelastic Problems," J. Roy. Aero. Soc., (June, 1954), p. 403.

10. Benscoter, S. U., and MacNeal, R. H., Equivalent Plate Theory for a Straight Multicell Wing, NACA TN-2786, Sept., 1952.

11. Levy, S., "Computation of Influence Coefficients for Aircraft Structures with Discontinuities and Sweep Back," J. Aero. Sci., (Oct., 1947), p. 547.

12. Wehle, L. B., and Lansing, W., "A Method for Reducing the Analysis of Complex Redundant Structures to a Routine Procedure," J. Aero. Sci., (Oct., 1952), p. 677.

13. Argyris, J. H., and Kelsey, S., Energy Theorems and Structural Analysis, Butterworths, 1960.

14. Levy, S., "Structural Analysis and Influence Coefficients for Delta Wings," J. Aero Sci., (July, 1953), p. 449.

15. Archer, J. S., and Samson, C. H., "Structural Idealization for Digital Computer Analysis," 2nd Conf. on Electronic Computation, ASCE, (Sept. 8-9, 1960), p. 283.

16. Herennikoff, A., "Solutions of Problems of Elasticity by the Frame Work Method," Trans. ASME, Vol. 63 p. A-169.

17. McHenry, D., "A Lattice Analogy for the Solution of Stress Problems," J. of Inst. Civil Engineers, (Dec., 1943), p. 59.

18. Turner, M. J., Clough, R. W., Martin, H. C., and Topp, L. J., "Stiffness and Deflection Analysis of Complex Structures," J. Aero. Sci., (Sept., 1956), p. 805.

19. Clough, R. W., "The Finite Element Method in Plane Stress Analysis," 2nd Conf. on Electronic Computation, ASCE, (Sept. 8-9, 1960), p. 345.

20. Frazer, R. W., Duncan, W. J., and Collar, A. R., Elementary Matrices, Cambridge Univ. Press, 1950.

21. Klein, B., "A Simple Method of Matric Structural Analysis," J. Aero. Sci., (Jan., 1957), p. 39.

22. Clough, R. W., "Use of Modern Computers in Structural Analysis," J. Str. Div., Proc. ASCE, (May, 1958), No. 1636.

23. Archer, J. S., "Digital Computation for Stiffness Matrix Analysis," J. Str. Div., Proc. ASCE, (Oct., 1958), No. 1814.

24. Clough, R. W., "Structural Analysis by Means of a Matrix Algebra Program," Proc. ASCE. Conf. on Electronic Computation, Kansas City, Nov., 1958.

25. Berg, G. V., Computer Analysis of Structures, Part I, Matrix Methods of Structural Analysis, Preliminary edition, College of Engineering, The University of Michigan, Ann Arbor, Michigan, 1963.

26. Faddeeva, V. N., Computational Methods of Linear Algebra, Dover Pub., 1959.

SELECTED BIBLIOGRAPHY

1. A Guide for the Analysis of Ship Structures, U. S. Government Research Report, Dept. of Commerce, 1960.

2. Argyris, J. H., "On the Analysis of Complex Elastic Structures," Appl. Mech. Rev., Vol. 11, (July, 1958), p. 331.

3. Carpenter, J. E., "Structural Model Testing Compensation for Time Effect in Plastics," J. PCA, Vol. 5, (Jan., 1963), p. 47. (Includes list of references for plastic model testing)

4. Cornick, H. F., Dock and Harbour Engineering, The Design of Docks," C. Griffin and Co., London, 1958.

5. Crandall, S. H., Engineering Analysis, New York: McGraw Hill Book Co., 1957.

6. Crandall, P. S., "Reconstruction of Charles River Dam Lock Gates," J. Boston Soc. Civil Eng., (Oct., 1960), p. 357.

7. Galler, B. A., The Language of Computers, McGraw-Hill, 1962.

8. Gravey, S. J., "The Quadrilateral Shear Panel," Aircraft Engineering, (May, 1951), p. 134.

9. Hendry, A. W., and Jaeger, L. G., Grid Frame Works and Related Structures, Chatto and Windus Ltd., 1959.

10. Hendry, A. W., and El-turbi, D. A., "Theoretical and Measured Stresses in Welded Steel Dock Gates," The Inst. of Civil Engineers Proc., (Aug., 1961), p. 537.

11. Leliavsky, S., "Skin Plating on Steel Gates," The Engineer, (Oct., 1954), p. 510.

12. Memorandum on Construction and Equipment of Dry Docks, issued by the Institute of Civil Engineers in 1952.

13. Panc, V., "Modern Thin-Walled Structures and their Statical Solution, with Application to Flap Gates," Czechoslovak Heavy Industry, No. 6, (1959), p. 3.

14. Reissner, E., "The Effect of Transverse Shear Deformation on the Bending of Elastic Plates," Trans. ASME, Vol. 67, (1945), p. A69.

15. Salvadori, M. G., and Baron, M. L., Numerical Methods in Engineering, Prentice-Hall, Inc., 1959.

16. Schade, H. A., "Bending Theory of Ship Bottom Structure," Trans. Soc. Nav. Arch. and Marine Eng., 1938.

17. Schade, H. A., "Application of Orthotropical Plate Theory to Ship Bottom Structures," 5th Int. Congress for Applied Mechanics, 1938.

18. Schuerch, H., "Structural Analysis of Sweep, Low Aspect Ratio Multispar Aircraft Wings," Aero. Eng. Rev., Vol. 11, (Nov., 1952), p. 34.

19. Thomson, W., and Tait, P. G., Treatise on Natural philosophy Vol. 1, Part II, Cambridge Univ. Press, 1883.

20. Timoshenko, S., and Kriger, S. W., Theory of Plates and Shells, McGraw-Hill, Inc., 1959.

21. Walker, P. B., "The Experimental Approach to Aircraft Structural Research," J. Aero. Sci., (March, 1952), p. 145.

22. Zender, G. W., Comparison of Theoretical Stresses and Deflections of Multicell Wings with Experimental Results Obtained from Plastic Models, NACA TN-3813, Nov., 1956.